

# NORTHERN NEW MEXICO

## AND THE K-T BOUNDARY



PTYS594: PLANETARY GEOLOGY FIELD STUDIES - FALL 2013  
UNIVERSITY OF ARIZONA - LUNAR AND PLANETARY LABORATORY

*Letter from the Editor*

Welcome to New Mexico, 'Land of Enchantment', and to 'Colorful' Colorado!



Thank you to James for the cover art, the LPL field trip logo, the field geology reference guide, origami dinosaurs, and the grad students and deadlines plot. Thank you to Kelly for the crossword puzzle and to Ali for the LPL wordsearches.



*Catherine M. Elder*  
editor

# Table of Contents

## General Information & Geology Reference

**Trip Itinerary**

**Field Geology Reference Guide**

## Presentations

**Shane Byrne** - Provinces

**Michelle Thompson** – Continental divide

**Ali Bramson** – Lava tubes and perennial ice

**Corey Atwood-Stone** – Jemez Lineament

**Hannah Tanquary** – McCarthy flow and El Malpais history in general

**Kelly Miller** – Thermodynamics of lava flows

**Tad Komacek** – Rheology of lava flows

**Jess Vriesema** – Inflation and flow morphology

**Sky Beard** – Hydrothermal springs from volcanoes and impacts

**Donna Viola** – Astrobiology of hot springs

**Ning Ding** – Supervolcanoes & the Valles Caldera eruptions

**Catherine Elder** – Resurgent domes

**Ingrid Daubar** – Bandelier Tuff and ash fall vs. surge deposits

**Sarah Peacock** – Environmental effects of large volcanic events

**Youngmin JeongAhn** – Rio Grande Rift

**Xianyu Tan** – K/T Layer structure & continental vs. oceanic differences

**Margaret Landis** – Chicxulub and large crater formation in general

**Xi Zhang** – Environmental changes & extinctions from large impacts

**Christa Van Learhoven** – Impact hazards and impact rates for the terrestrial planets

**In-Car Entertainment**

**Note Paper**

**Scale Bar**

For locations:

<https://www.google.com/maps/ms?msid=217623034326340334094.0004e42c4afe41217322d&msa=0>

**Day 1 – 9/26**

8AM Leave the loading dock. Drive north on Campbell. Turn left on River and right on Oracle (AZ 77). After 95 miles (at Globe), turn left onto the US 70 for two miles and then right onto US 60. After 130 miles, turn left on US 180/US 191. Travel 14 miles to Lyman Lake State Park.

1PM Lunch at Lyman Lake State Park or nearby location...

2PM Leave Lyman Lake. Continue north on US 191, it transitions to AZ 61. After 41 miles, take a right to stay on AZ 61; it transitions to NM 53 in 14 miles at the border. Travel 59 miles further within NM and take a left onto State Route 57. Travel 9.8 miles and continue onto Zuni Canyon road – stop location uncertain probably travel about 2 miles.

Along this road we cross the continental divide

- **Michelle Continental divide**

4.40PM Arrive at Zuni Canyon.

5.30PM Backtrack on Zuni Canyon Road and State Route 57 for 8 miles. Take a left on an unmanned road toward a cinder cone. Travel about 1.3 miles to camp site.

5.50PM Camp in the Cibola National Forest. Elevation: 7800 feet.

(Sunset is ~6.05pm.)

**Day 2: 9/27**

8AM Leave Camp and drive back to NM 53. Turn left and travel 2 miles until the Ice Cave Road.

8.30 – 9.30AM Ice cave

- **Ali**                    **Lava tubes and Perennial Ice**

9.30AM Go North on NM 53 for 25 miles. In the town of Grants, turn right onto Santa Fe Avenue, 2.7 miles later continue onto Hwy 66 (left turn). After 5.3 mile transition to NM 117 and go south for 30 miles. Turn right on Lava Falls Road.

11.15AM Arrive at McCarthy Flow stop (include 30 minute stop in Grants)

- **Corey**                **Jemez Lineament**
- **Hannah**        **McCarthy Flow and El Malpais History in general**
- **Kelly**              **Thermodynamics of Lava Flows**
- **Tad**                **Rheology of Lava flows**
- **Jess**                **Inflation and flow morphology**

Lunch at McCarthy Flow

3 PM Drive north on NM 117 for 18 miles. Enter I40 East and drive 69 miles. Transition to I25 North in Albuquerque and drive 16 miles. Exit 242 onto US 550 West and travel 24 miles. Turn right onto NM 4, travel 8.4 miles and turn right onto Camino Amarillo. Two right turns after 0.6 and 0.4 miles respectively. After the second right turn we can pull off and camp.

5.40PM Camp in the Santa Fe National Forest. Elevation 6300 feet.

### Day 3 – 9/28

8AM Return to NM 4. Drive north for 11 miles to reach Soda Dam. Stop in Jemez Springs for 30 minutes on the way to powder our noses.

9AM Arrive at Soda Dam – explore old dam and cave with new spring

- **Sky**            **Hydrothermal springs from Volcanoes and Impacts**
- **Donna**        **Astrobiology of hot springs**

If there's time stop at an outcrop of three Rhyolite units at 12.8 miles from Soda Dam.

10AM Leave Soda Dam. Drive through Valles Caldera on NM 4 After 20 miles take a left onto a dirt road.

10:40AM Arrive at Cerro La Jara – views of the caldera floor and Redondo Peak

- **Ning**            **Supervolcanoes & the Valles Caldera Eruptions**
- **Catherine**    **Resurgent domes**
  
- **Talk about lava domes and hike around this dome (~500m across)**

12.10-12:50PM Drive to Bandelier NM on NM4.  
Lunch here.

- **Ingrid**        **Bandelier Tuff and Ash fall vs. surge deposits**
- **Sarah P.**      **Environmental effects of large volcanic events**

3.30PM Exit Bandelier National Monument and continue east on NM 4 for 12 miles. After it transitions into NM 502, go another 4 miles. Take NM 30 north for 9 miles. Turn left into US-285 (Paseo De Onate), after 8 miles turn right to stay on US 285 (cross Rio Chama), travel 27 more miles. Turn right into NM 567 and travel 5 miles until turning right into South Carson Road. Follow this dirt road for about 6 miles to the campsite.

5.15PM After walking 200m to the south-east, we should have a great view of the Rio Grande Gorge. If it's too late for this then we'll do it tomorrow at the Rio Grande Gorge bridge.

- **Youngmin**    **Rio Grande Rift**

Arrive at camp in the Carson National Forest. Elevation: 6800 feet.

## Day 4 – 9/29

8AM Leave Camp. Drive north, back to NM 567 (6 miles) and travel east 4 miles. Turn left on Taos County Rd Cb-115 and travel 8.2 miles. Take a right turn (almost doubling back on ourselves) onto US 64 (there's a small road called Sheep Herder's road at this junction). Travel 103 miles on US 64 (requires a right turn after 8.6 miles and a left 4.1 miles later in Taos) to I25. Join I25 north and travel 25 miles to exit 11 in Colorado. Take 30-minute break at freeway stop.

Cross the freeway and double back on CO 69.1 for <1 miles. Take a slight right onto CO 69 and immediately a right onto CO 18.3 for 3 miles. Take a left onto CO 12 and travel 6 miles. Turn left and cross the river at Madrid Bridge. This is CO18.3 again; the outcrops 1.2 miles further.

12PM Arrive at the Madrid KT exposures – no sampling

- **Xianyu**      **K/T Layer structure & Continental vs. Oceanic Differences**
- **Margaret**    **Chicxulub and large crater formation in general**
- **Xi**            **Environmental changes & extinctions from large impacts**

Continue on CO 18.3 for 2 miles. Turn left at a T-junction to stay on CO 18.3, travel another 0.5 miles to the Long Canyon parking area. Walk north about 400-500m to see the Long Canyon KT exposure – *no sampling*.

Lunch at Long Canyon. Leave Long Canyon and return to exit 11 of I25. Travel south on the eastern frontage road for 2.5 miles.

Starkville south KT exposures – sampling permitted.

- **Ingrid**        **Seismic effects of impacts from Chicxulub to INSIGHT.**
- **Christa**      **Impact hazards and impact rates for the terrestrial planets**

3PM When finished rejoin the I25 at exit 11. Travel 164 miles and take exit 307. Cross under the freeway and backtrack along the frontage road for 1.3 miles. Turn right onto state route 34 and travel 1.8 miles, turn left and reach campsite 0.2 miles later.

5.30PM Arrive at campsite in Santa Fe National Forest. Elevation 7600 feet.

**Day 5 – 9/30**

South on I25 towards the I10 to Tucson (taking the Hatch-Demming cutoff).  
7.5 hours driving, 1.5 hours various stops.

Back to LPL at ~5pm

**Participants**

---

Atwood-Stone, Corey  
Baker, Vic  
Beard, Sky  
Bramson, Ali  
Byrne, Shane  
Chung, Youngmin  
Daubar, Ingrid  
Ding, Ning  
Elder, Catherine  
Hamilton, Christopher  
Komacek, Tad

Landis, Margaret  
Miller, Kelly  
Peacock, Sarah  
Tan, Xianyu  
Tanquary, Hannah  
Thompson, Michelle  
Van Learhoven, Christa  
Viola, Donna  
Vriesema, Jess  
Zhang, Xi



Figure 12. The Madrid East site (above), with prominent vertical cliffs of sandstone directly overlying the boundary sequence (below).



Courtesy of Barb Cohen



Figure 13. Photograph of the Long's Canyon K/T boundary site showing mudstone and siltstone beds in the lower part overlain by the carbonaceous coaly sequence of the K/T boundary interval and the white K/T boundary claystone (shown by arrow) directly beneath a 7- to 8 foot thick ledge-forming sandstone.

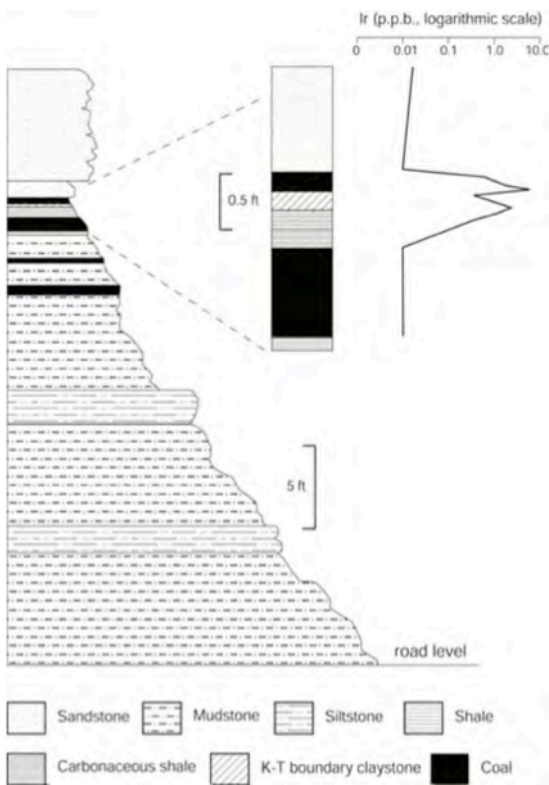


Figure 14. Iridium contents in the Long's Canyon site

Courtesy of Barb Cohen

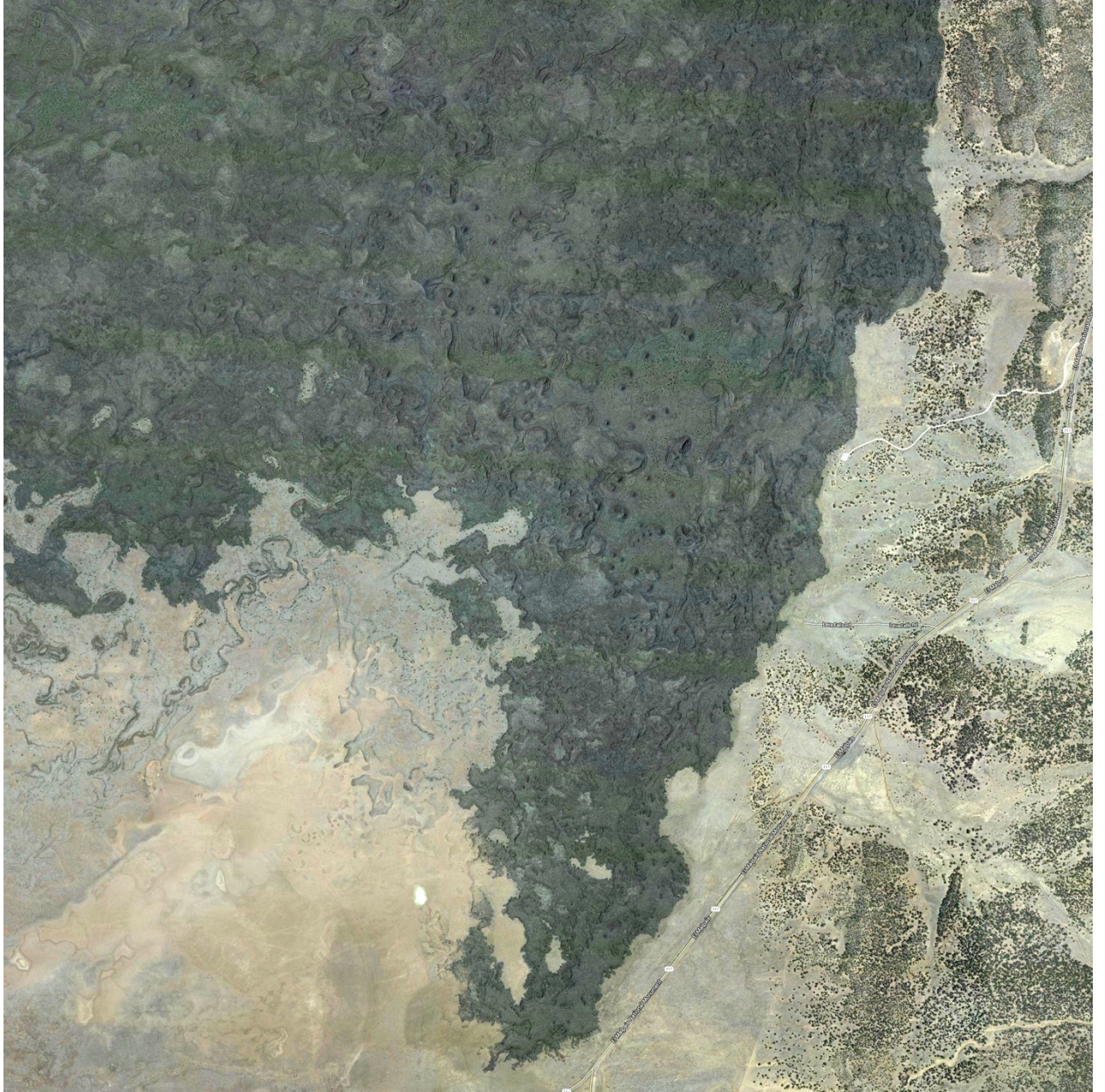


Figure 17. Photograph of the Starkville South site, looking east, showing the position of the K/T boundary claystone interval about 6 ft above a 23-ft-thick point-bar sandstone. Arrow points to the K/T boundary claystone layer.



Figure 18. Photograph of the K/T boundary sequence at the Starkville south site showing the light gray boundary claystone and overlying thin coal bed that contains the fern-spore spike.

Courtesy of Barb Cohen



# Common Rock Forming Minerals

Dark-Colored minerals			
Hardness	Cleavage	Physical Properties	Name
Hardness >5	Excellent or good	Dark gray, Blue-gray or black. May be iridescent. Cleavage in 2 planes at nearly right angles. Striations. Hardness-6	<b>Plagioclase Feldspar</b>
		Brown, gray, green or red. Cleavage in 2 planes at nearly right angles. Exsolution Lamellae. Hardness-6	<b>Potassium Feldspar</b>
		Opaque black. 2 cleavage planes at 60° and 120°. Hardness- 5.5	<b>Hornblende (Amphibole)</b>
	Poor or absent	Opaque red, gray, hexagonal prisms with striated flat ends. Hardness- 9	<b>Corrundum</b>
		Gray, brown or purple. Greasy luster. Massive or hexagonal prisms and pyramids. Transparent or translucent. Hardness- 7	<b>Quartz Black or brown-Smoky , Purple-Amethyst</b>
		Opaque red or brown. Waxy luster. Hardness- 7. Conchoidal Fracture	<b>Jasper</b>
		Opaque black. Waxy luster. Hardness- 7	<b>Flint</b>
Transparent- translucent dark red to black. Hardness- 7	<b>Garnet</b>		
Hardness < 5	Excellent or good	Colorless, purple, green, yellow, blue. Octahedral cleavage. Hardness- 4	<b>Flourite</b>
		Green. Splits along 1 excellent cleavage plane. Hardness- 2-3	<b>Chlorite</b>
		Black to dark brown. Splits along 1 excellent cleavage plane. Hardness- 2.5-3	<b>Biotite mica</b>
	Poor or absent	Opaque green, yellow or gray. Silky or greasy luster. Hardness- 2-5	<b>Serpentine</b>
		Opaque white, gray or green. Can be scratched with fingernail. Soapy feel. Hardness- 1	<b>Talc</b>
		Opaque earthy red to light brown. Hardness- 1.5-6	<b>Hematite</b>

Light-colored minerals			
Hardness	Cleavage	Physical Properties	Name
Hardness >5	Excellent or good	White or gray. Cleavage in 2 planes at nearly right angles. Striations. Hardness-6	<b>Plagioclase Feldspar</b>
		Orange, brown, white, gray, green or pink. Cleavage in 2 planes at nearly right angles. Exsolution Lamellae. Hardness-6	<b>Potassium Feldspar</b>
		Pale brown, white or gray. Long slender prisms. Cleavage in 1 plane. Hardness- 6-7	<b>Sillimanite</b>
	Poor or absent	Opaque red, gray, white hexagonal prisms with striated flat ends. Hardness- 9	<b>Corrundum</b>
		Colorless, white, gray or other colors. Greasy luster. Massive or hexagonal prisms and pyramids. Transparent or translucent. Hardness- 7	<b>Quartz White-Milky, Yellow-Citrine, Pink-Rose</b>
		Opaque gray or white. Waxy luster. Hardness- 7. Conchoidal Fracture	<b>Chert</b>
		Colorless, white, yellow, light brown. Translucent opaque. Laminated or massive. Cryptocrystalline. Hardness- 7	<b>Chalcedony</b>
Pale olive green. Conchoidal fracture. Transparent or translucent. Hardness- 7	<b>Olivine</b>		
Hardness < 5	Excellent or good	Colorless, white, yellow, blue, green. Excellent cleavage in 3 planes. Breaks into rhombohedrons. Effervesces in HCl. Hardness- 3	<b>Calcite</b>
		Colorless, white, yellow, blue, green. Excellent cleavage in 3 planes. Breaks into rhombohedrons. Effervesces in HCl only if powdered. Hardness- 3.5-4	<b>Dolomite</b>
		White with tints of brown. Short tabular crystals or roses. Very heavy. Hardness- 3-3.5	<b>Barite</b>
		Colorless, white or gray. Massive or tabular crystals, blades or needles. Can be scratched by fingernail. Hardness- 2	<b>Gypsum</b>
		Colorless, white. Cubic crystals. Salty taste. Hardness- 2.5	<b>Halite</b>
		Colorless, purple, green, yellow, blue. Octahedral cleavage. Hardness- 4	<b>Flourite</b>
	Poor or absent	Colorless, yellow, brown. Splits along 1 excellent cleavage plane. Hardness- 2-2.5	<b>Muscovite mica</b>
		Yellow crystals or earthy masses. Hardness 1.5-2.5	<b>Sulfur</b>
		Opaque green, yellow or gray. Silky or greasy luster. Hardness- 2-5	<b>Serpentine</b>
		Opaque white, gray or green. Can be scratched with fingernail. Soapy feel. Hardness- 1	<b>Talc</b>
Opaque earthy white to light brown. Hardness- 1-2	<b>Kaolinite</b>		

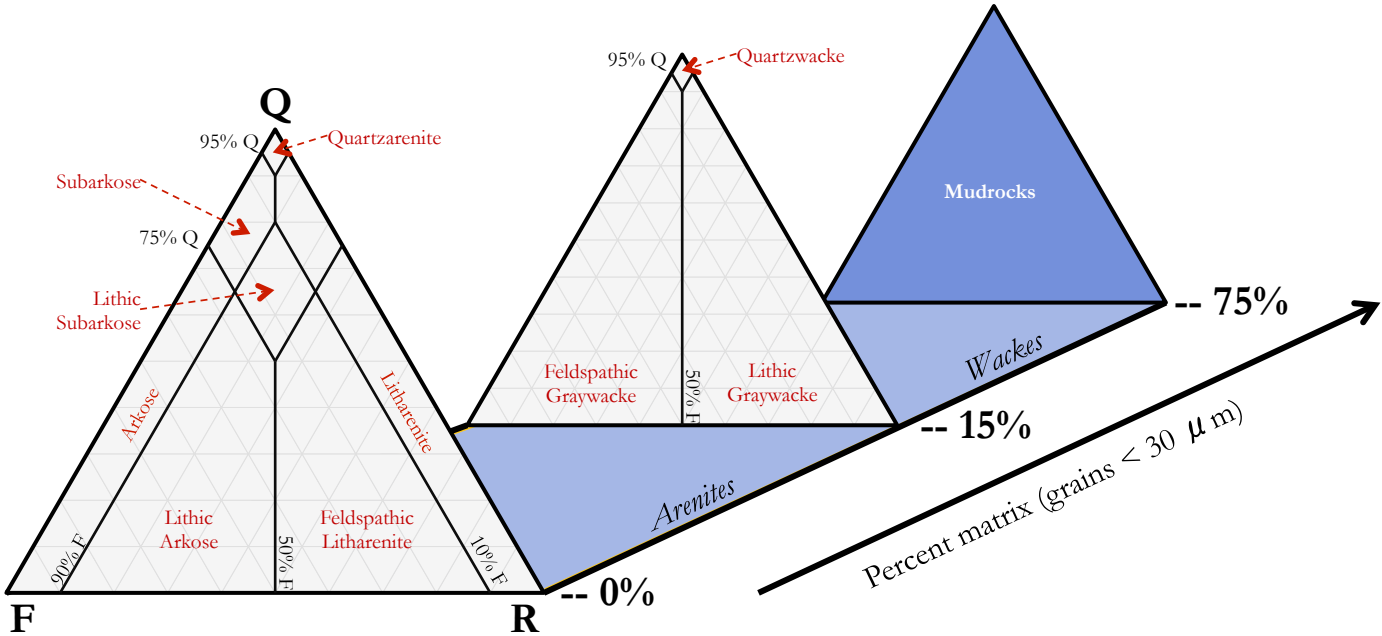
Metallic			
	Streak	Physical Properties	Name
Hardness > 5	Dark Gray	Brass yellow	<b>Pyrite</b>
		Dark gray-black, attracted to magnet	<b>Magnetite</b>
	Brown	Silvery black to black tarnishes gray	<b>Chromite</b>
Hardness < 5	Red-Red/Brown	Silvery gray, black, or brick red	<b>Hematite</b>
	Dark Gray	Brass yellow, tarnishes dark brown or purple	<b>Chalcopyrite</b>
		Iridescent blue, purple or copper red, tarnishes dark purple	<b>Bornite</b>
		Silvery gray, tarnishes dull gray Cleavage good to excellent	<b>Galena</b>
		Dark gray to black, can be scratched with fingernail	<b>Graphite</b>

# Sedimentary Rocks

## McBride, 1963 & Dott, 1964 Classification Scheme for Clastic Sedimentary Rocks

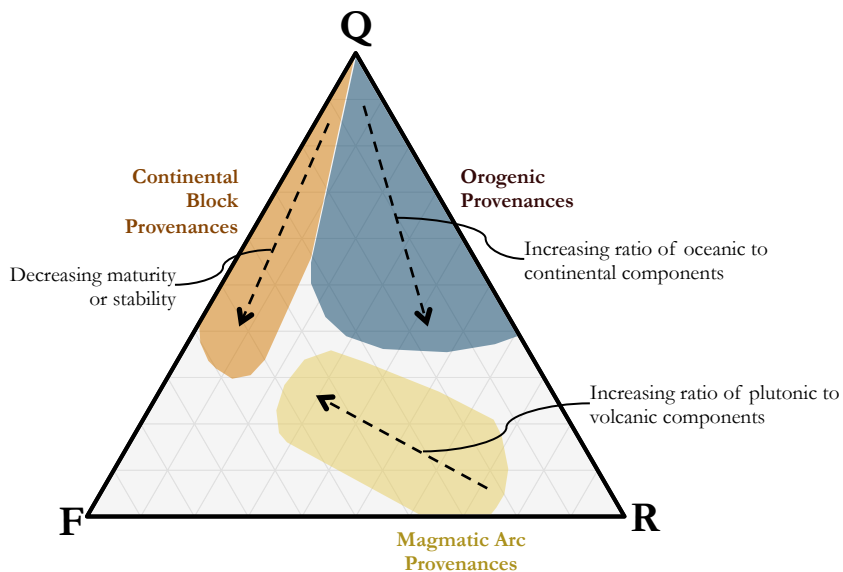


Scheme based on the normalized percentages of the visible grains: quartz and chert (Q), feldspar (F), and lithic rock fragments (R) – as well as the percent composed of matrix (mud & silt)



## Tectonic Setting for Clastic Sedimentary Rocks

Scheme based on the normalized percentages of the visible grains: quartz and chert (Q), feldspar (F), and lithic rock fragments (R) – as well as the percent composed of matrix (mud & silt). Regions based upon field data.



# Sedimentary Rocks

## Classification Scheme for Mudrocks



Scheme based on clay/silt content, and whether the rock is laminated (layered) or not.

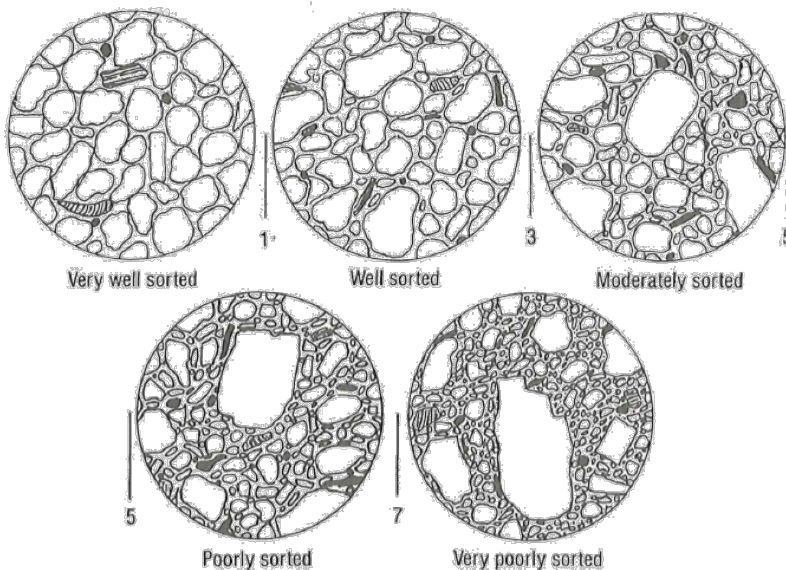
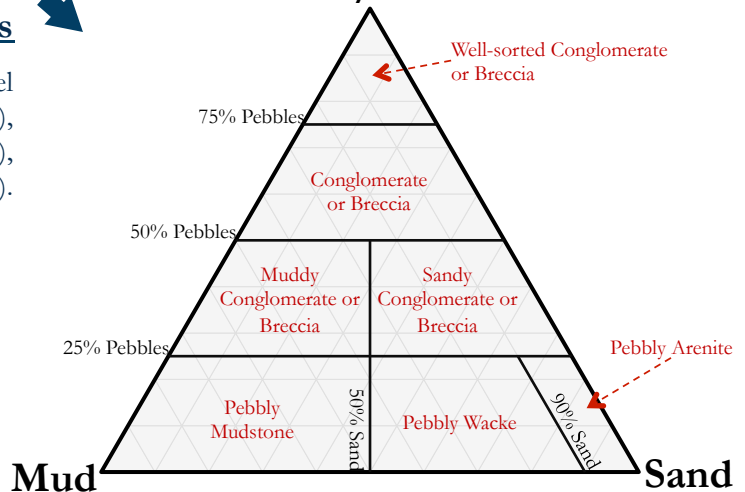
	Mudrocks (containing > 50% mud)			Rocks with <50% mud
	Silt dominant (> 2/3 of rock)	Clay and Silt	Clay dominant (> 2/3 of rock)	
<b>Non-laminated</b>	Siltstone	Mudstone	Claystone	Conglomerates, Breccias, Sandstones, etc.
<b>Laminated</b>	Laminated Siltstone	Mudshale	Clayshale	

## Classification Scheme for Sub-Conglomerates and Sub-Breccias



Scheme based on percent of a rock composed of: gravel or pebbles (size >2 mm), sand (2 mm > size > 1/16 mm), and mud (size < 1/16 mm).

## Gravel/Pebbles



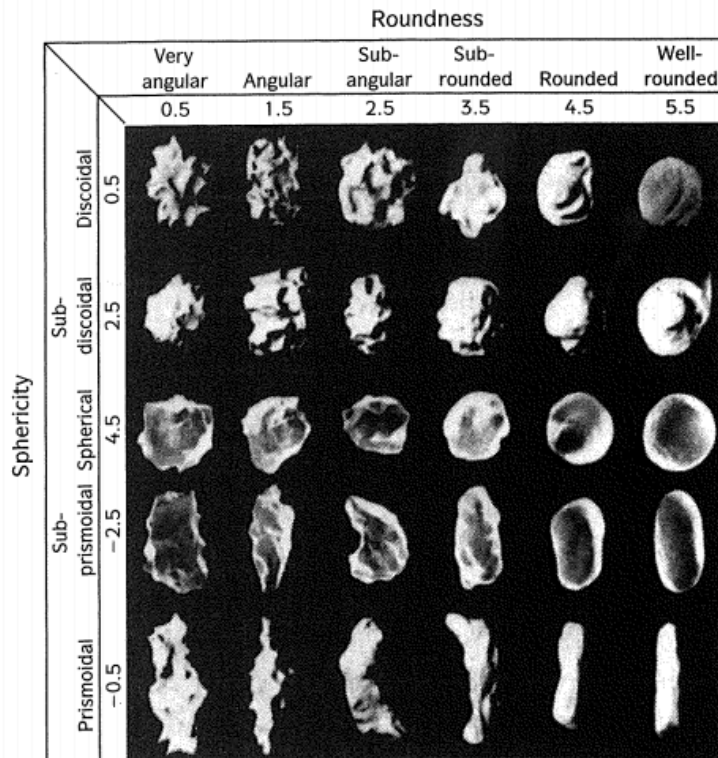
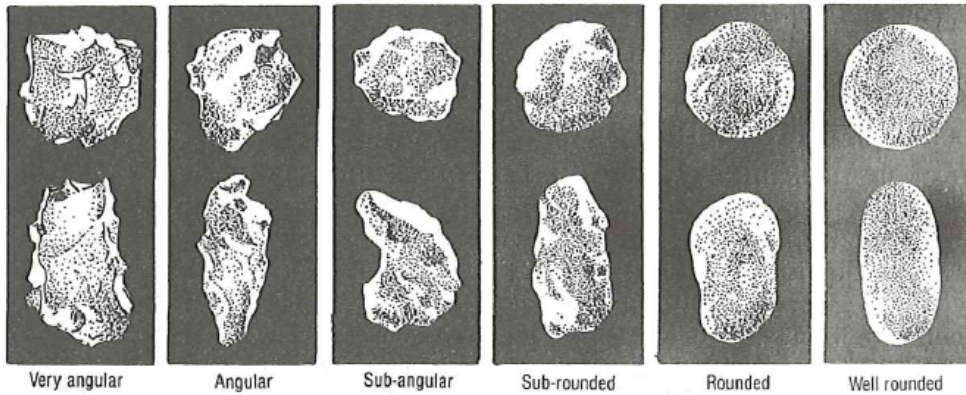
## Estimating Sorting

Example hand-lens view of detritus.  
From Compton, 1985

# Sedimentary Rocks

## Degrees of Rounding

Example hand-lens view of detritus of varying degrees of roundedness. The top row are equidimensional (spherical) grains, while the lower row are elongated grains. From Compton, 1985 and Davis & Reynolds, 1996, respectively.

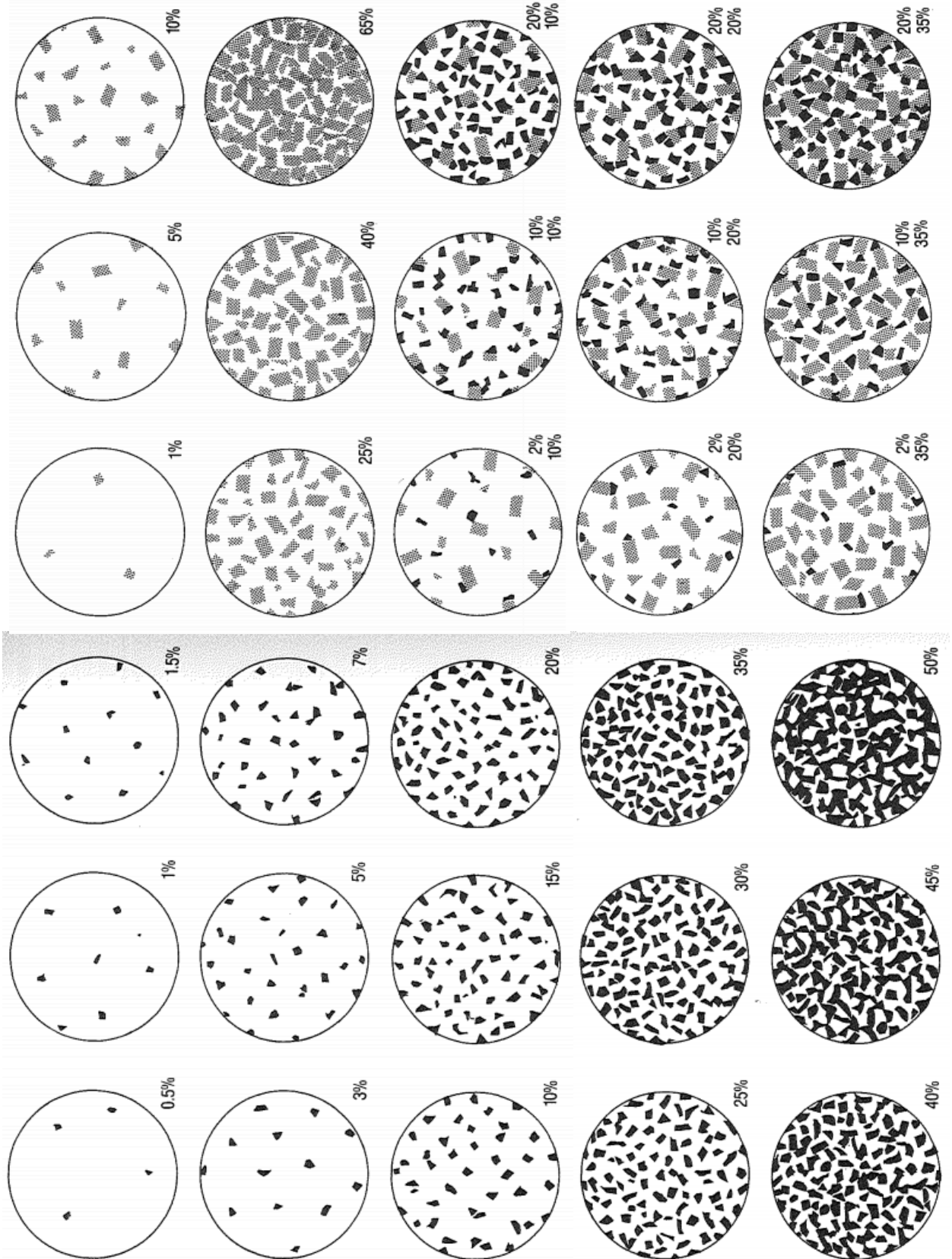


# Sedimentary Rocks

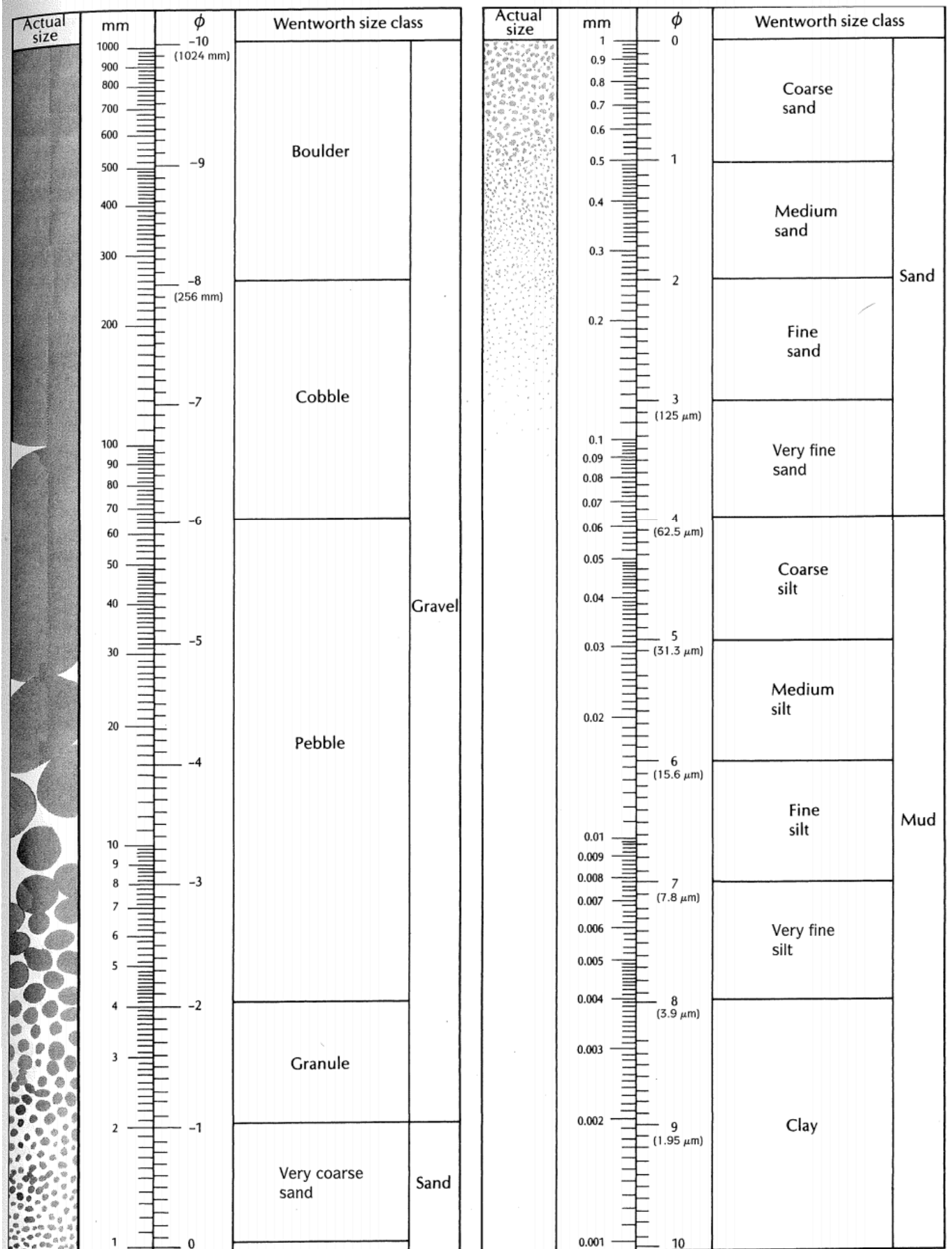
## Percentage Diagrams for Estimating Composition by Volume



Example hand-lens view of rocks with varying composition. To find weight percents, simply multiply each volume percent by the specific gravity of that mineral, and re-normalize. Compton, 1985



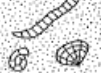
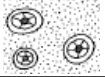
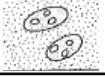
# Sedimentary Rocks



# Sedimentary Rocks: Carbonates

## Folk Classification Scheme for Carbonate Rocks

Folk's classification scheme is based upon the composition (and type of allochems) within a limestone. Figures from Prothero and Schwab, 2004

Principle Allochems in Limestone	Limestone Type			
	Cemented by Sparite		Cemented by Micritic Matrix	
Skeletal Grains (Bioclasts)	Biosparite		Biomicrite	
Ooids	Oosparite		Oomicrite	
Peloids	Pelsparite		Pelmicrite	
Intraclasts	Intrasparite		Intramicroite	
Limestone formed in place	Biolithite		Terrestrial Limestone	

## Dunham Classification Scheme for Carbonate Rocks

Dunham's classification scheme is based upon depositional textures within a limestone.

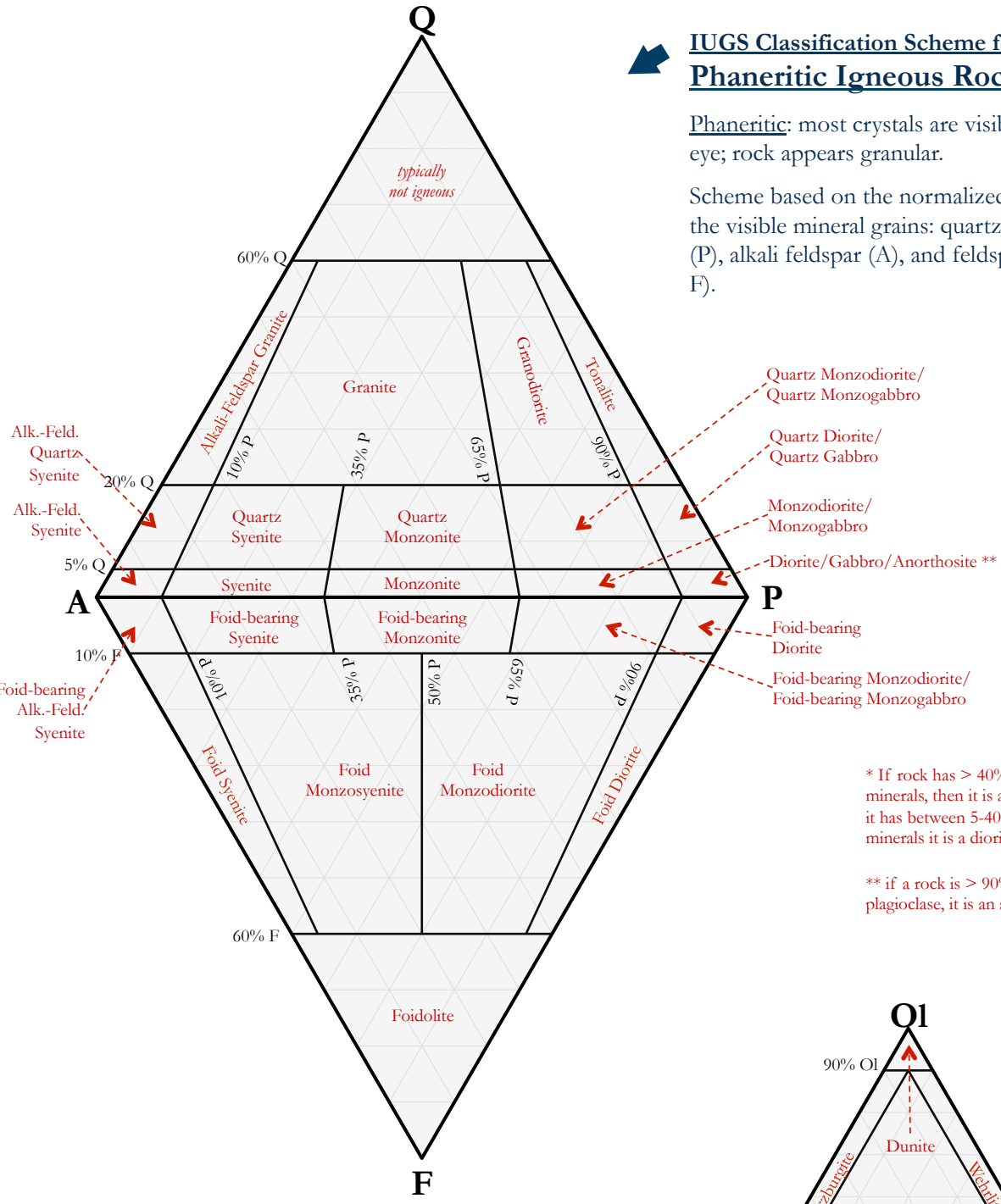
Allochthonous Limestone (original components not organically bound during deposition)				Autochthonous Limestone (original components organically bound during deposition; reef rocks)						
Of the allochems, less than 10% are larger than 2 mm			Of the allochems, greater than 10% are larger than 2 mm							
Contains carbonate mud		No mud		Matrix supported	Grain supported	Organisms acted as baffles	Organisms are encrusting and binding	Organisms building a rigid framework		
Grain supported		Grain supported								
Less than 10% grains	More than 10% grains									
Mudstone	Wackestone	Packstone	Grainstone	Floatstone	Rudstone	Bafflestone	Bindstone	Framestone		

# Igneous Rocks

## IUGS Classification Scheme for Phaneritic Igneous Rocks

Phaneritic: most crystals are visible to the naked eye; rock appears granular.

Scheme based on the normalized percentages of the visible mineral grains: quartz (Q), plagioclase (P), alkali feldspar (A), and feldspathoids (foids, F).



- Quartz Monzodiorite/  
Quartz Monzogabbro
- Quartz Diorite/  
Quartz Gabbro
- Monzodiorite/  
Monzogabbro
- Diorite/Gabbro/Anorthosite \*\*
- Foid-bearing  
Diorite
- Foid-bearing Monzodiorite/  
Foid-bearing Monzogabbro

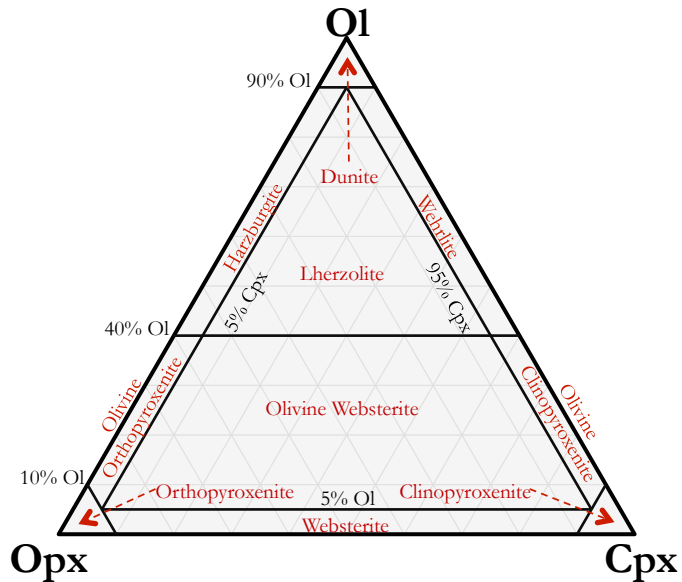
\* If rock has > 40% mafic minerals, then it is a gabbro. If it has between 5-40% mafic minerals it is a diorite.

\*\* if a rock is > 90% plagioclase, it is an anorthosite

## IUGS Classification Scheme for Phaneritic Ultramafic Igneous Rocks (1)

Ultramafic: more than 90% of the total minerals are mafic.

Scheme based on the normalized percentages of the visible minerals: olivine (Ol), orthopyroxene (Opx), and clinopyroxene (Cpx).



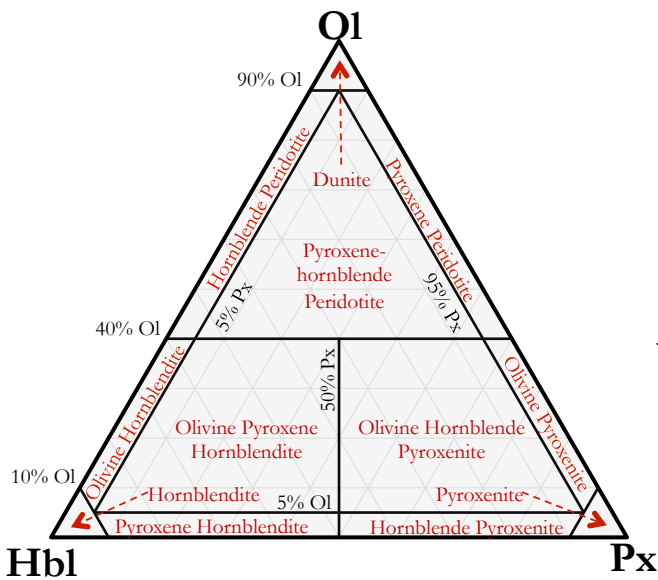
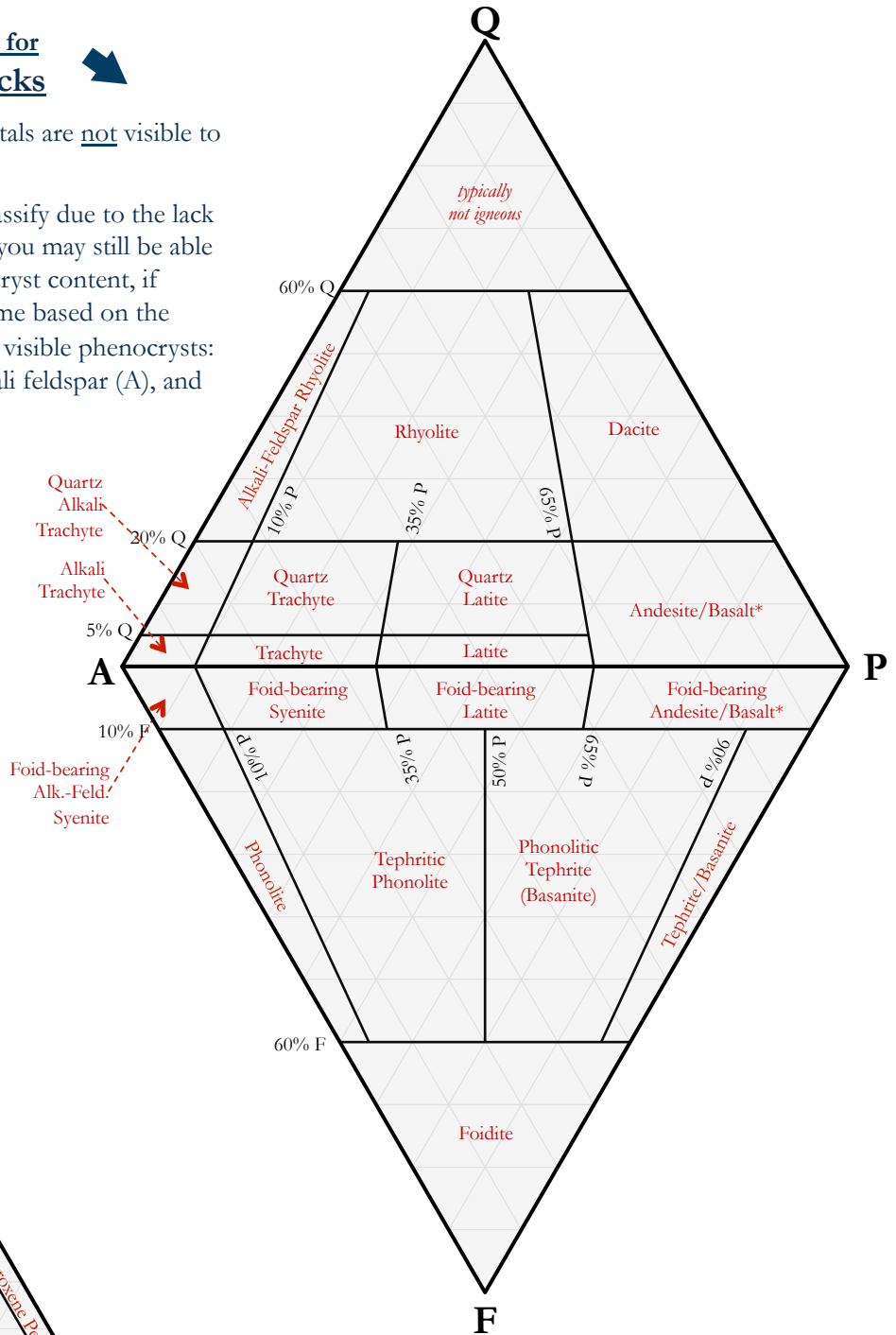
Opx Cpx

# Igneous Rocks

## IUGS Classification Scheme for Aphanitic Igneous Rocks

**Aphanitic:** the majority of crystals are not visible to the naked eye.

Aphanitic rocks are hard to classify due to the lack of visible minerals. However, you may still be able to identify them based on phenocryst content, if phenocrysts are present. Scheme based on the normalized percentages of the visible phenocrysts: quartz (Q), plagioclase (P), alkali feldspar (A), and feldspathoids (foids, F).



## IUGS Classification Scheme for Phaneritic Ultramafic Igneous Rocks (2)

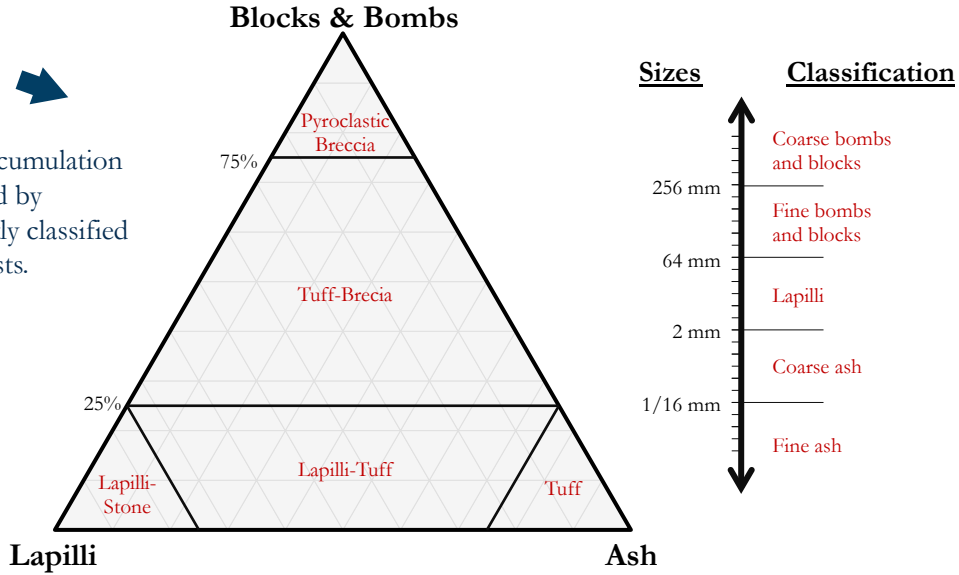
**Ultramafic:** more than 90% of the total minerals are mafic.

Scheme based on the normalized percentages of the visible minerals: olivine (Ol), hornblende (Hbl), and pyroxene (Px).

# Igneous Rocks

## Classification Scheme for Pyroclastic Igneous Rocks

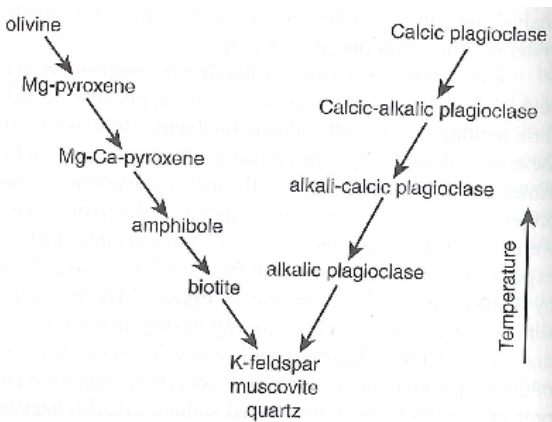
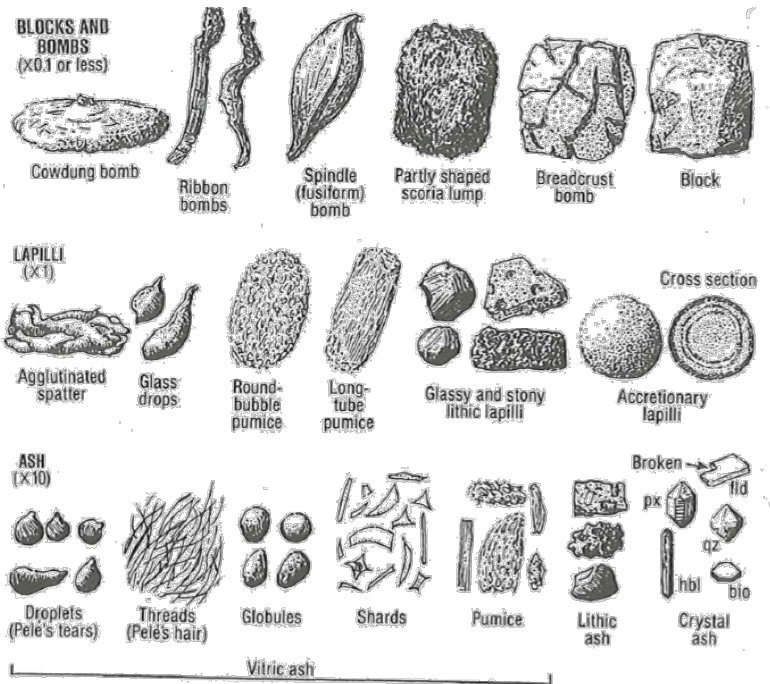
Pyroclastic rocks are formed via the accumulation of fragments of volcanic rock scattered by volcanic explosions. They are frequently classified based upon the size distribution of clasts.



## Types of Tephra (Pyroclasts)



In each row, the viscosity of the lava increases to the right. From Compton, 1985.



## Bowen's Reaction Series

From Winter, 2010.

# Metamorphic Rocks



## Classification Scheme for Metamorphic Rocks

Based upon texture and mineralogical composition.

Structure & Texture	Characteristic Properties	Characteristic Mineralogy	Rock Name	
Foliate (layered)	Increasing grain size, and degree of metamorphism ↓	Dull luster; very flat fracture surface; grains are too small to readily see; more dense than shale	No visible minerals	Slate
		Silky sheen; Crenulated (wavy) fracture structure; A few grains visible, but most are not	Development of mica and/or hornblende possible	Phyllite
		Sub-parallel orientations of individual mineral grains; wavy-sheet like fracture; often contains porphyroblasts; thinly foliated	Abundant feldspar; Quartz and mica are common; hornblende possible	Schist
		Sub-parallel, alternating bands or layers of light and dark material; coarsely foliated; blocky fracture	Abundant feldspars; Quartz, mica, and hornblende are common	Gneiss
Foliate (layered)	Interlocking crystals; effervesces in dilute HCl; softer than glass	Calcite	Marble	
	Nearly equigranular grains; fracture across grains (not around them); sub-vitreous appearance; smooth feel compared to sandstone	Quartz	Quartzite	



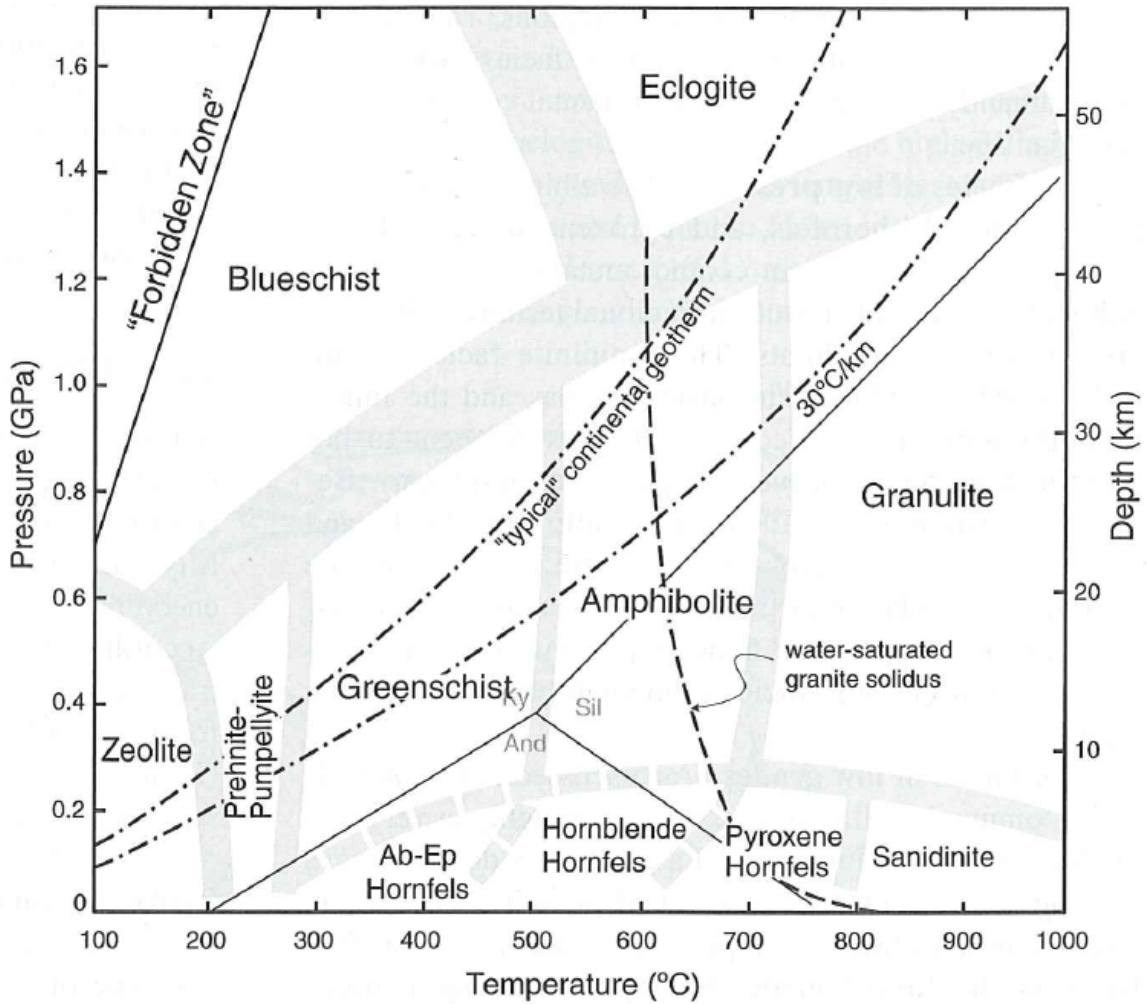
## Mineralogy for Metamorphic Rock Facies

Facies	Definitive Mineral Assemblages in Mafic Rocks
Zeolite	zeolites: especially laumontite, wairakite, analcime (in place of other Ca-Al silicates such as prehnite, pumpellyite and epidote)
Prehnite-Pumpellyite	prehnite + pumpellyite (+ chlorite + albite)
Greenschist	chlorite + albite + epidote (or zoisite) + actinolite ± quartz
Amphibolite	hornblende + plagioclase (oligoclase, andesine) ± garnet
Granulite	orthopyroxene + clinopyroxene + plagioclase ± garnet
Blueschist	glaucophane + lawsonite or epidote/zoisite (± albite ± chlorite ± garnet)
Eclogite	pyralspite garnet + omphacitic pyroxene (± kyanite ± quartz), no plagioclase
Contact Facies	mineral assemblages in mafic rocks of the facies of contact metamorphism do not differ substantially from those of the corresponding regional facies at higher pressure

# Metamorphic Rocks

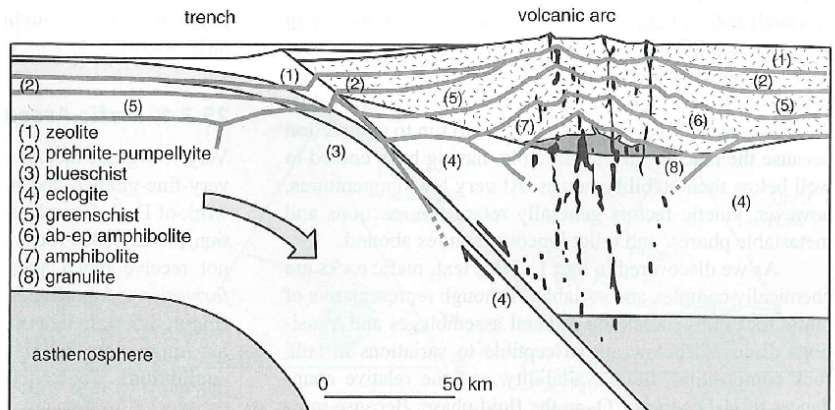
## Metamorphic Rock Facies, P vs. T diagram

From Winter, 2010



## Schematic of Island Arc, and the origins of Metamorphic Facies

A schematic cross section of an island arc. Light gray lines are isotherms. From Winter, 2010

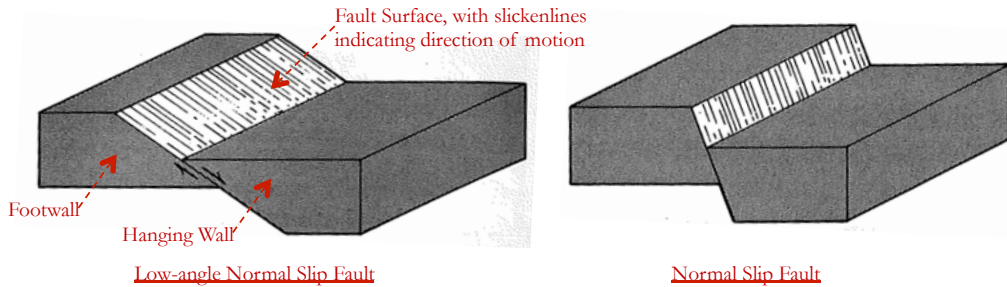


# Structural Geology: Normal Faults

## Normal Faults



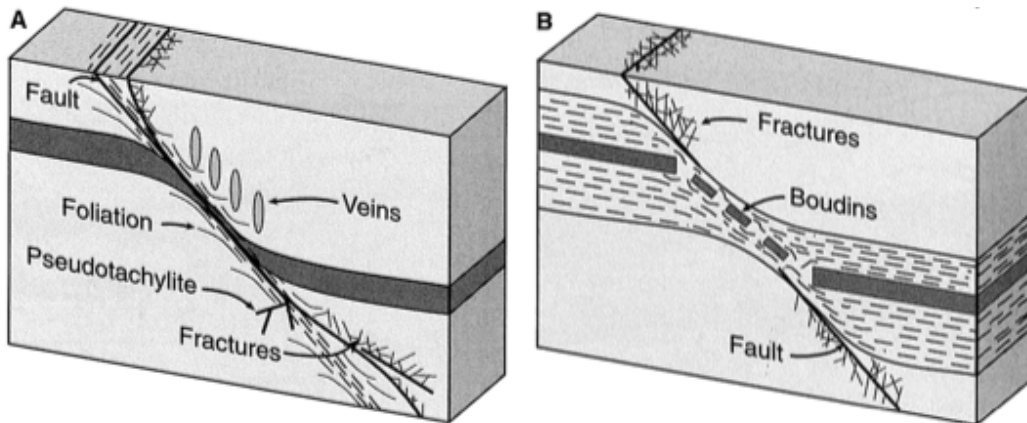
In normal faults, the footwall goes up with respect to the hanging wall. Normal faults are indicative of extension. Figures from Davis & Reynolds, 1996.



## Effects of Brittle or Ductile Shear in Normal Faults



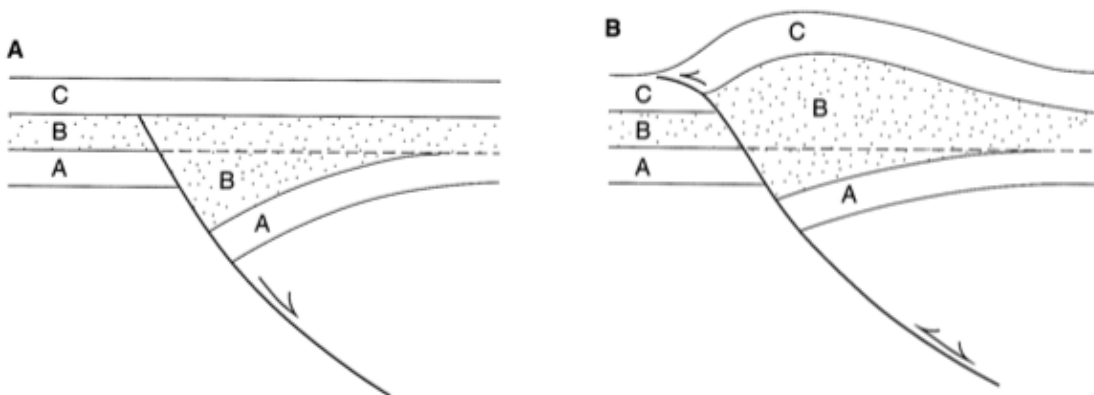
The block diagrams below illustrate the effects of changing the nature of deformation, between brittle deformation (which results in clear fault planes, fractures and fault rocks), ductile deformation (which causes deformation over a larger shear zone). Often, strata of different rheologies will behave differently, as is shown in the figure at right. The dashed layer was weak and deformed ductilely, while the middle grey layer was rigid and formed boudins. Figures from Davis & Reynolds, 1996.



## Inversion Tectonics



If the regional stresses change, previously inactive faults can reactivate, and change their sense of motion. In the figure at left, layer-A was formed prior to the formation of a normal fault. Layer-B and layer-C were deposited after the formation, and shut down of the fault. In the figure at the right, the fault has reactivated, though as a reverse fault. The resulting stratigraphic sequence is a combination of effects one would expect from both normal and reverse faults. Figures from Davis & Reynolds, 1996.

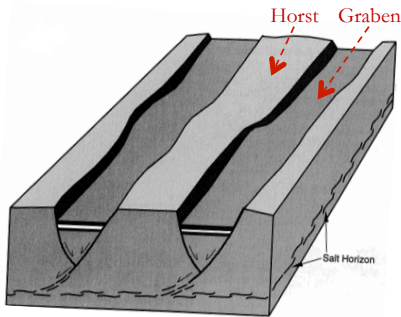
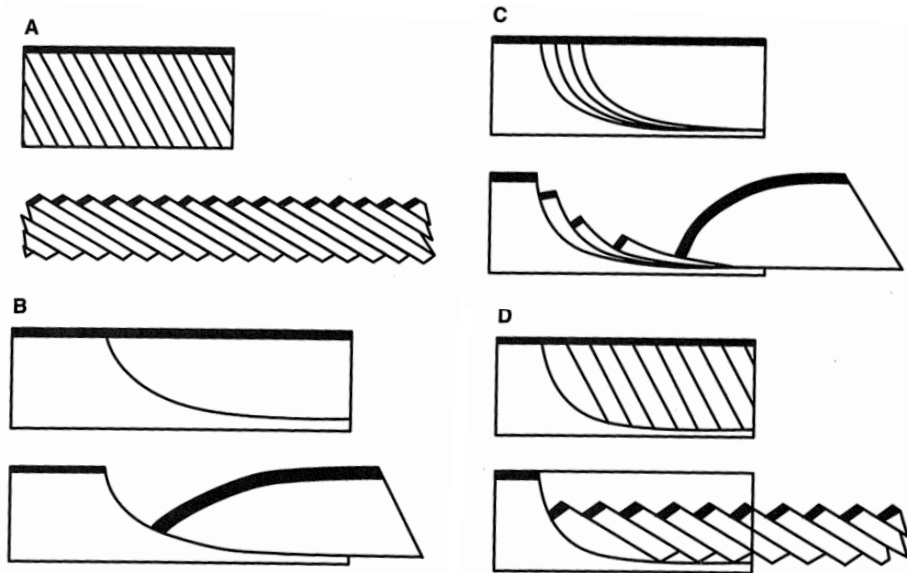


# Structural Geology: Normal Faults

## Normal Faults Geometries



Various normal fault geometries are possible. They all allow for lithospheric extension. (A) Domino style faulting. (B) Listric normal faulting with reverse drag. (C) Imbricate listric normal faulting. Note that listric faulting can cause extreme rotation of faulted blocks. (D) Listric normal faulting bounding a family of planar normal faults. Figures from Davis & Reynolds, 1996.



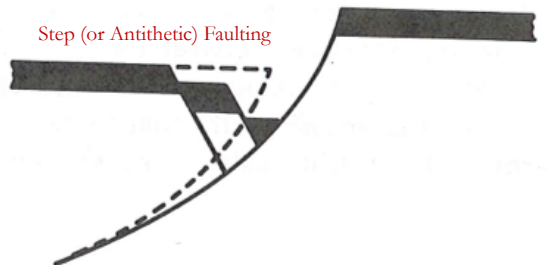
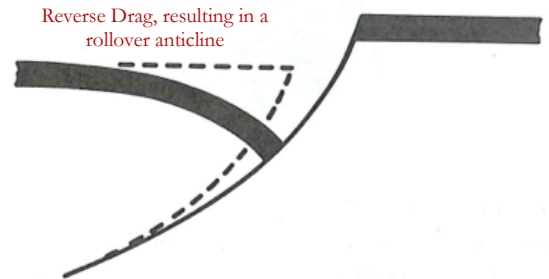
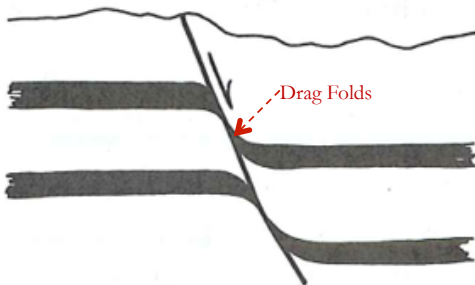
## Horsts & Grabens

Classical formation describing fault-bounded uplifted (horsts) and down-dropped blocks (grabens). Figures from Davis & Reynolds, 1996.

## Drag Folds, Reverse Drag, and Step Faulting



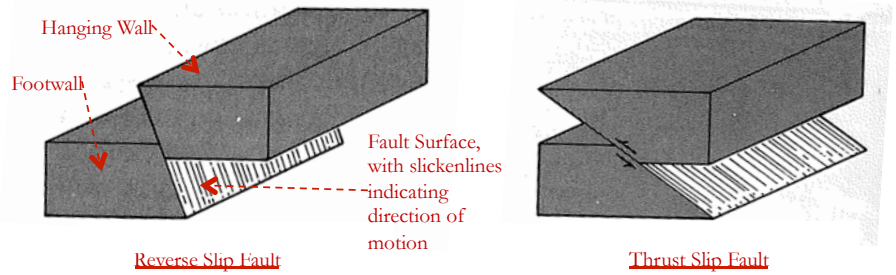
Faulting does not always produce clean displacement along the fault surface. Fault blocks are frequently folded or fractured, and the nature of these deformations are non-trivial. Figures from Davis & Reynolds, 1996.



# Structural Geology: Reverse & Thrust Faults

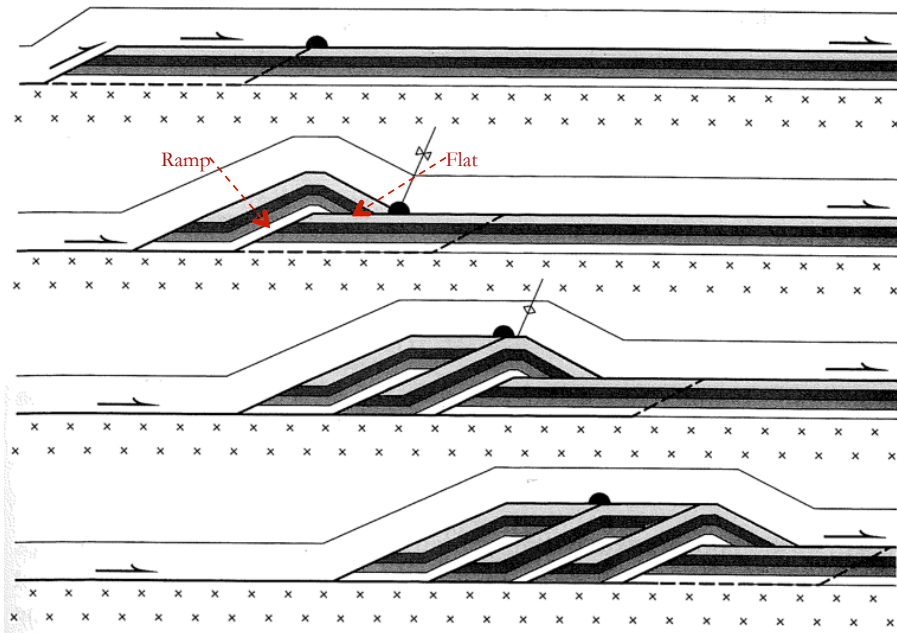
## Reverse Faults ➡

In reverse faults, the footwall goes down with respect to the hanging wall. Normal faults are indicative of compression. Thrust faults are reverse faults with fault dips <45 degrees. Figures from Davis & Reynolds, 1996.



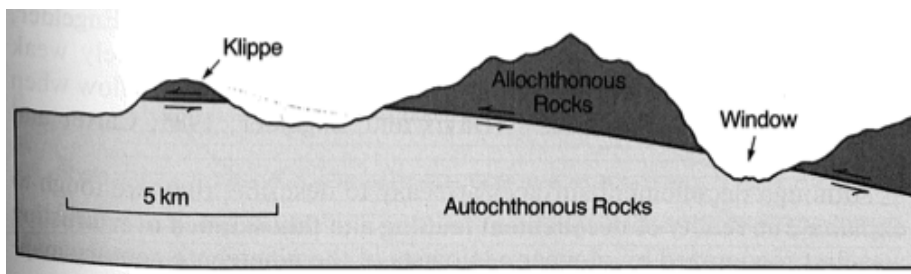
## “Ramp-Flat” Geometry of Typical Thrust Fault Systems ↓

In a regional thrust, faulted blocks are “thrust” on top of younger strata. The exact geometry of these thrust systems can vary significantly. Figures from Davis & Reynolds, 1996.

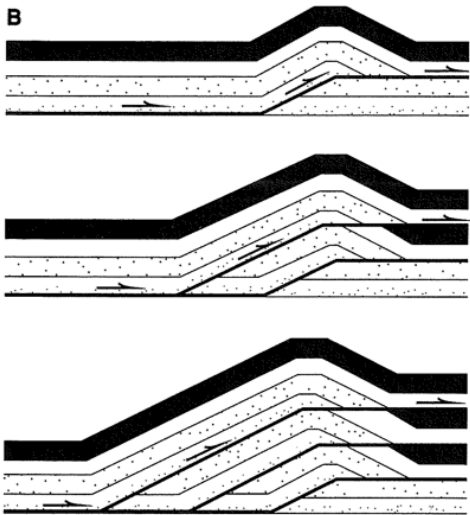


## Klippe & Windows ↓

Thrust faults move large blocks of non-indigenous rock (referred to as “allochthonous” rock) over emplaced rock (referred to as “autochthonous” rock). If the overlying allochthonous rock is eroded, it can create windows into the lower underlying autochthonous rock. Erosion can also create islands of isolated allochthonous rock, called klippe. Figures from Davis & Reynolds, 1996.



# Structural Geology: Reverse & Thrust Faults

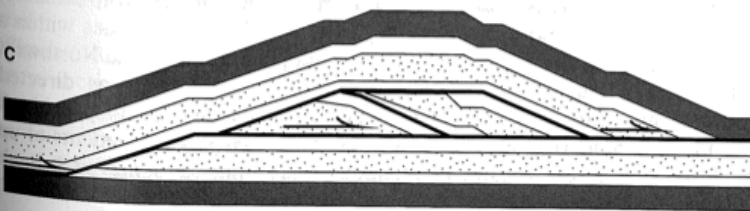
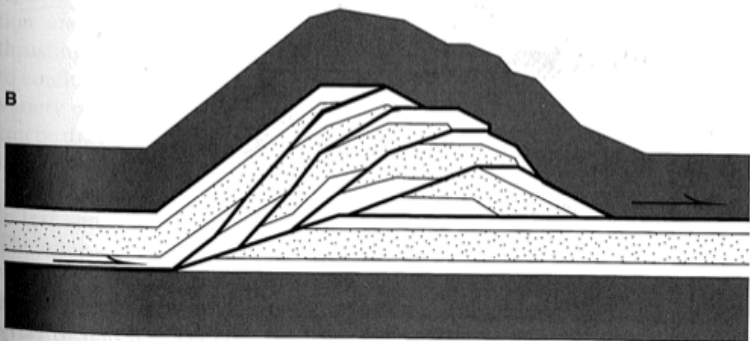
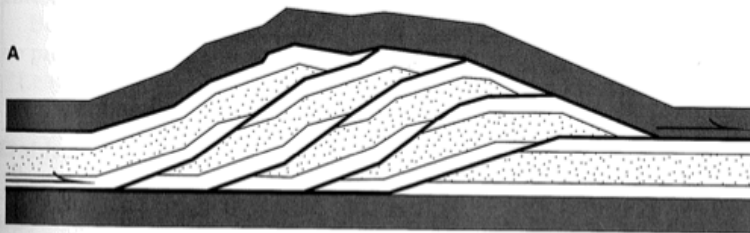
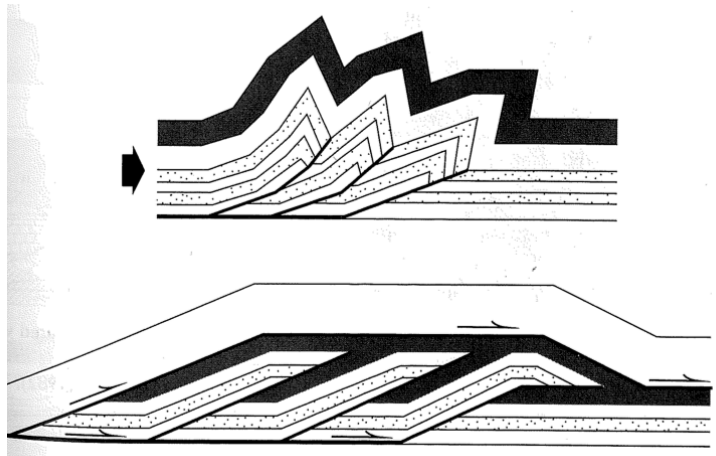


## ← Out-of-Sequence Thrust Fault System

Unlike “in-sequence” thrust fault systems (as shown on the previous page, the “roof” of the thrust block in an out-of-sequence system becomes the “flat” for subsequent fault blocks. Figures from Davis & Reynolds, 1996.

## Imbricate Fans vs. Duplexes ↓

Two thrust fault geometries: imbricate fans (top) and duplexes (bottom). Figures from Davis & Reynolds, 1996.



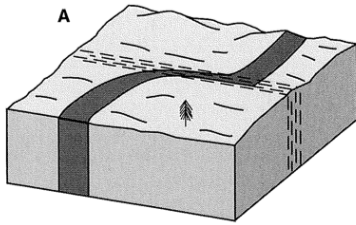
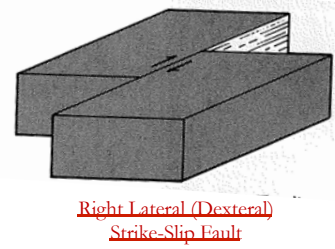
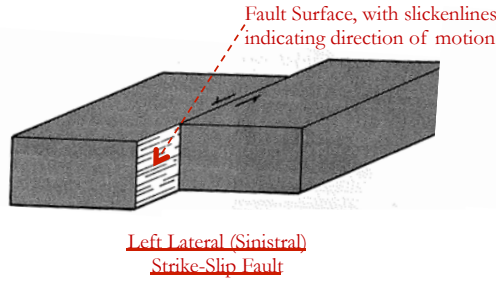
## ← Forms of Duplexes

The exact form of a duplex or imbricate fan depends on the spacing of ramps and the amount of slip. (A) A normal duplex develops when slice length exceeds the fault slip. (B) An antiformal duplex develops when slice length and fault slip are effectively equal. (C) A forward-dipping duplex develops when the fault slip is greater than the slice length. Figures from Davis & Reynolds, 1996.

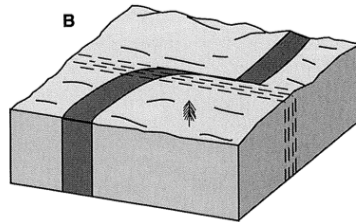
# Structural Geology: Strike-Slip or Transform Faults

## Strike-Slip Faults ➡

In reverse faults, the footwall goes down with respect to the hanging wall. Normal faults are indicative of compression. Thrust faults are reverse faults with fault dips <45 degrees. Figures from Davis & Reynolds, 1996.



Continuous Shear Zone



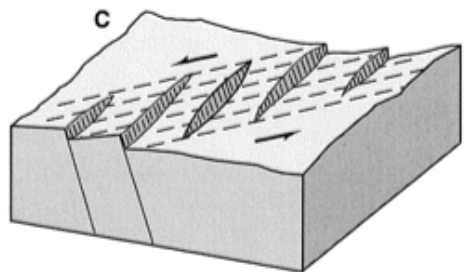
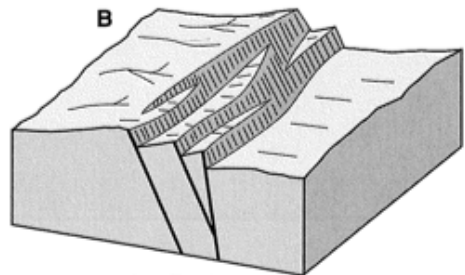
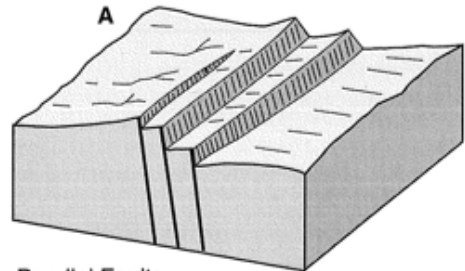
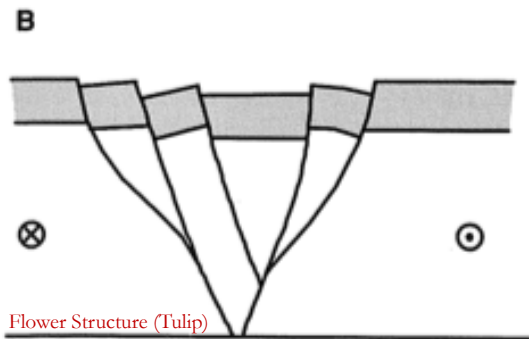
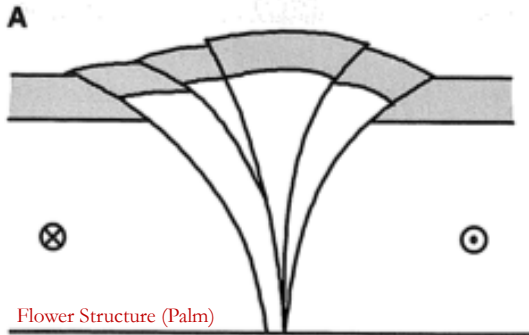
Discontinuous Shear Zone

## ➡ Ductile Shear Zones

Shear in a strike-slip fault is not always located in a single plane. Sometimes, shear takes place over an extended region. Figures from Davis & Reynolds, 1996.

## Brittle Shear Zones ➡

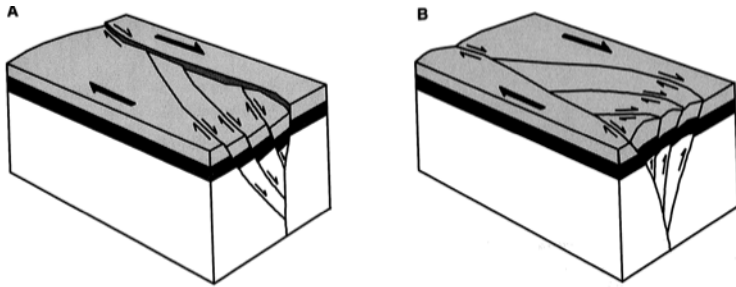
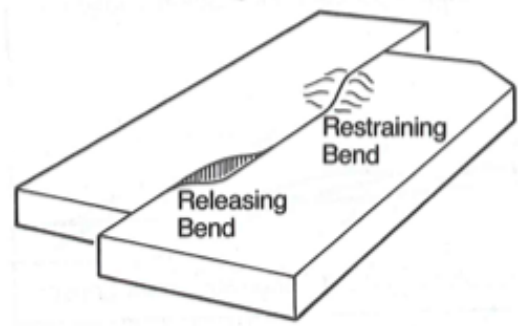
Figures from Davis & Reynolds, 1996.



# Structural Geology: Strike-Slip or Transform Faults

## Bends in Strike-Slip Faults →

Strike-slip faults along irregularly curved faults creates localized regions of extension and compression. Figures from Davis & Reynolds, 1996.

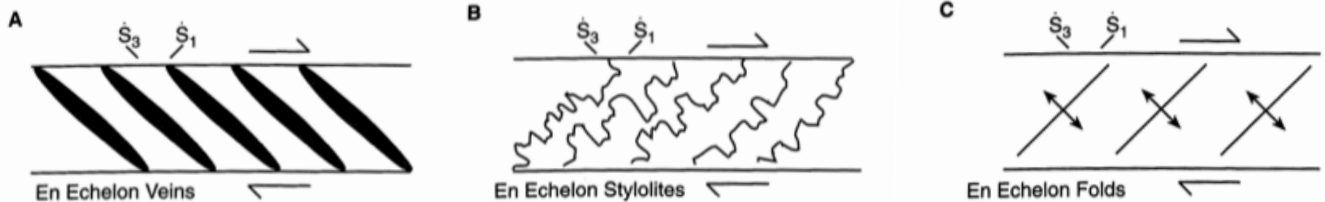


## ← Strike-Slip Duplexes

(A) Extensional duplexes can form at releasing bends. (B) Compressional duplexes can form at restraining bends. Figures from Davis & Reynolds, 1996.

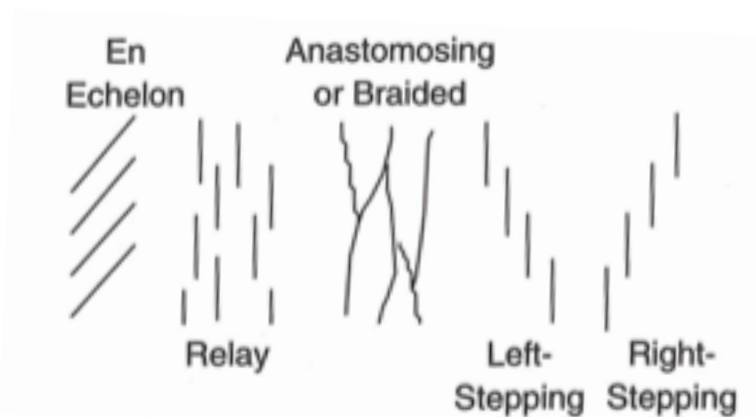
## Slip Indicators in Strike-Slip Systems ↓

In strike-slip systems, the maximum ( $S_1$ ) and minimum compressional stresses ( $S_3$ ) are at an angle with respect to the sense of shear. This can lead to the formation of both large scale folds and faults, or small scale fractures or veins, which are indicative to the sense of motion. Figures from Davis & Reynolds, 1996.



## Even more Geometric Arrangements of Strike-Slip Faults →

Figures from Davis & Reynolds, 1996.

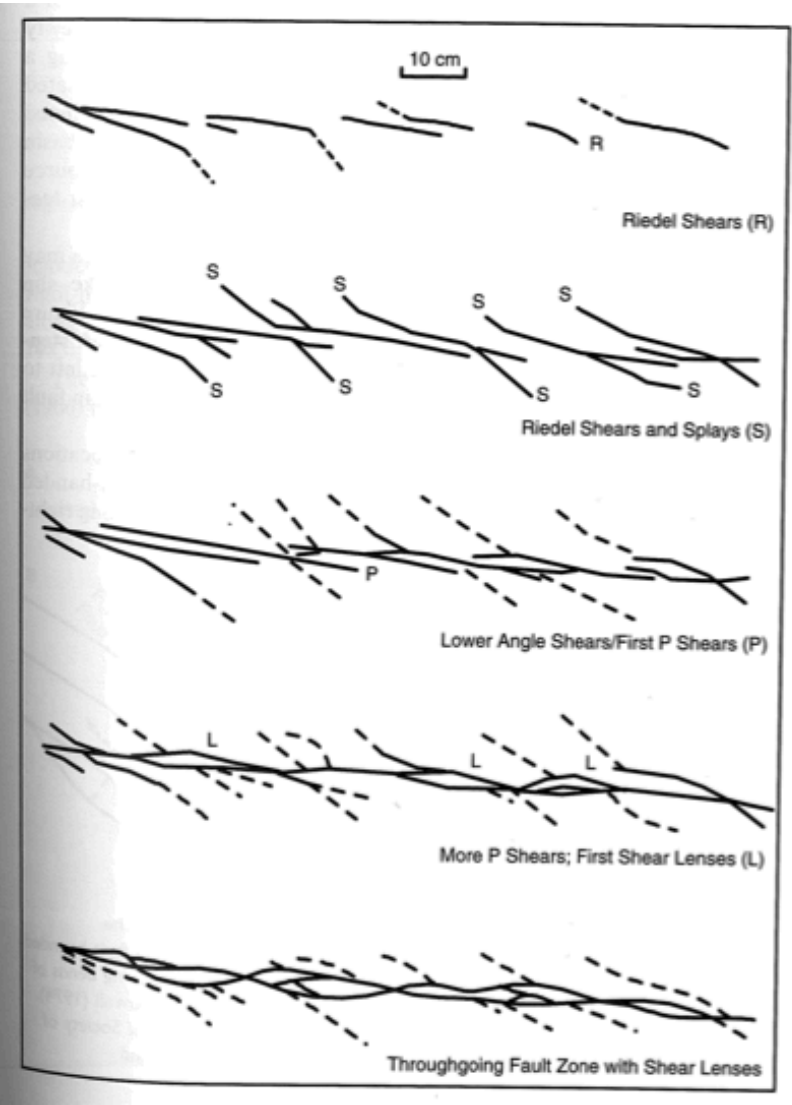
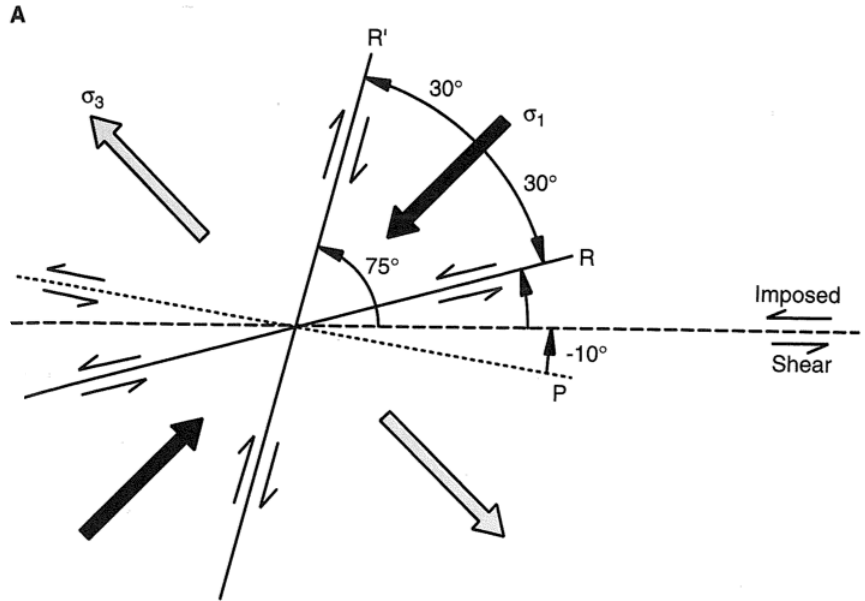


# Structural Geology: Strike-Slip or Transform Faults

## Riedel Shears



When under compression, rocks tend to form fail with faults forming  $30^\circ$  from the primary compressional stress. In a strike-slip fault, the primary compressional stress ( $\sigma_1$ ) is  $45^\circ$  away from the plane of strike-slip shearing. The combination of these two facts results in fractures at interesting angles with respect to the motion of shear. These are called Riedel shears. The figure below shows a left-handed strike-slip zone. Figures from Davis & Reynolds, 1996.

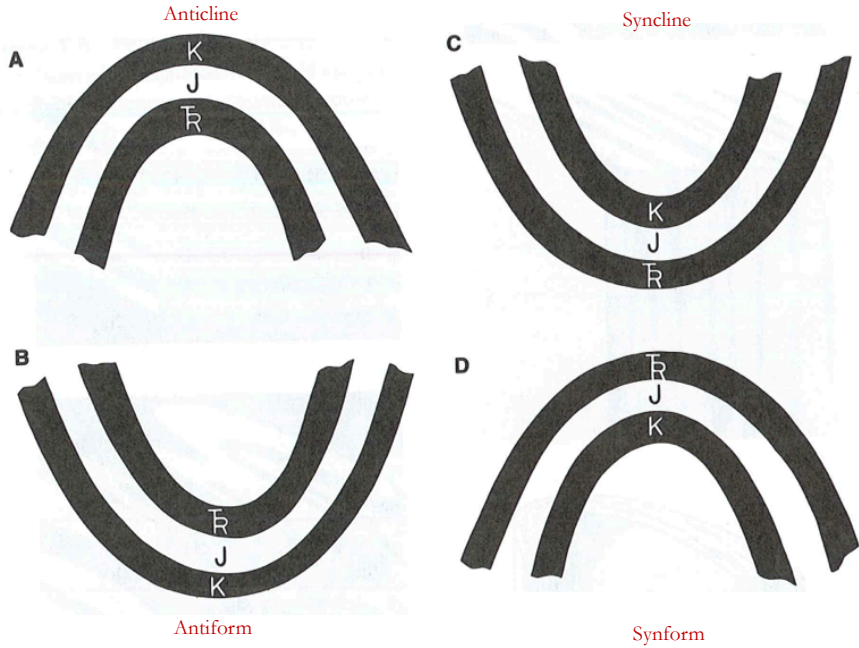


The figure at left illustrate the formation sequence of Riedel shears and other splays and shears in a right-handed strike-slip zone. Figures from Davis & Reynolds, 1996.

# Structural Geology: Folds

## Anticlines & Antiforms, and Synclines & Synforms

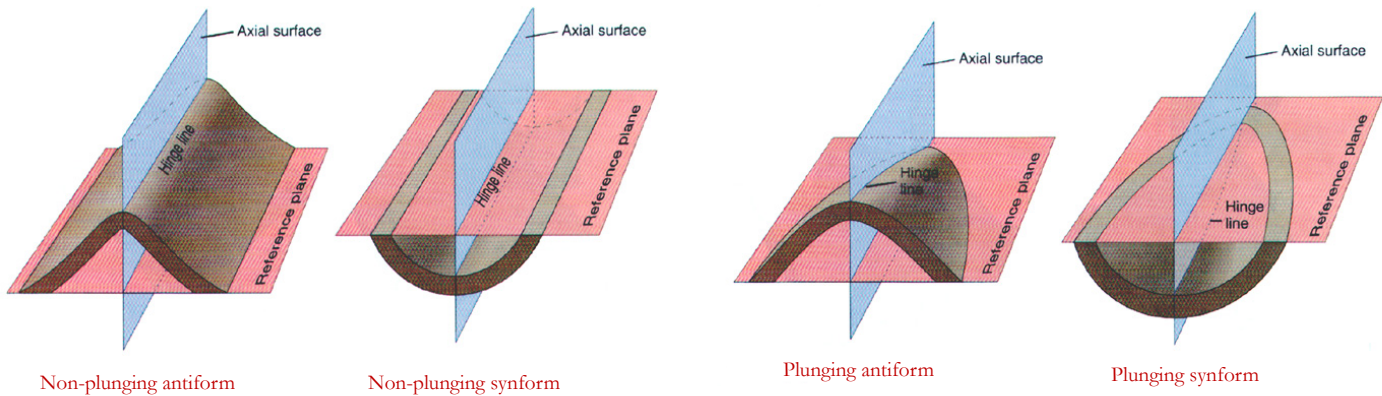
Antiforms are concave-down folds, while Synforms are concave-up folds. Anticlines are antiforms where we know that the younger strata lie on top of older strata. Similarly, Synclines are antiforms where younger strata lie on top of older strata. Figures from Davis & Reynolds, 1996.



## Plunging Folds



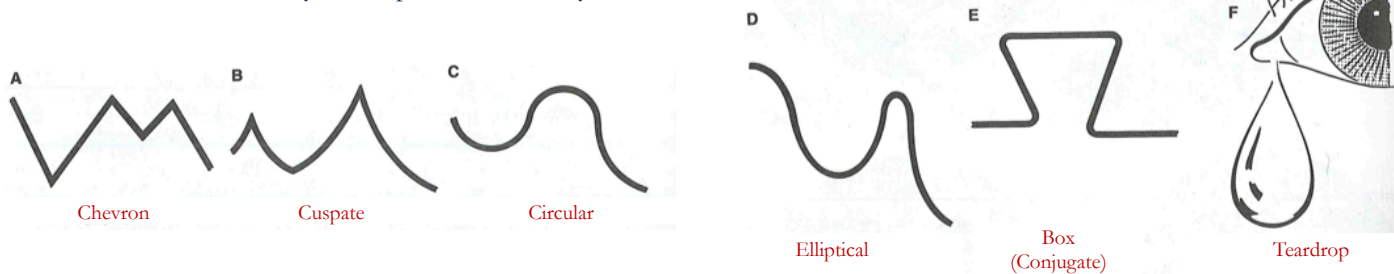
Folds (defined by hinge lines and axial surfaces) are not necessarily perpendicular to the Earth's surface. They can be dipping into or out of the surface. This can create interesting patterns of exposed surface rock, or even topography. Figures from Jones, 2001.



## Fold Shapes



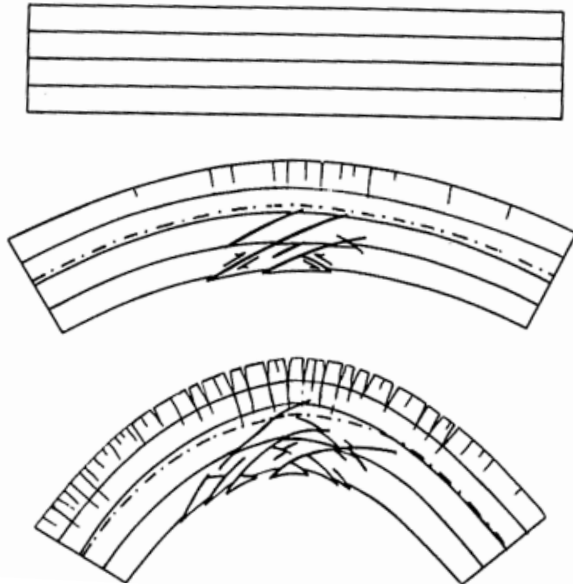
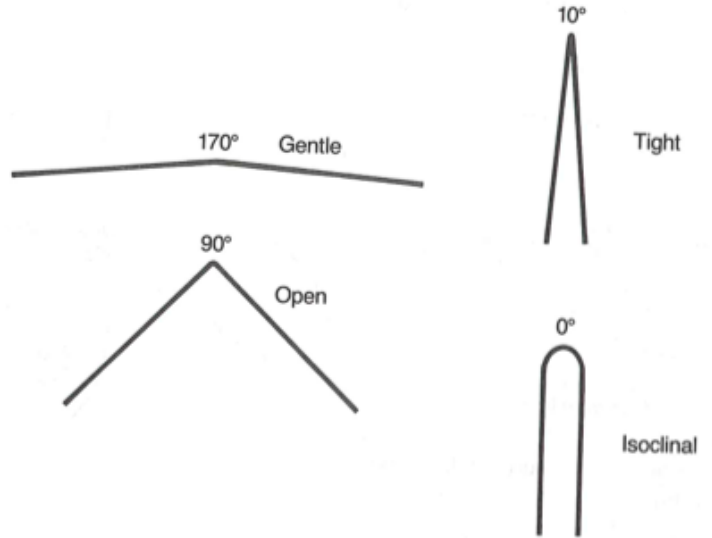
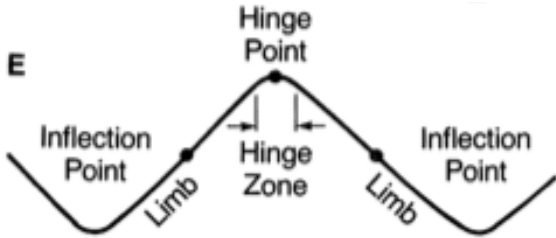
Folds can come in a variety of shapes. Davis & Reynolds, 1996.



# Structural Geology: Folds

## Fold Tightness

Fold tightness is based upon the size of the inter-limb angle. Figures from Davis & Reynolds, 1996.

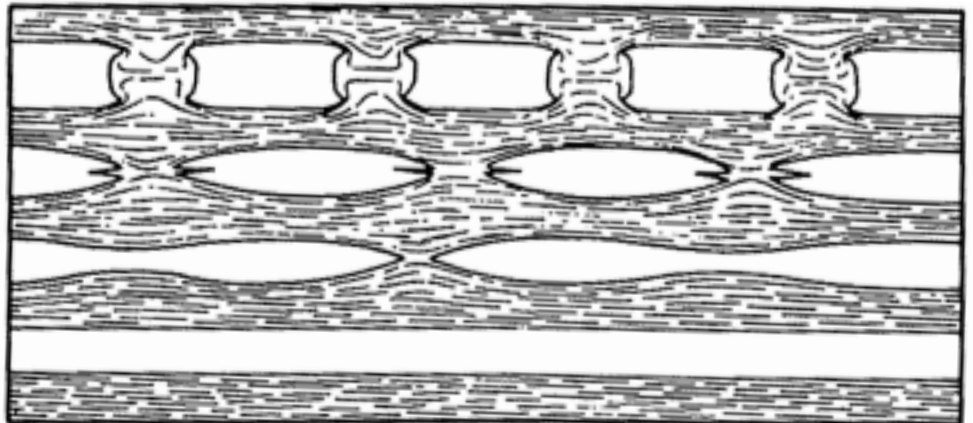


## Minor Structures in Folds

When folding layers of strata, layer-parallel stretching occurs in the outer arc of a folded layer, while layer-parallel shortening occurs in the inner arc. Figures from Davis & Reynolds, 1996.

## Boudins

Layer-parallel stretching can pinch off layers of strata, depending on the ductility contrast between layers. This can result in pinch-and-swell structures or boudins (where the pinching completely pinches off portions of a given strata). Figures from Davis & Reynolds, 1996.



# Geologic Map Symbols

1		Contact, showing dip where trace is horizontal, and strike and dip where trace is inclined	42		Steeply plunging monocline or flexure, showing trace in horizontal section and plunge of hinges
2		Contact, located approximately (give limits)	43		Plunge of hinge lines of small folds, showing shapes in horizontal section
3		Contact, located very approximately, or conjectural	44		Strike and dip of beds or bedding
4		Contact, concealed beneath mapped units	45		Strike and dip of overturned beds
5		Contact, gradational (optional symbols)	46		Strike and dip of beds where stratigraphic tops are known from primary features
6		Fault, nonspecific, well located (optional symbols)	47		Strike and dip of vertical beds or bedding (dot is on side known to be stratigraphically the top)
7		Fault, nonspecific, located approximately	48		Horizontal beds or bedding (as above)
8		Fault, nonspecific, assumed (existence uncertain)	49		Approximate (typically estimated) strike and dip of beds
9		Fault, concealed beneath mapped units	50		Strike of beds exact but dip approximate
10		Fault, high-angle, showing dip (left) and approximate dips	51		Trace of single bed, showing dip where trace is horizontal and where it is inclined
11		Fault, low-angle, showing approximate dip and strike and dip	52		Strike and dip of foliation (optional symbols)
12		Fault, high-angle normal (D or ball and bar on downthrown side)	53		Strike of vertical foliation
13		Fault, reverse (R on upthrown side)	54		Horizontal foliation
14		Fault, high-angle strike-slip (example is left lateral)	55		Strike and dip of bedding and parallel foliation
15		Fault, thrust (T on overthrust side)	56		Strike and dip of joints (left) and dikes (optional symbols)
16		Fault, low-angle normal or detachment (D on downthrown side)	57		Vertical joints (left) and dikes
17		Fault, low-angle strike-slip (example is right lateral)	58		Horizontal joints (left) and dikes
18		Fault, low-angle, overturned (teeth in direction of dip)	59		Strike and dip of veins (optional symbols)
19		Optional sets of symbols for different age-groups of faults	60		Vertical veins
20		Fault zone or shear zone, width to scale (dip and other accessory symbols may be added)	61		Horizontal veins
21		Faults with arrows showing plunge of rolls, grooves or slickensides	62		Bearing (trend) and plunge of lineation
22		Fault showing bearing and plunge of net slip	63		Vertical and horizontal lineations
23		Point of inflection (bar) on a high-angle fault	64		Bearing and plunge of cleavage-bedding intersection
24		Points of inflection on a strike-slip fault passing into a thrust	65		Bearing and plunge of cleavage-cleavage intersections
25		Fault intruded by a dike	66		Bearings of pebble, mineral, etc. lineations
26		Faults associated with veins	67		Bearing of lineations in plane of foliation
27		Anticline, showing trace and plunge of hinge or crest line (specify)	68		Horizontal lineation in plane of foliation
28		Syncline (as above), showing dip of axial surface or trough surface	69		Vertical lineation in plane of vertical foliation
29		Folds (as above), located approximately	70		Bearing of current from primary features; from upper left: general; from cross-bedding; from flute casts; from imbrication
30		Folds, conjectural	71		Bearing of wind direction from dune forms (left) and cross-bedding
31		Folds beneath mapped units	72		Bearing of ice flow from striations (left) and orientation of striations
32		Asymmetric folds with steeper limbs dipping north (optional symbols)	73		Bearing of ice flow from drumlins
33		Anticline (top) and syncline, overturned	74		Bearing of ice flow from crag and tail forms
34		Antiformal (inverted) syncline	75		Spring
35		Synformal (inverted) anticline	76		Thermal spring
36		Antiform (top) and synform (stratigraphic sequence unknown)	77		Mineral spring
37		Separate dome (left) and basin	78		Asphaltic deposit
38		Culmination (left) and depression	79		Bituminous deposit
40		Vertically plunging anticline and syncline	80		Sand, gravel, clay, or placer pit
41		Monocline, south-facing, showing traces of axial surfaces			

# Geologic Map Symbols

81		Mine, quarry, or open pit
82		Shafts: vertical, inclined, and abandoned
83		Adit, open (left) and inaccessible
84		Trench (left) and prospect
85		Water wells: flowing, nonflowing, and dry
86		Oil well (left) and gas well
87		Well drilled for oil or gas, dry
88		Wells with shows of oil (left) and gas
89		Oil or gas well, abandoned (left) and shut in
90		Drilling well or well location
91		Glory hole, open pit, or quarry, to scale
92		Dump or fill, to scale

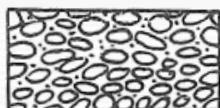
# Fossil and Structural Symbols for Stratigraphic Columns

	Algae		Tree trunk fallen		Foraminifers, general		Scour casts
	Algal mats		Trilobites		Foraminifers, large		Convolution
	Ammonites		Vertebrates		Fossils		Slumped beds
	Belemnites		Wood		Fossils abundant		Paleosol
	Brachiopods		Beds distinct		Fossils sparse		Mud cracks
	Bryozoans		Beds obscure		Gastropods		Salt molds
	Corals, solitary		Unbedded		Graptolites		Burrows
	Corals, colonial		Graded beds		Leaves		Pellets
	Crinoids		Planar cross-bedding		Ostracodes		Oolites
	Echinoderms		Trough cross-bedding		Pelecypods		Pisolites
	Echinoids		Ripple structures		Root molds		Intraclasts
	Fish bones		Cut and fill		Spicules		Stylolite
	Fish scales		Load casts		Stromatolites		Concretion
					Tree trunk in place		Calcitic concretion

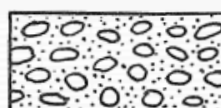
# Lithologic Patterns for Stratigraphic Columns & Cross Sections



1. Breccia



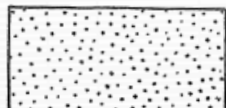
2. Clast-supported conglomerate



3. Matrix-supported conglomerate



4. Conglomeratic sandstone



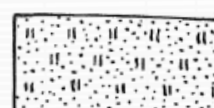
5. Coarse sandstone



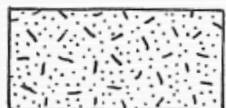
6. Fine sandstone



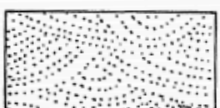
7. Feldspathic sandstone



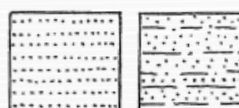
8. Tuffaceous sandstone



9. Graywacke



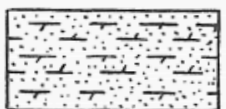
10. Cross-bedded sandstone



11. Bedded sandstone



12. Calcite-cemented sandstone



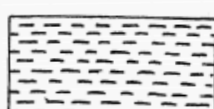
13. Dolomite-cemented sandstone



14. Silty sandstone



15. Siltstone



16. Mudstone



17. Shale



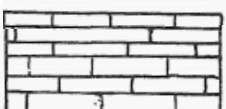
18. Coal bed with carbonaceous shale



19. Pebbly mudstone



20. Calcareous shale



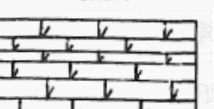
21. Limestone



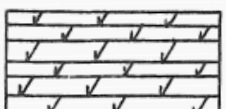
22. Cross-bedded limestone



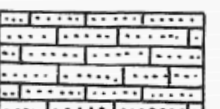
23. Dolomite (dolostone)



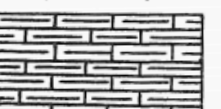
24. Dolomitic limestone



25. Calcitic dolomite



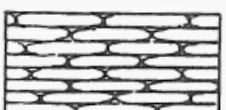
26. Sandy limestone



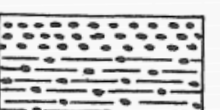
27. Clayey limestone



28. Cherty limestone



29. Bedded chert



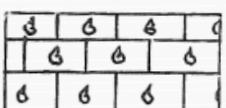
30. Phosphorite, phosphatic shale



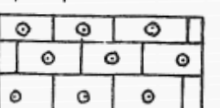
31. Chalk



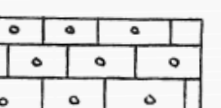
32. Marl



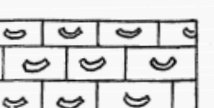
33. Fossiliferous limestone



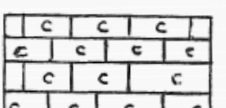
34. Oolitic limestone



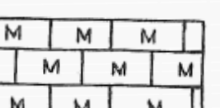
35. Pelletal limestone



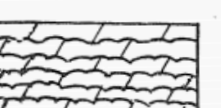
36. Intraclastic limestone



37. Crystalline limestone



38. Micritic limestone



39. Algal dolomite



40. Limestone conglomerate

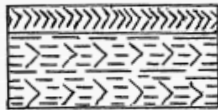
# Lithologic Patterns for Stratigraphic Columns & Cross Sections



41. Limestone breccia



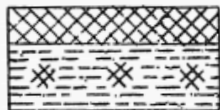
42. Algal dolomite breccia



43. Gypsum bed, gypsumiferous shale



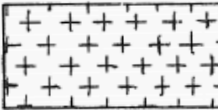
44. Anhydrite, anhydritic dolomite



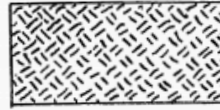
45. Rock salt, salty mudstone



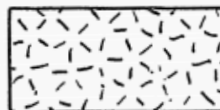
46. Peridotite



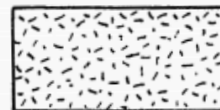
47. Gabbro



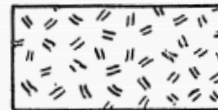
48. Mafic plutonic rock



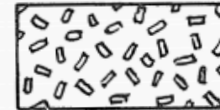
49. Coarse granitic rock



50. Fine granitic rock



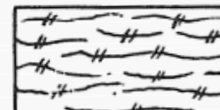
51. Porphyritic plutonic rock



52. Porphyritic plutonic rock



53. Mafic lava



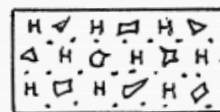
54. Silicic lava



55. Intrusive volcanic rocks



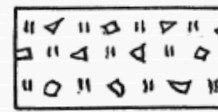
56. Pillow lava



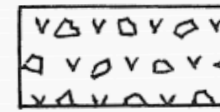
57. Hyaloclastite



58. Tuff



59. Tuff-breccia



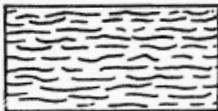
60. Volcanic breccia



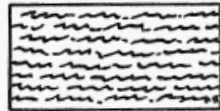
61. Massive serpentinite



62. Foliated serpentinite



63. Schist



64. Crenulated schist



65. Folded schist



66. Semischistose sandstone



67. Semischistose limestone



68. Semischistose gabbro



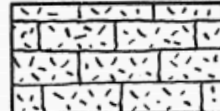
69. Greenstone



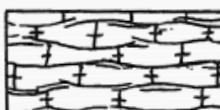
70. Silicic gneiss



71. Mafic gneiss



72. Marble



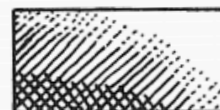
73. Foliated marble



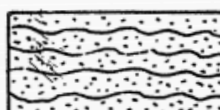
74. Foliated calc-silicate rock



75. Massive skarn



76. Alteration zones



77. Quartzite



78. Quartzite

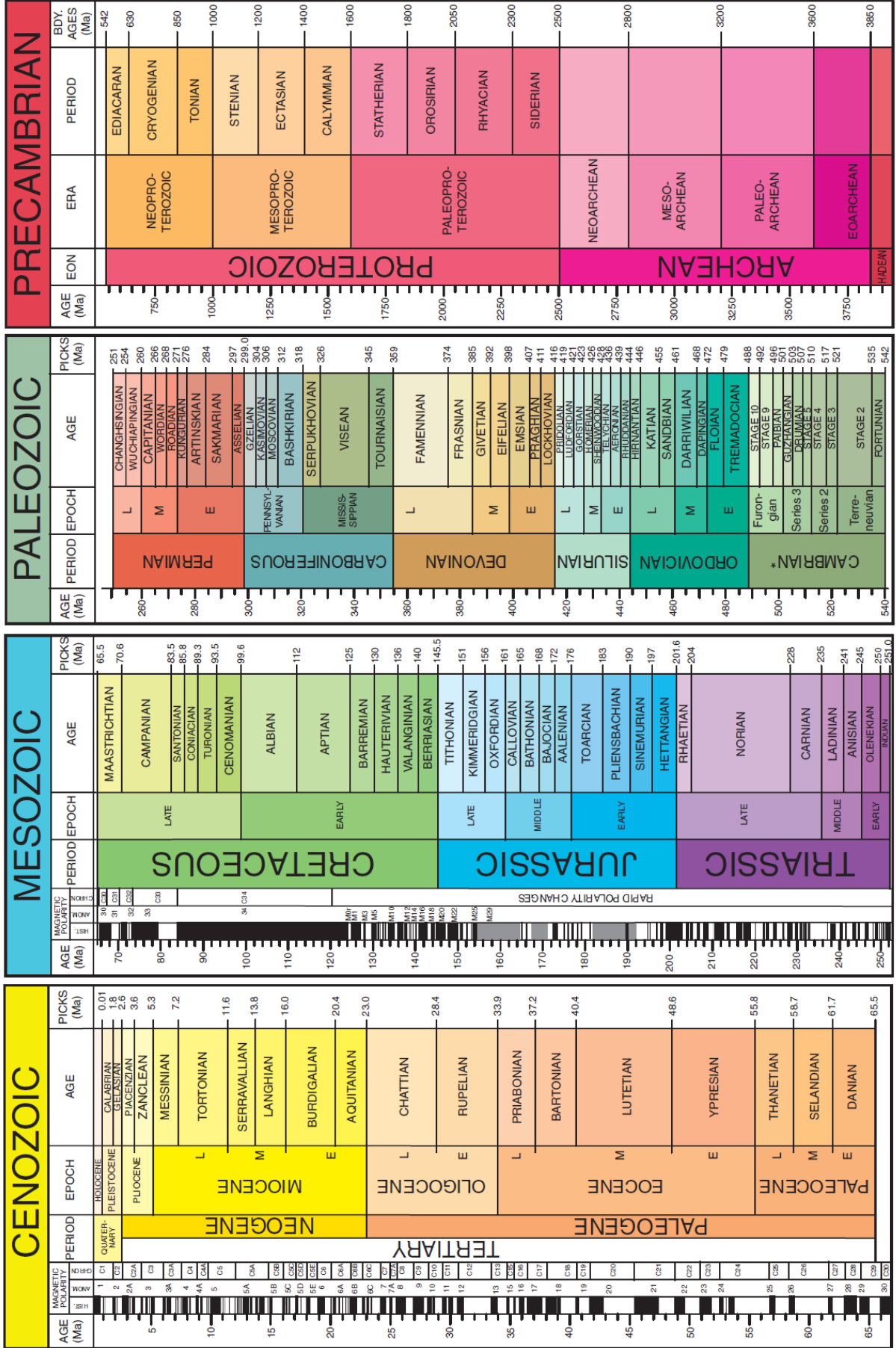


79. Silicic migmatite



80. Mafic migmatite

# Geologic Timescale

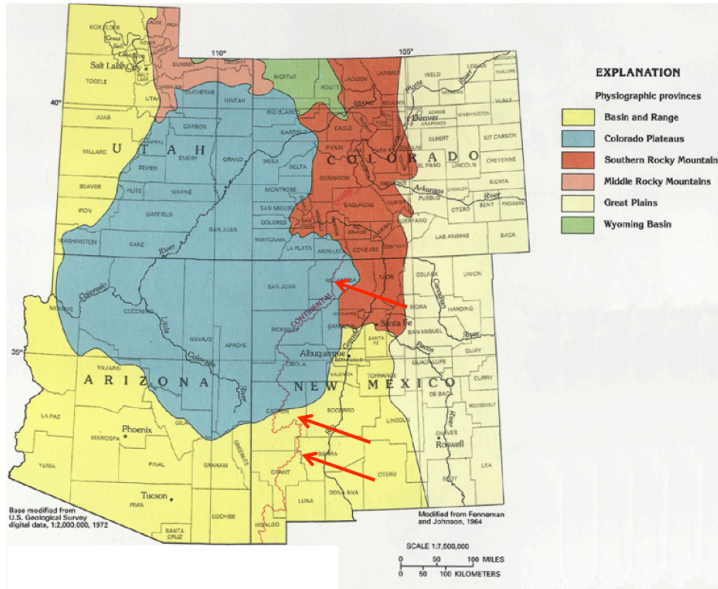


# Physiographic Provinces & Plateau Uplift & Other Miscellaneous stuff

## Shane Byrne

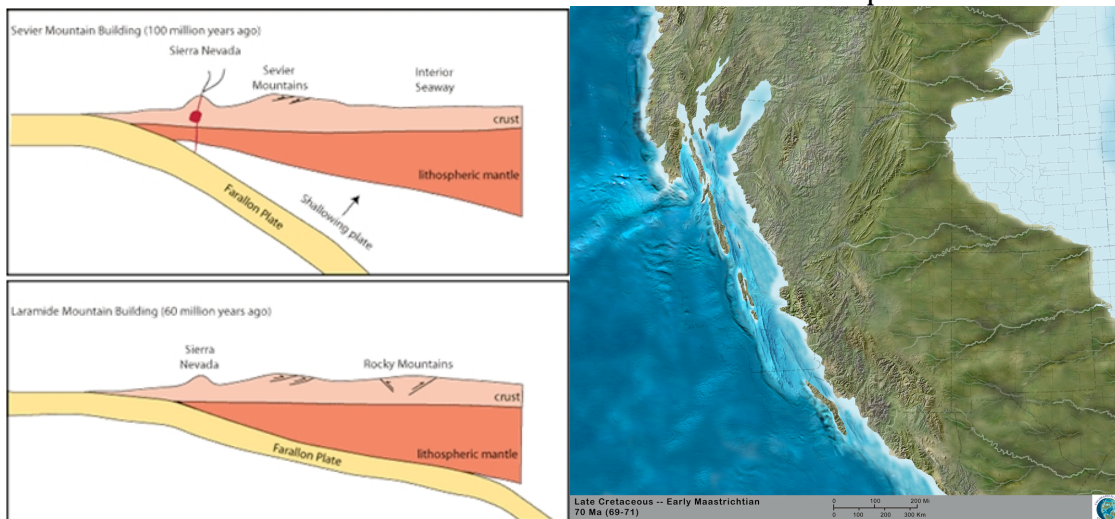
**SUPER-EXCITING!!**

This may be the only fieldtrip where we sample four physiographic provinces that dominate the south-western United States.

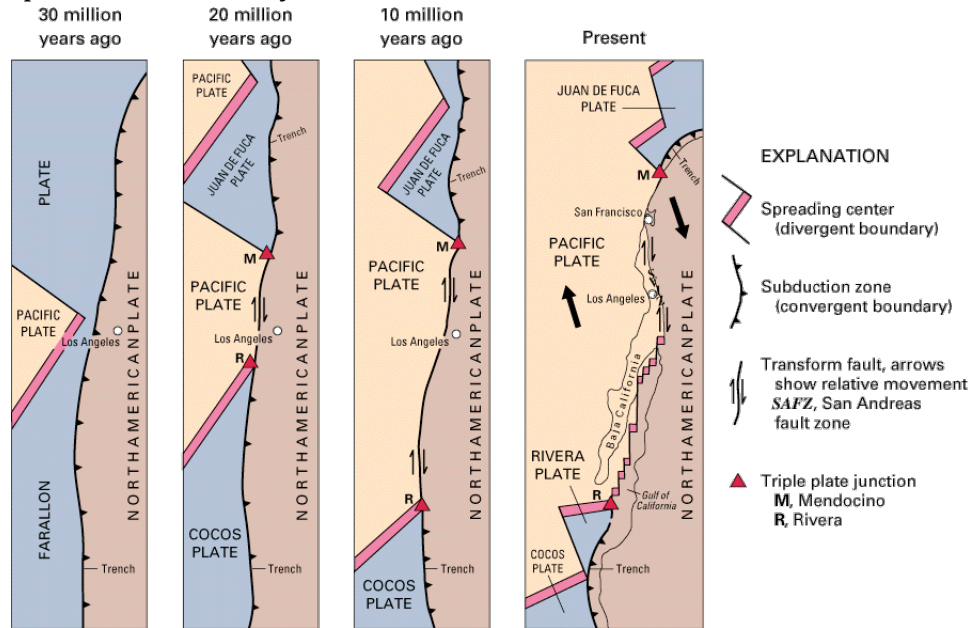


- **Basin & Range:** Tucson to ~Showlow and again at the Rio Grande Rift. Set of quasi-parallel horst and graben formed in an extensional period over the past 30 Myr. The eroded horsts are the ranges and infilled graben the basins.
- **Rocky Mountains:** Formed in a broad regional compression about 60-70 Myr ago known as the Laramide Orogeny. The result of the subduction of an oceanic slab off the western seaboard at an especially shallow angle.
- **Colorado Plateau:** Region uplifted over the past few 10s of Myr as a coherent crustal block. There's still a lot of debate about how this was accomplished and the timing.
- **Great Plains:** Relatively undeformed continental interior. Mostly marine and coastal sediments deposited by an inland sea during the Cretaceous.

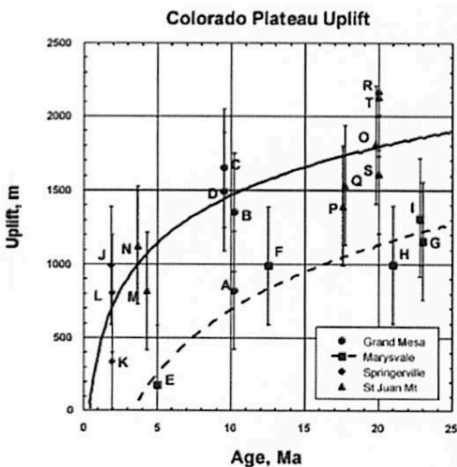
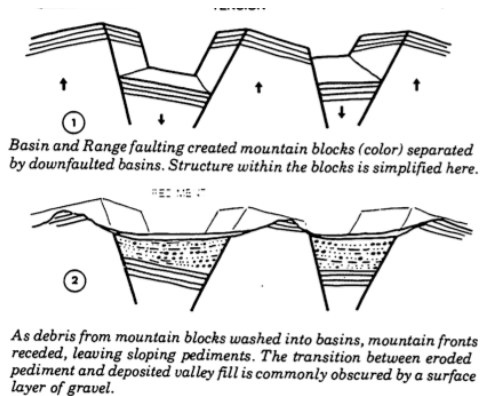
Most of these divisions can be tied to the subduction of the Farallon plate



Subduction creates the large Sevier-Mogollon range (like the Andes) along the west coast. Then ~60Myr ago (really 80-40 Myr) the subduction angle of the slab became much shallower. The subducting slab began to grate along the underside of North America's lithosphere transmitting stresses far inland to where an inland sea existed. Compression in this period produced the Rocky Mountains – far inland from the subduction zone.



The spreading center west of the Farallon plate reached north America ~30 Myr ago. Compression ends and the strike-slip San Andreas Fault is created. Without the constant compressive stresses the Sevier Mogollon range collapses and the crust spreads outward. This extension propagates from west to east and creates the basin and range province



Colorado Plateau uplift occurred during this period. Possibly from:

- Mantle flow
- Intra-crustal flow
- Delamination of the lithosphere.

Dating of the uplift is controversial e.g.:

- Paleo-botany studies
- Vesicle-sizes in lava flows

Basin and range continues to nibble at the edges of the Colorado Plateau. The Farallon plate continues diving toward the core-mantle boundary.

## The Continental Divide

The 'Continental Divide' (also called the Great Divide) is the hydrological boundary for the continent of North America. All watersheds to the west of the divide drain to the Pacific Ocean, and those to the East flow towards the Atlantic Ocean (which, here, includes the Gulf of Mexico and the Caribbean Sea). The divide exists primarily in mountainous terrain and spans the entirety of the North and South American continents, running from the Bering Strait offshore of Alaska down to the Strait of Magellan off the southernmost tip of South America. There are also lesser known divides which also represent the division of drainage between the Atlantic, Pacific and Arctic Oceans. Figure 1 shows the location of the Continental Divide in the United States.

**Fun Fact:** Every continent has at least one hydrological divide except Antarctica. 10 points to Gryffindor for anyone who can tell me why Antarctica doesn't have one.



**Figure 1:** The location of the continental divide as it traverses the United States (shown as green line). Notice there are small 'loops' which are closed drainage areas (USGS).

**Fun Fact:** There are many lakes and rivers that straddle the divide, with lake outflows draining in both directions, and rivers often splitting and draining to both oceans.

In North America, the continental divide tends to follow the peaks of the high elevation Rocky Mountains. While generally at an elevation of >7000 ft, in southern New Mexico the elevation of the divide falls below 4500 ft. Figure 2 is a map of the Continental Divide as it exists in the four corners area. Hopefully we will get to straddle the divide this trip. Sadly, many rivers in the southwest that are bound for the Pacific Ocean never make it as they empty into the desert.

**Fun Fact:** While a triple point (Atlantic-Pacific-Arctic) exists in Montana, Canadians generally consider theirs, which occurs on the Alberta-British Columbia border, to be of greater importance because it is 1000 m higher in elevation and receives more precipitation. I think it is of greater importance because it is in Canada. This point is referred to by people who know things about hydrogeology as the hydrological apex of North America.

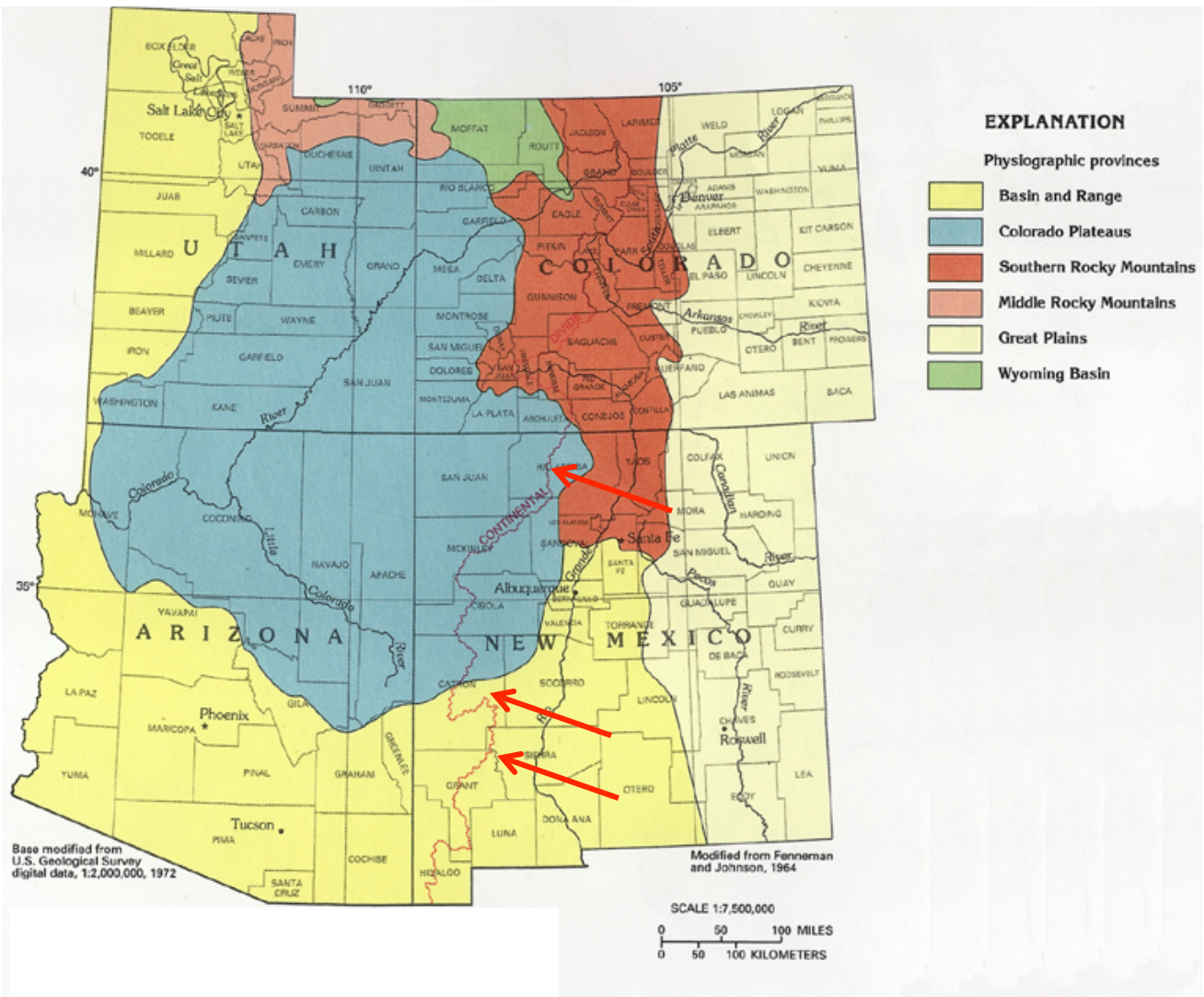


Figure 2: The Continental Divide on a map of the South West (red line, annotated by red arrows). Physiographic provinces (shown as different colours here) with unique geology terrain and climate (USGS).

**Fun Fact:** there is a hiking trail that follows the divide from Mexico to Canada. It is aptly (and surprisingly) named the Continental Divide Trail. Next field trip?

#### References:

I am ashamed to admit, a lot of this information came from:

[http://en.wikipedia.org/wiki/Continental\\_Divide\\_of\\_the\\_Americas](http://en.wikipedia.org/wiki/Continental_Divide_of_the_Americas)

But more respectfully, also from: Ground Water Atlas of the United States: Arizona, Colorado, Utah, New Mexico. Can be found at [http://pubs.usgs.gov/ha/ha730/ch\\_c/C-text1.html](http://pubs.usgs.gov/ha/ha730/ch_c/C-text1.html)

Figures 1 and 2, both USGS.

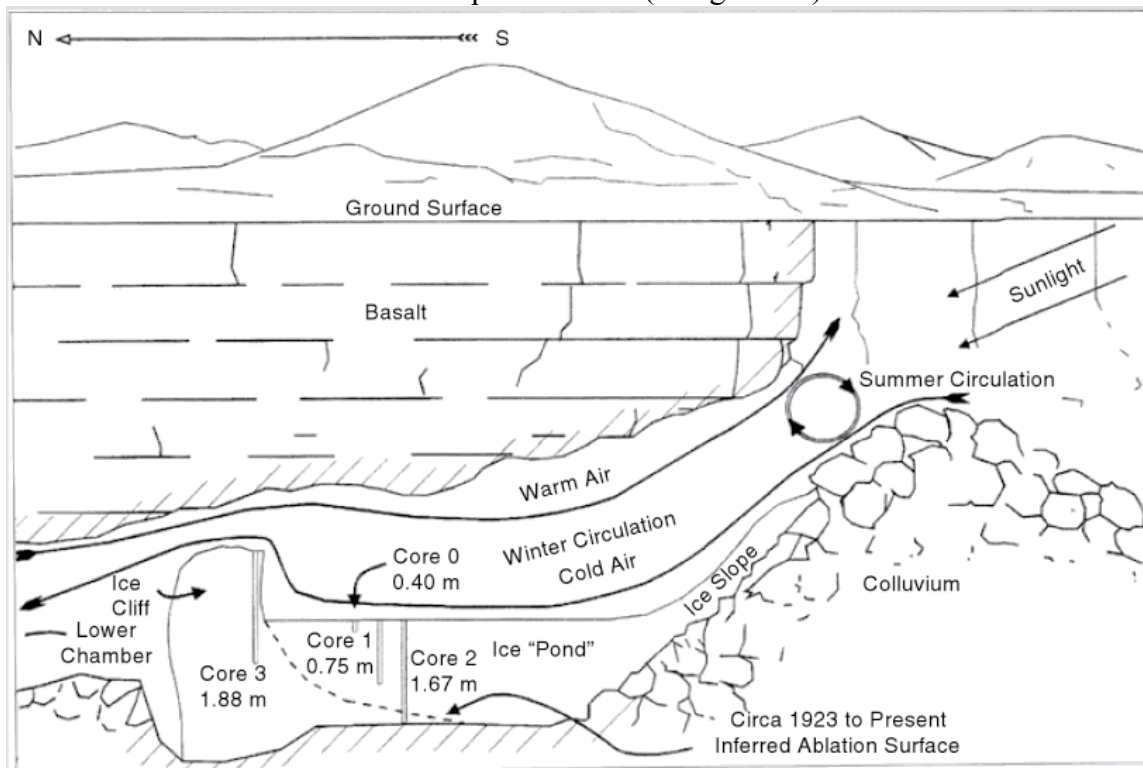
## Lava Tubes and Perennial Ice

Ali Bramson

### **Background**

Caves that contain perennial ice (commonly limestone caves or lava tubes) are often called “ice caves”. Water can percolate through the ground into the cave and freeze if the cave draws in freezing air from the outside (US EPA 2002). Ice can also form in caves through crystallization of water vapor. If summer melting overcomes winter freezing, the ice exists seasonally and is dependent on annual freeze/thaw cycles. However, if ice survives the melting season, the ice can remain permanently or continue growing, giving perennial ice (Perşoiu & Onac 2012).

The ice can remain permanently as perennial ice if the average temperature is less than  $0^{\circ}\text{C}$  or if air circulation patterns are favorable to trapping colder air from the outside and expelling warmer air. In these circulation patterns, the latent heat from the freezing process gets removed and replaced by colder, outside air (Barry & Gan 2011). In the winter, the cold air can get sucked into the cave but trapped there in the spring and summer because it is denser. In the more static case where there is simply a cavity that leads down to the cave, dense, cold air can sink into this cavity and get trapped. The geometry of lava tubes lends itself towards these cold-trapping air circulation patterns that lead to favorable conditions for perennial ice (Yonge 2004).



Schematic diagram of the air circulation in Candelaria Ice Cave, NM, in summer and winter (from P. V. Dickfoss *et al.* 1997).

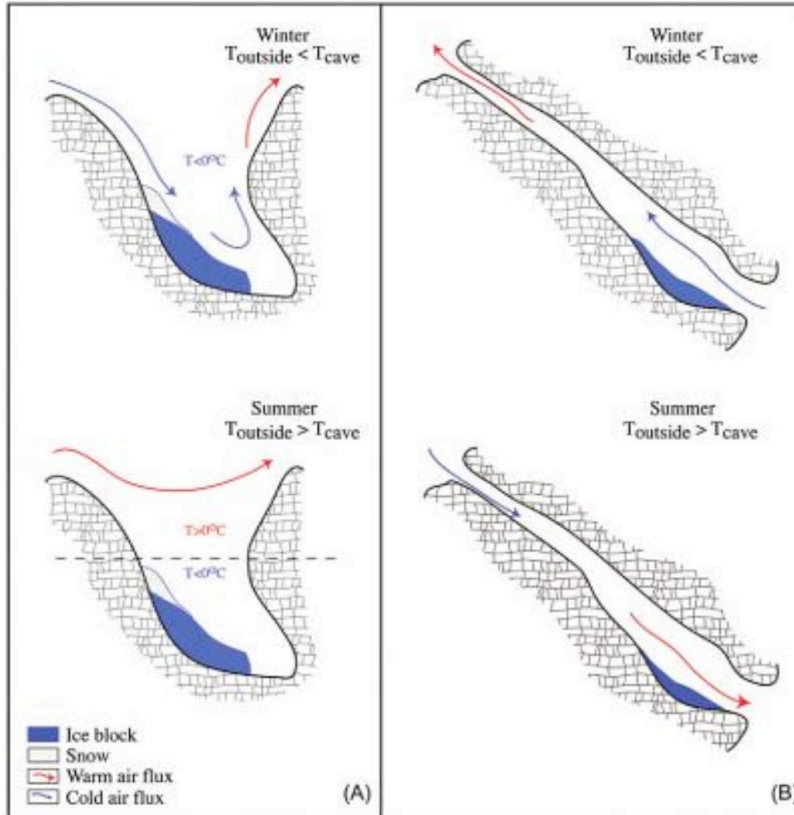


Figure 2 from Perşoiu & Onac 2012: Schematic diagram showing the most common cave cooling mechanisms. Left: Cold air trapping, Right: Unidirectional ventilation

Ice features in caves:

- Ponded water that collects in the depressions in caves and then freezes into large, thick, clear masses of ice
- Accumulated snow blown into caves through the wind
- Ice needles- Centimeter-long slivers of ice that form in moist soils when air temperatures drop below freezing (Pidwirny & Jones 2010, Carter). The soil must have enough pore space so that the water will get sucked to the surface but small enough to keep it in place against gravity (Carter)
- Ice formations (ice stalactites, stalagmites, flowstone, etc)
- Water vapor/atmospherically deposited hoarfrost (dew that forms a white coating on a surface) that can form large, hexagonal crystals that line the cave walls (US EPA 2002)

Note: Seasonal ice generally forms icicles and ice stalagmites whereas the perennial ice usually takes the form of stratified chunks of ice meters thick like in flowstone and frozen ponds or as ice needles and ice crystals (Perşoiu & Onac 2012, National Park Service 2012).

## Lava Tubes and Ice Caves in New Mexico

Along the Continental Divide, there are 100+ lava tubes and crevices within the El Malpais National Monument area (35° N, 108° W, 2,000-2,5000 feet elevation) where perennial ice accumulates (Barry & Gan 2011). Dickfoss et al. 1997 dated an ice core from Candelaria Ice Cave and found the lowest meter of ice (to 4.5 m depth) was 1,800-3000 years old. The upper 3 m of ice dates between 1600-1850. They found 0.05 m/yr accumulation in the ice pond between 1924 and 1936, a decrease until 1947 and then varying rates of accumulation until the early 1990s when ablation started to occur. The recent variations were due to 1986-1991 being the wettest spell the region had had in the last 2,000 years with the ablation in the 90's occurring in the subsequent drought. The most common places on Earth to find ice caves are in the Western United States (California, Idaho, New Mexico), the limestone Alps of Bavaria, northern Austria and Switzerland.

At El Malpais National Monument, there are 15 major lava tubes (Marinakis 1997) that stretch a combined total length of 100 km. The Bandera lava tube is the longest (and would be the longest identified system in North America if most of it hadn't collapsed). When a lava tube cools, it contracts and often causes piles of rubble and debris (called breakdown) due to the collapse that happens from cooling. A skylight forms when the collapse happens vertically and reaches the surface, allowing atmospheric gases to mix and combust with the hot gas of the flow (National Park Service 2012). The interaction of gases can cause the formation of lava speleothems (lavacicles, shelves, flowstones, etc) from flowing, dripping, splashing and movement of the molten (or partially molten) lava (National Park Service 2012). This can give rise to features similar to limestone speleothems but they form much quicker than the limestone processes.

Ice accumulations are very common in El Malpais National Monument. Rainwater and snowmelt percolate into the freezing region of a lava tube cave. Seasonal ice features such as icicles and ice stalagmites form, melting by late summer (sad panda) but perennial accumulations lead to flowstone, frozen ponds, and ice needles and crystals (National Park Service 2012). Most of the ice is clear-white but part of the floor in Candelaria Ice Cave is a pale green due to the flourishing of algae in this part where direct sunlight is received (National Park Service 2012).



*LEFT: Ice stalagmite (Perşoiu & Onac, 2012)*

*RIGHT: Ice Needles (Carter)*





**Figure 31. Perennial ice. Perennial ice accumulations produce ice flowstone, frozen ponds, and frozen floors. Some ice accumulations at El Malpais have persisted for more than 3,000 years. This photograph was taken in the Red Room of Crystal Ice Cave at Lava Beds National Monument, where similar ice accumulations occur. National Park Service photograph.**

*Figure 31 from National Park Service 2013*

Fun Fact #1: Native Americans would use ice caves as *natural refrigerators* to freeze and store meat. Archaeologists found that ice caves in the Snake River Plain and Wilson Butte Cave region of Idaho for at least 8,000 years (Wilson Butte Cave 2013).

Fun Fact #2: El Malpais' ice caves are also culturally relevant because *soldiers* in the 1860's would take the ice back to Fort Wingate (National Park Service 2012).

Fun Fact #3: All ice caves combined make up the smallest part of the terrestrial cryosphere. The largest amount of ice in a terrestrial cave is 100,000 m<sup>3</sup>. Kern & Perşoiu 2013 say this about how much scientists care about cave ice: “both speleologists and glaciologists, regard cave ice as a “*stepchild*” in their discipline” and while calcareous speleothems are treated as valuable scientific targets, “ice is often seen as an *annoying slippery decoration* that should be avoided.” ☹

## Planetary Analogs

There is evidence for lava tube caves on Mars and some studies predict they could hold ice. Williams et al. 2010 modeled airflow of a subterranean room with a small “chimney” opening in the ceiling to predict stability of ice deposits in martian caves. They found a lack of stable cave ice in the polar regions, with lower latitude caves being more likely candidates for ice. This is because low-latitude caves could get flushed with new air every night and because the air at lower-latitudes could be more humid (low latitudes have higher mean annual outside and ground temperatures). The volcanic province of Tharsis could be especially stable to ice caves due to the region’s lower thermal inertia compared to other regions at the same longitude. This is shown in figure 5a from Williams et al. 2010. An interpretation of the regions that are undergoing losses in the ice mass could mean that a 1 m thick ice plate in a cave could still last ~34,000 years despite undergoing (slow) sublimation. Thicker ice deposits could last much longer, and may be remnants from ice deposition that took place during higher obliquity periods (up to 35°) within the last several 100,000 years. Figure 11b from Williams et al. 2010 shows a region interpreted to be collapsed lava tubes, which could contain stable cave ice.

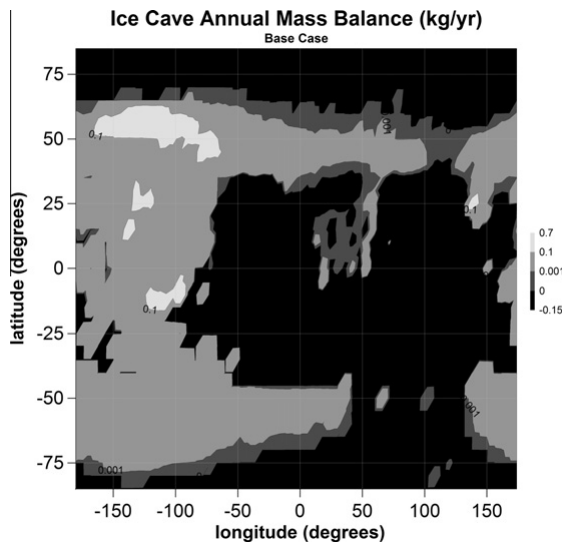


**Fig. 5a.** Base case: the annual ice mass balance within hypothetical Mars ice caves. For each gridpoint, a cave was modeled for one Mars year. The mass balance indicates how much ice mass was gained or lost from the 30 kg of ice initially placed within the cave. The lighter-toned areas indicate regions where cave ice is either stable or would grow. Black areas are where ice would not be stable for annual timescales.

*Figures from Williams et al 2010*

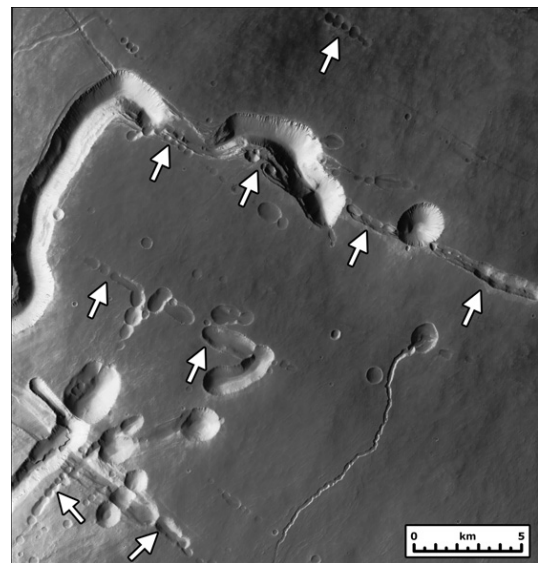
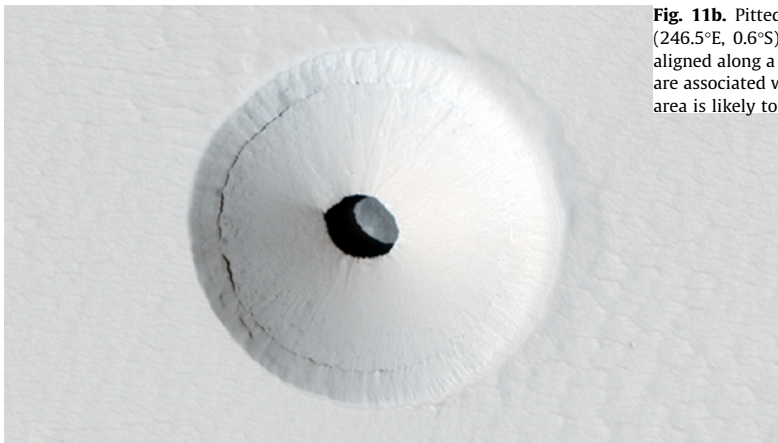


**Fig. 11b.** Pitted crater chains (white arrows) along the flanks of Pavonis Mons (246.5°E, 0.6°S), one of the Tharsis Montes volcanoes (Fig. 5). Crater chains are aligned along a NW-SE trend and sinuous rilles of volcanic and larger collapse pits are associated with them. Many of these features have undergone collapse and this area is likely to be the site of conditions conducive to the formation of ice caves.



*Skylight (35 m across) to underground cavern on Mars (3.735° N, 248.485° E)*

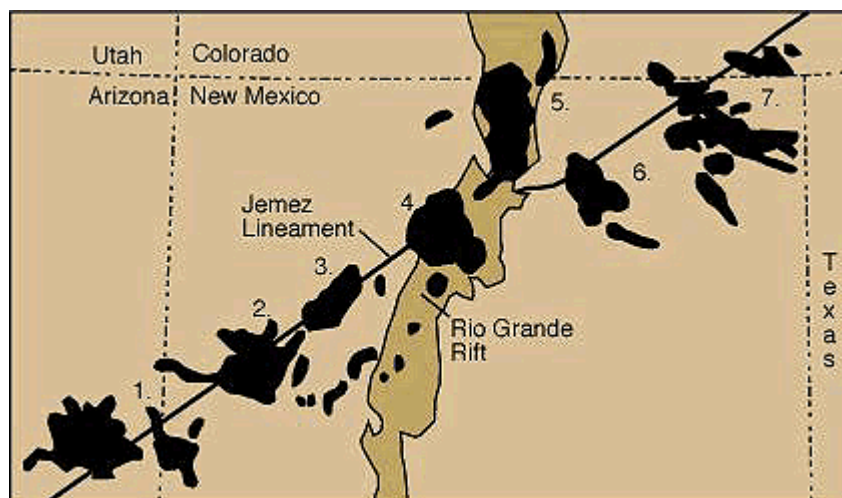
## References

- Barry, R. & Gan, T.Y., (2011) *The Global Cryosphere: Past, Present and Future*, Cambridge University Press page 180-181.
- Carter, J.R., Needle Ice: <http://my.ilstu.edu/~jrcarter/ice/needle/> (accessed 9/21/2013)
- Dickfoss, P.V., et al. (1997) In K. Mabery, (Ed.) Natural history of El Malpais National Monument Bulletin 156. (pp 91-112) New Mexico Bureau of Mines and Mineral Resources.
- Kern, Z. & Perşoiu, A. (2013) *Quaternary Science Reviews*, 67, 1-7.
- National Park Service, (2012) *El Malpais National Monument: Geologic Resources Inventory Report*, Natural Resource Stewardship and Science.
- Perşoiu, A. & Onac, B.P. (2012), Ice in Caves, In W.B. White & D.C. Culver (Ed.), *Encyclopedia of Caves* (pp. 399-404). Academic Press.
- Pidwirny, M. & Jones, S. (2010). Periglacial Processes and Landforms, *Physical Geography Fundamentals eBook*:  
<http://www.physicalgeography.net/fundamentals/10ag.html> (accessed 9/21/2013)
- United States Environmental Protection Agency, (2002) *Lexicon of Cave and Karst Terminology with Special Reference to Environmental Karst Hydrology*, National Center for Environmental Assessment: <http://www.karstwaters.org/files/glossary.pdf>
- Williams, K.E., et al. (2010) *Icarus*, 209, 358-368.
- Wilson Butte Cave (2013), U.S. Department of the Interior Bureau of Land Management Website- *Hunting and Gathering*:  
[http://www.blm.gov/id/st/en/prog/cultural/wilson\\_butte\\_cave/prehistoric\\_idaho/hunting\\_and\\_gathering/ice\\_caves.html](http://www.blm.gov/id/st/en/prog/cultural/wilson_butte_cave/prehistoric_idaho/hunting_and_gathering/ice_caves.html) (accessed 9/21/2013).
- Yonge, C. (2004), Ice in Caves, In J. Gunn (Ed.), *Encyclopedia of Cave and Karst Science* (pp. 435-437). New York: Fitzroy-Dearborn Publishers.

# The Jemez Lineament

## Corwin Atwood-Stone

Northeast trending 600 km lineament of Tertiary-Quaternary volcanic centers and faults running from East-Central Arizona to North-East New Mexico. This pattern of volcanism is not a hotspot as the ages of the fields do not form a progression. The faulting seems to be due to faster spreading of the Espanola basin to the south than the area to the north. This lineament appears to correspond to a boundary between Pre-Cambrian crustal provinces. This structural boundary is from the Mazatzal island arc accreting onto the Yavapai craton. This weakness in the crust allows magma to leak upwards thus forming these volcanic fields. This boundary in the basement is seen from: a south dipping low velocity seismic anomaly at depth, high heat flow, and high electrical conductivity.



Map of the Jemez Lineament and its constituent volcanic fields, listed below with their ages of activity.

0: San Carlos -	4.2 – 1.0 Ma
1: Springerville -	2.5 – 0.3 Ma
2: Zuni Bandera -	4.0 – 0.001 Ma
3: Mount Taylor -	3.5 – 1.5 Ma
4: Jemez Mountains -	14 Ma - Nowish
5: Taos -	10 – 1.8 Ma
6: Ocate -	8.3 – 0.8 Ma
7: Raton-Clayton -	8.2 Ma – 2.3 ka

The magmas in the volcanic fields along the lineament are primarily basaltic, with some transitional lavas and a few highly silicic eruptions. The basaltic lavas show significant petrologic variation, due to different source zones and crustal contaminants.

Brief highlights of the various fields from SW to NE

- 0: San Carlos** – Cones and lava flows. This field, especially Peridot Mesa, is known for its peridotite xenoliths in basaltic flows, which here contain significant amounts of large gem quality olivine.
- 1: Springerville** – A classic cinder cone field with ~380 vents. Possibly associated with nearby White Mountains Baldy, and 8 Ma old volcano which may also be related to the lineament.
- 2: Zuni Bandera** – 74 vents representing a wide variety of eruptive types both effusive and pyroclastic. Cinder cones, spatter ramparts, small shields, maars and collapse pits. Also found here are lava tube ice caves.
- 3: Mount Taylor** – 20 km diameter strato-volcano and a surrounding volcanic field. The field is notable for having a large number of maar craters. Also found here are prominent fissure eruptions, trachyte dome and volcanic necks.
- 4: Jemez Mountains** – Field at the intersection with the Rio Grande Rift. Several distinct periods of volcanism:
  - 14-10 Ma – Rhyolite lava domes and basaltic lava flows
  - 10-7 Ma – Huge andesite complex volcanoes
  - 5-2 Ma – Large dacite lava dome complex and several basaltic lava fields
  - 2 Ma-Recent – Large Plinian Eruptions at 1.45 & 1.12 Ma (from Valles Caldera), each followed by pyroclastic outflows and pumice/ash falls creating the massive Bandelier Tuff. Smaller eruptions of this type have continued up until the recent geologic past – still considered active.
- 5: Taos** – Concentric pattern of large volcanoes. Basaltic shields in the center moving out to andesite volcanoes and the dacite volcanoes.
- 6: Ocate** – Cones with basaltic to dacite flows. An interesting feature of these flows is that older flows form high mesas, while younger flows are at lower elevation in canyons carved in these mesas.
- 7: Raton-Clayton** – 125 basaltic cinder cones and also andesitic & dacitic volcanic necks and domes.

# The El Malpais Region and McCarty's Lava Flow

Hannah Tanquary 2013

## El Malpais Overview

- The El Malpais Region is located in western New Mexico. *Malpais* means “badlands” in Spanish.
- The Zuni-Bandera volcanic field is the second largest in the Basin and Range Province and covers 2,460 km<sup>2</sup>, the majority of the El Malpais Region.<sup>1</sup>
- The easternmost lava flow in this field is known as McCarty's (or McCarthy's) Flow (shown in red below).
  - At only ~3000 years old, this flow is one of the youngest in the continental US.<sup>2</sup>
- Zuni-Bandera exhibits features of “Hawaiian-style” volcanism, with both a-a and Pahoehoe lavas.
  - This is of particular interest because these very young flows can be compared to their much older counterparts that, in many cases, have been obscured by erosion.
- Flows reach 145 meters thick in some areas, and the total volume of the flows is ≥ 74 km<sup>3</sup>.<sup>2</sup>

Geologic Map of the Zuni-Bandera Volcanic Field

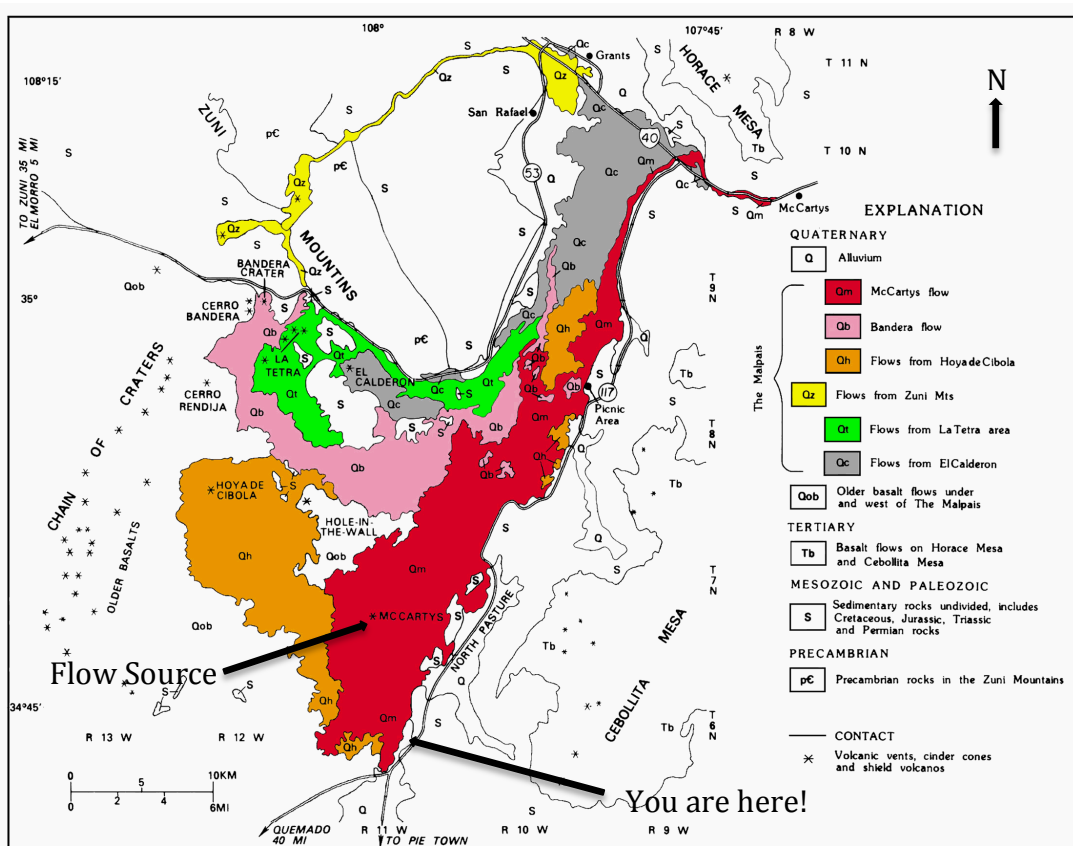


Figure 1. Geologic map of El Malpais and surrounding area, New Mexico.

After: New Mexico Bureau of Geology and Mineral Resources. 2007-2008

# The El Malpais Region and McCarty's Lava Flow

Hannah Tanquary 2013

## McCarty's Flow

- All flows in the Zuni-Bandera region are thought to have occurred as a result of its location along the Jemez Lineament.
  - This lineament extends from east central Arizona to northeastern New Mexico and is ~600 km long.<sup>3</sup>
  - Lavas are believed to have originated from great depth since the Lineament is thought to penetrate to great depth.
    - Further evidence of this are the apparently mantle-derived melts that comprise the Zuni-Bandera region's basaltic lavas.<sup>5</sup>



LANDSAT image of the Zuni-Bandera lava flow in the El Malpais region.



Cinder cone marking the source vent of McCarty's Flow. Credit: Google Maps

- The source of McCarty's Flow is a small shield volcano located in the southeast portion of the flow.
- Marking the vent is an 8 meter high cinder cone.
- Some lava flowed 8-9 km southward, but most flowed north with the slope of the land and then east into the Rio San Jose Valley. (Along I-40)
- The flow is mostly a vesicular, porphyritic basalt having distinctive plagioclase phenocrysts 0.20 to 1.5 cm long, which is indicative of the extrusive processes that formed the flows.<sup>6</sup>

The El Malpais Region and McCarty's Lava Flow  
Hannah Tanquary 2013

References

<sup>1</sup>"Zuni-Bandera". Global Volcanism Program, Smithsonian Institution.

<sup>2</sup>Laughlin, W.A., Charles, R.W., Reid, K., and White, C., 1993, Field-trip guide to the geochronology of El Malpais National Monument and the Zuni-Bandera volcanic field, New Mexico: New Mexico Bureau of Mines and Mineral Resources Bulletin 149

<sup>3</sup>Wood, Charles Arthur; Kienle, Jürgen (1992). *Volcanoes of North America: United States and Canada*. Cambridge University Press.

<sup>4</sup>"McCarty's Flow, Zuni-Bandera Volcanic Field, New Mexico"  
[http://volcano.oregonstate.edu/vwdocs/volc\\_images/north\\_america/mccartys\\_flow.html](http://volcano.oregonstate.edu/vwdocs/volc_images/north_america/mccartys_flow.html)

<sup>5</sup>Laughlin, A. W., M. J. Aldrich Jr., M. E. Ander, G. H. Heiken, D. T. Vaniman, Tectonic setting and history of late Cenozoic volcanism in west-central New Mexico, Field Conf. Guideb. N. M. Geol. Soc. 1982

<sup>6</sup>Carden, J. R., and Laughlin, A. W., 1974, Petrochemical variations within the McCarty's basalt flow, Valencia County, New Mexico: Geological Society of America, Bulletin, v. 85, pp. 1479-1.8

# Thermodynamics of Lava Flows

Kelly Miller

## Pāhoehoe

- Smoother appearance
  - o Formation of “toes” and ropy structures
  - o Often radar dark
- Forms from lava at  $\sim 1135^\circ\text{C}$  with 15-20% crystals



Figure 1 Toes of pāhoehoe lava in Hawaii.  
Credit: J.D. Griggs via USGS

## ‘A‘ā

- Rougher appearance
  - o Formation of “clinkers”
  - o Radar bright
- Forms from lava at  $\sim 1100^\circ\text{C}$  with 40% crystals



Figure 2: ‘A‘ā crust forms as a flow overtakes ropy pāhoehoe lava emplaced earlier. Credit: USGS

- Pāhoehoe  $\rightarrow$  slabby pāhoehoe  $\rightarrow$  Scoriaceous-spinose ‘a‘ā  $\rightarrow$  clinker ‘a‘ā transition common
  - o Transition occurs as lava cools, or as a function of effusion rates
- Hon et al., 2003 argue that the reverse process also occurs
  - o In flatter areas, pāhoehoe dominates; on steeper slopes, ‘a‘ā dominates
    - Flatter areas have lower shear-strain rates
    - Change in shear stress more important than temperature
    - Pāhoehoe resembles Newtonian rheology while ‘a‘ā is non-Newtonian (Bingham or other); more on this from Thad!

## Pāhoehoe crust

- McCarty’s flow is dominated by pāhoehoe
  - o Has examples of the transition from slabby to normal pāhoehoe
    - Transition occurs where lava breaks through a narrow opening, causing slabby pāhoehoe to form from the initially fast flow, and then normal pāhoehoe once the flow rate slows



Figure 3: Slabby pāhoehoe is characterized by buckling features; the wedge shape is typical of continuously advancing sheet flows. Credit: GEOL 205 lecture notes, Hawaii.edu

- At 1070 °C lava hits the solidification temperature; below 800 °C it transitions from viscoelastic to brittle behavior.
  - o Tensile strength containing a flow determined by the viscoelastic surface between 800-1070 °C below the brittle surface
    - Can result in storage of fluid that later breaks through
- Pāhoehoe tends to form from flows that initially have roughly isothermal liquid
  - o Indicative of constant flow of liquid
  - o Can result in inflation of sheets

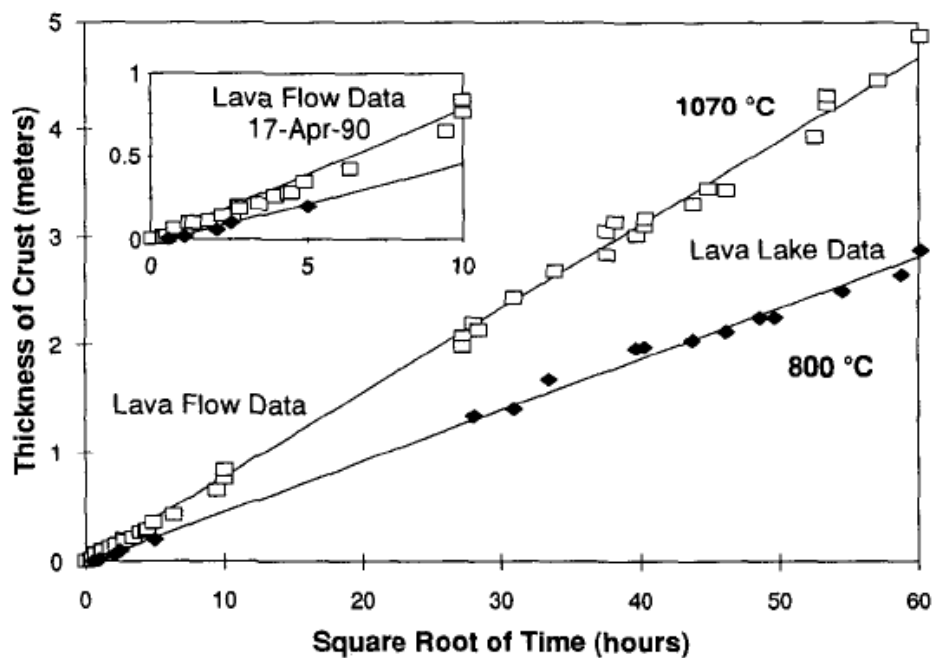


Figure 4: Thickness of the pāhoehoe crust on lava as a function of time. Credit: Hon et al., 1994

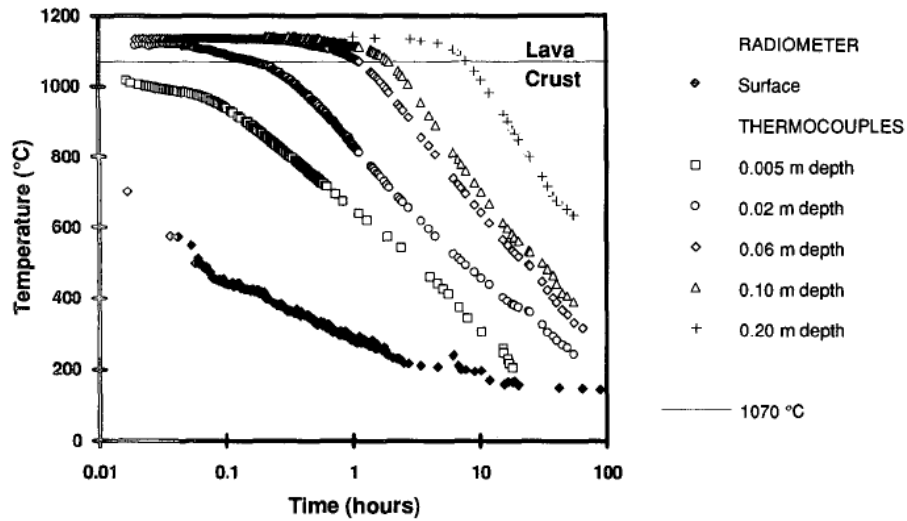


Figure 5: Temperature at different depths of a lava flow as a function of time. Credit: Hon et al., 1994

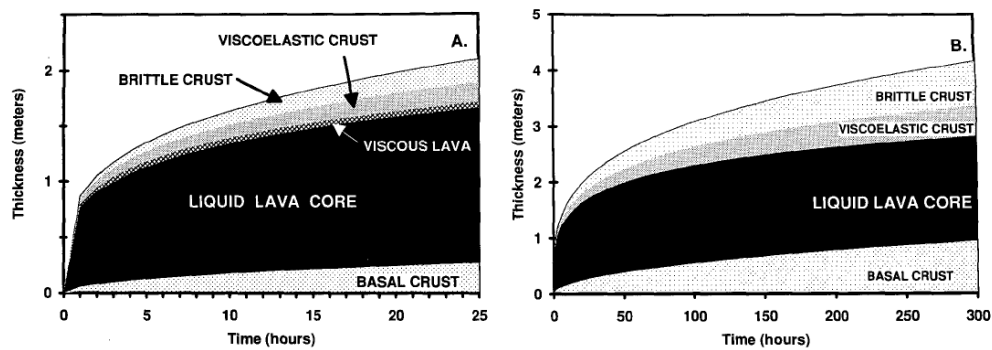
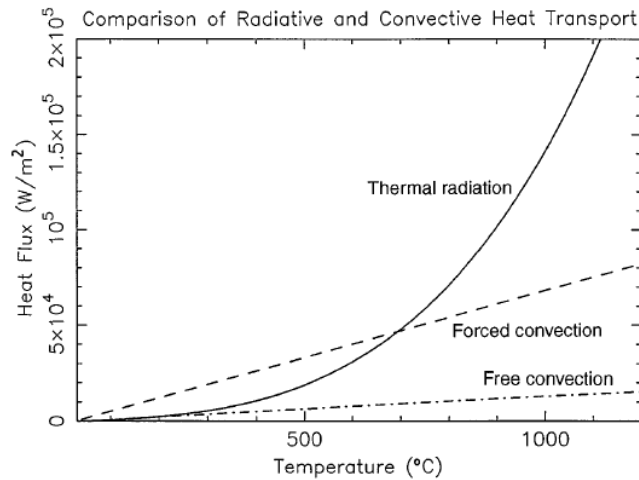
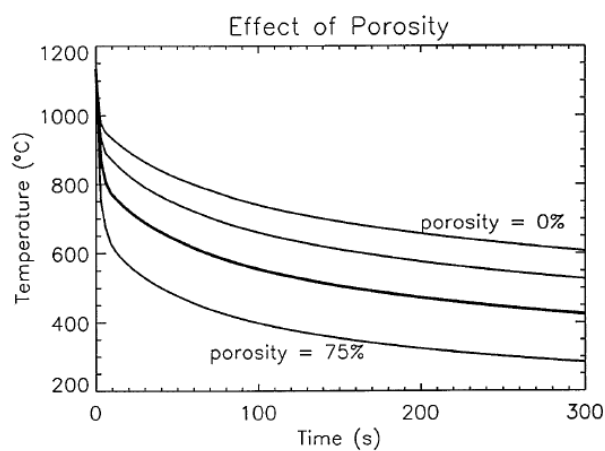


Figure 6: Composition of the flow as a function of time based on models. Credit: Hon et al., 1994

- Initial cooling is influenced by
  - o Radiative cooling at the surface
  - o Convection of the atmosphere above the surface
  - o Conduction of heat within the flow
  - o Heat released by crystallization



**Figure 7: Comparison of heat flux from the surface of lava flows via different mechanisms as a function of temperature. Credit: Keszthelyi and Denlinger, 1996**



**Figure 8: Changing the porosity of modeled materials has a significant impact on the cooling rate in the first five minutes; lines correspond to 0, 25, 50, and 75% porosity. Credit: Keszthelyi and Denlinger, 1996**

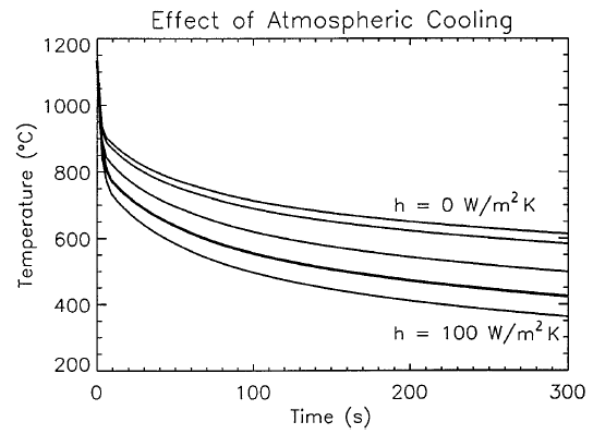


**Figure 9: The effects of increasing atmospheric flux are more variable; shown above are lines for  $h = 0$  (no atmospheric cooling), 10 (stagnant air), 40 (minimal wind), 70 (average wind), 100 (very windy)  $W/m^2K$ . Credit: Keszthelyi and Denlinger, 1996**

## References

Hon, K., Kauahikaua, J., Denlinger, R., & Mackay, K. (1994). Emplacement and inflation of pahoehoe sheet flows: Observations and measurements of active lava flows on Kilauea Volcano, Hawaii. *Geological Society of America Bulletin*, 106(3), 351-370.

Keszthelyi, L., & Denlinger, R. (1996). The initial cooling of pahoehoe flow lobes. *Bulletin of Volcanology*, 58(1), 5-18.

Hon, K., Gansecki, C., & Kauahikaua, J. (2003). The Transition from 'A'a to Pahoehoe Crust on Flows Emplaced During the Pu'u'u'6-Kupaianaha Eruption. *US Geological Survey professional paper*, 1676, 89.

# Lava Flow Rheology

Thaddeus D. Komacek

## 1 Introduction

The theoretical understanding of lava flow rheology, when coupled with an understanding of the thermodynamics of such flows, aids in our interpretations of ancient flows such as the McCarthy flow we will see on this trip. The morphology of lava flows (its flow structure and features) further help us understand the lava rheology and provide model constraints [3]. There are many different morphologies of lava flows, such as channelized basalt flow, pahoehoe, pillow basalts, rhyolite flows, and lava domes. The McCarthy flow is distinctly pahoehoe, and an image of the ropy pahoehoe structure observed in the flow is shown in Figure 1. This is the most common surface texture of pahoehoe flows, and is formed when the thin, partially solidified crust of a flow is slowed, with the crust continuing to move forward, causing the ropy structures observed [1].



Figure 1: An image of ropy pahoehoe lava in the McCarthy flow. From <http://nmnaturalhistory.org/>.

In this brief I will discuss the theoretical underpinnings of lava rheology, and leave in-depth discussion of the McCarthy flow and lava cooling mechanisms and thermodynamics to the other reviewers.

## 2 Viscosities

Lava rheology is dependent on a variety of parameters: lava composition, temperature, crystal content, and bubble content. Viscosity, a measure of the resistance of a fluid to flow, is an important parameter in rheological modeling. To model lava as a viscous fluid, we generally use four different shear viscosity components [3]: melt viscosity of the liquid phase,  $\eta_m$ ; actual lava viscosity  $\eta = d\sigma/d\dot{\epsilon}$  with  $\sigma$  the applied shearing stress and  $\dot{\epsilon}$  the strain rate of the lava; apparent lava viscosity  $\eta_A = \sigma/\dot{\epsilon}$ ; and apparent flow viscosity  $\eta_F$  that is essentially an averaged effective viscosity over a lava flow. The melt viscosity is identical to the lava rheology for small crystal and bubble fractions. However, the actual and apparent

lava viscosities are the relevant macroscopic viscosities that govern the flow due to the microphysics of the liquid-crystal bubble mixture that makes up the flow [3]. Due to the various crystal (<5% to 50%) and bubble contents (few % to >90%) of lava flows, there are many types of lava flow regimes. Examples of the microstructures of pahoehoe and 'a'a lava structures are shown in Figure 2.

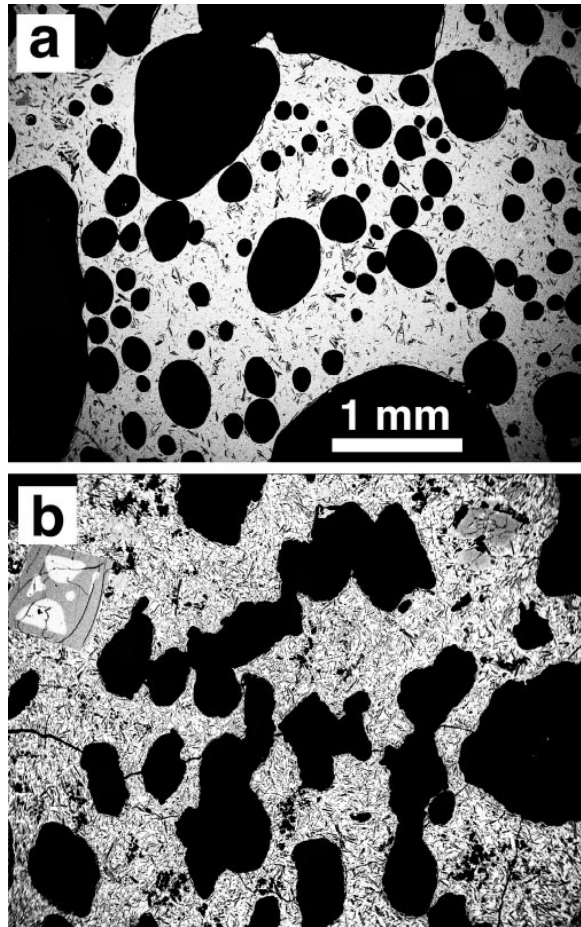


Figure 2: Vesicle structures for a) pahoehoe and b) 'a'a samples. Scale bar is same for both images. Figure reprinted from [2].

### 3 Rheological Relationships

A simple approximation for lava rheology is the Bingham flow law:

$$\sigma = \sigma_0 + \eta \dot{\epsilon} \quad (1)$$

where  $\sigma_0$  is the yield stress and  $\eta$  is the plastic viscosity, a constant. Deformation only occurs for stresses greater than  $\sigma_0$ , and once this stress limit is reached the flow is characterized by an apparent viscosity  $\eta_A$  [3]:

$$\eta_A = \eta + \sigma_0 / \dot{\epsilon} \quad (2)$$

Elastic deformation is ignored for lava flows due to the small length scale of shearing in lava flows.

For basaltic lavas (like we will observe on the trip), the apparent viscosity follows the Einstein-Roscoe

relationship, and is a function of the temperature  $T$  and the volume fraction of crystals  $\phi$ :

$$\eta_A(T, \phi) = \eta_0(1 - \phi/\phi_{max})^{-2.5} e^{\gamma(T_0 - T)} \quad (3)$$

with  $\phi_{max}$  the maximum crystal fraction where flow still occurs,  $\gamma \approx 0.04$  a constant, and  $T_0$  and  $\eta_0$  reference values. Equation 3 hence shows that lava flows reach a limit of large apparent viscosity due to the onset of yield stress at a given critical crystal fraction. For basalt flows, this critical yield strength occurs at  $\phi \approx 40\% - 50\%$  [2].

Large bubbles can cause shear-thinning behavior in lava flows. This behavior can be modeled using a power law stress-strain rate relationship [3]:

$$\phi_{ij} = (K\dot{\epsilon}^{n-1} + \sigma_0/\dot{\epsilon})\epsilon_{ij} \text{ for } \sigma > \sigma_0 \quad (4)$$

with  $\epsilon_{ij} = 0$  for  $\sigma \leq \sigma_0$ . Here  $\sigma_{ij}$  are the deviatoric stresses,  $\epsilon_{ij}$  are elements of the strain rate tensor,  $K$  is the consistency, and  $n$  is an index. For  $n = 1$ , we recover the Bingham fluid; for  $n < 1$  shear leads to a reduction of applied stress required to achieve a given shear rate; and for  $n > 1$  the fluid will be shear thickening.

## 4 Applications to Planetary Geology

The understanding of lava flows is very important for understanding the observed surface morphology of the terrestrial planets and various moons, and hence their geological histories. Lava flows due to volcanism are known to have been extensive on all of the terrestrial planets, and the formation of our moon also involved massive basaltic lava flows. Hence, to invert our observations of geological features on bodies such as Mars, Venus, and Io, we must have an in-depth understanding of the rheological and thermodynamic properties of lava flows that helped create many of the surface features observed. Combining the previous brief on thermodynamics of lava, this on rheology, and the next on flow morphology we can construct a simple picture of how the effects of volcanism are preserved on planetary surfaces.

## References

- [1] USGS Volcano Hazards Program, 2013.
- [2] K.V. Cashman, C. Thornber, and J.P. Kauahikaua. Cooling and crystallization of lava in open channels, and the transition of pāhoehoe lava to 'a'ā. *Bulletin of Volcanology*, 61:306–323, 1999.
- [3] R.W. Griffiths. The dynamics of lava flows. *Annual Reviews of Fluid Mechanics*, 32:477–518, 2000.
- [4] M. Manga, J. Castro, K.V. Cashman, and M. Lowenberg. Rheology of bubble-bearing magmas. *Journal of Volcanology and Geothermal Research*, 87:15–28, 1998.
- [5] M. Manga and G. Ventura, editors. *Kinematics and Dynamics of Lava Flows*. The Geological Society of America, 2005.
- [6] R.S.J. Sparks and H. Pinkerton. Effect of degassing on rheology of basaltic lava. *Nature*, 276:385–386, 1978.

## Inflation and Morphology in Lava Flows

Jess Vriesema

### Introduction:

Lava flows produce a remarkable variety of morphological features. Land-based lava flows are generally classified as being either “‘a’a” or “pahoehoe.” In this document, we will introduce ‘a’a and pahoehoe lava flows and explore some of the morphological features of pahoehoe flows.

‘A’a lava is formed when lava flows rapidly, causing the lava to lose heat quickly. As the lava cools, its viscosity increases and the lava hardens. The high flow rates cause surface strains to gouge and tear the surface into jagged pieces, which, in bulk, have come to be known as “clinker.” This characteristic clinker layer is found above and below the interior of ‘a’a lava flows. (Miller et al. 1997) The general form of ‘a’a lava is blocky due in part to the rapid cooling and hardening of the flow.



**Figure 1:** Representative ‘a’a flow. (USGS, T.N. Mattox)

Pahoehoe lava, in contrast, forms at lower flow rates. Its relatively lower viscosity allows it to form its characteristic smooth or “ropy” surface texture through flow-related surface shears. Pahoehoe advances primarily by inflation and breakouts of lobes. Individual pahoehoe flows are rarely more than a meter or two thick, but they thicken by subsequent injection of sub-surface lava (Walker 1991). Unlike ‘a’a lava, pahoehoe exhibits numerous pits and cavities called vesicles, which are formed when the lava hardens before the gas bubbles are able to escape the flow.

**Figure 2:** Representative pahoehoe flow. (USGS, T.N. Mattox)



There are a few interesting similarities between ‘a’a and pahoehoe lava. Both ‘a’a and pahoehoe lava have the same chemical composition and high permeabilities when cooled (due mainly to ‘a’a’s surface clinker layer and pahoehoe’s natural voids and vesicles [Miller et al. 1997]). ‘A’a and pahoehoe can be produced by the same eruption and are commonly found at the same eruption site. Pahoehoe lava often transitions into ‘a’a lava as the distance to the eruptive vent increases (Miller et al. 1997) or if the lava is forced to flow with a sufficiently high shear and viscosity (Peterson and Tilling 1980).

### Tumuli:

Tumuli were named after ancient burial mounds by Daly (1914) due to a close resemblance. A typical tumulus is a mound of rock between 3-6 meters tall and about twice as long with slopes usually between 20-30 degrees (see Fig. 3).

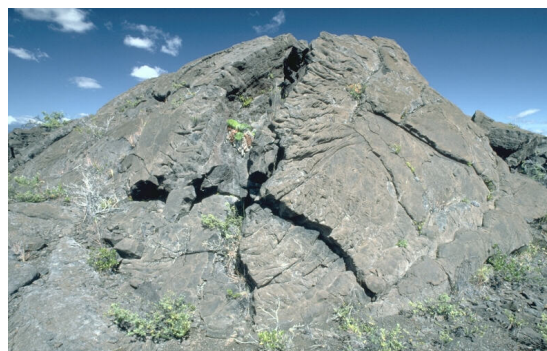


**Figure 3:** Tumulus about 30 m in diameter on the Hilina Pail road on the south flank of Kilauea Volcano, Hawaii. (VHP Photo Glossary)

Tumuli are typically elongated along the direction of flow, with one side being higher and

steeper than the other. They exhibit a major axial cleft up to a few meters wide as well as a few smaller radial clefts. These clefts are at least a meter or two deep, narrow with depth and are usually partially filled with debris. (Walker 1991) Occasionally, lava seeps out from these cracks, partially or fully covering the tumulus (Walker 1991, Rossi and Gudmundsson 1996).

Tumuli are formed when lava is injected just underneath a surface crust. The added pressure lifts the crust into a dome shape. The process of uplifting puts tensile stress in the uplifted crust (Daly 1914), which creates tensile cracks that propagate along the axis of the tumulus and along its sides. The maximum lava overpressure is approximately equal to the hydrostatic pressure due to the height difference between the tumulus and the surface of the lava lake feeding the lava injection (Walker 1991). Rossi and Gudmundsson (1996) observed that the variation in pressure with height affects tumulus

formation, as different kinds of tumuli are formed at different elevations with respect to the lava lake surface. As the cracks propagate downward, they help cool the interior, which causes the cracks to widen as uplift progresses (see Fig. 4).

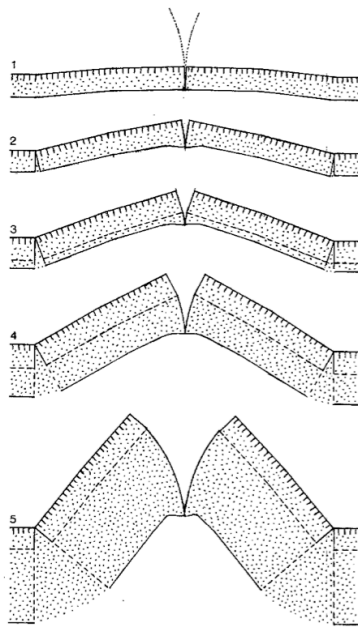


**Figure 4:** Tumulus growth stages. (Walker 1991)

Tumulus formation requires a few conditions to be met. In order to push the crust upwards, the lava needs to be topographically confined in a basin or channel. There also needs to be a balance between the lava pressure and supply rate, the crustal cooling rate, and the size of the

uplift area (Rossi and Gudmundsson 1996). Lower supply rates give the crust time to build tensile strength by cooling so that it is more resistant to cracking as it is raised (Holcomb 1981). Higher supply rates cause lobe breakage without uplift.

#### **Pressure Ridges:**

Pressure ridges are similar in appearance to tumuli, but are formed by a horizontal compression of the crust rather than a vertical pressure from an underlying lava layer. As a result, their total cross-profile crustal width is greater than the width of the structure (Walker 1991). Macdonald (1972) explained pressure ridges as the upheaval and pressure of a lava crust up against some obstacle, a view which others have accepted (e.g. Gary et al. 1972, Bullard 1976).

#### **Lava Rises:**

Previously called “pressure plateaus” due to their plateau-like appearance, lava rises have a formation mechanism similar to that of tumuli. Unlike tumuli, however, lava rises cover much more horizontal ground (tens to hundreds of meters across), are relatively flat on top, and occasionally cave in. (Walker 1991)

#### **Inflation Rifts:**

Previously called “cracks” (Hon et al. 1994) and “lava-inflation clefts” (Walker 1991, 2008); Hoblitt et al. (2012) coined “inflation rifts” to describe the narrow cracks in lava rocks due to lava-induced inflation. Inflation rifts are especially common in pahoehoe tumuli and sheet flows (Hoblitt et al. 2012).

Inflation rifts are formed when a small crack penetrates the viscoelastic layer of a subsurface flow. This greatly reduces the tensile strength of the surrounding rock to the point where lava can begin pushing through. This new lava supply widens the rift, exposing the lava to the air and cooling the lava (Hoblitt et al. 2012) (see Fig. 5). The wider the final rift is, the closer the balance of crustal cooling and lava supply must have been as it formed.

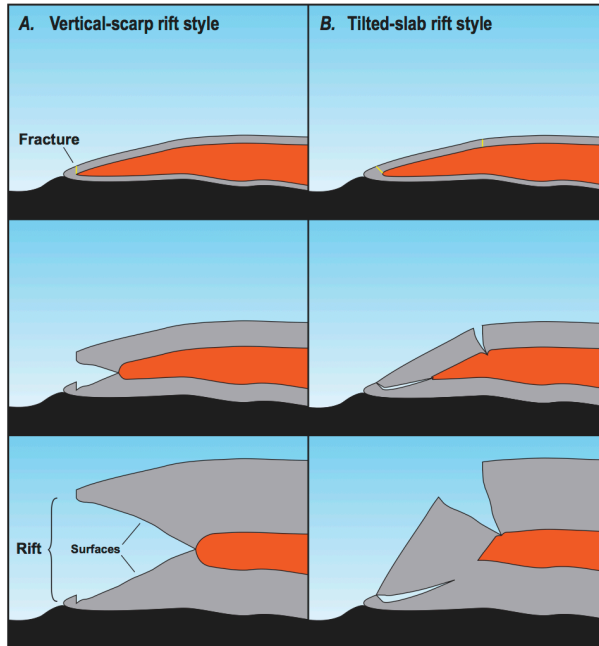


**Figure 5:** Mechanisms for inflation rift growth. (Hoblitt et al. 2012)

### Lava Pits:

Lava pits are simply negative topographic regions where the crust around them was elevated (see Fig. 6). Incorrectly called “subsidence pits,” lava pits do not show evidence of sinking, but rather the upheaval of the crust around them, with their walls closely resembling the walls of lava rises (Walker 1991).

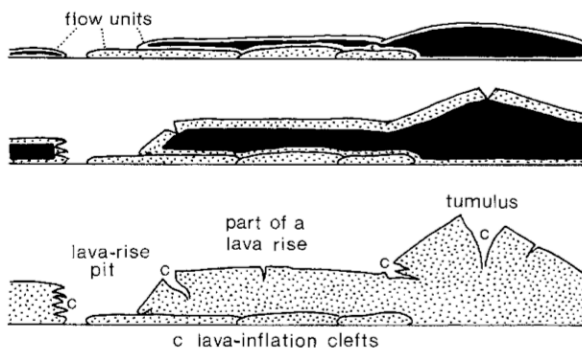


**Figure 6:** Stages of formation of a tumulus, lava rise, and lava pit. Solid black denotes fluid lava injected below the surface crust. (Walker 1991)

### Conclusion:

Walker (1991) estimates that tumuli and lava rises cover over 50% of Hawaiian pahoehoe flow fields. Inflation mechanisms therefore play an important role in shaping lava flows. Understanding these morphologies and their mechanisms has implications for lava flows on Earth as well as other terrestrial planets.

### References:

- Bullard, F.M. (1976). *Volcanoes of the Earth*. University of Texas Press, Austin.
- Daly, R.S. (1914). *Igneous rocks and their origin*. McGraw Hill, New York.
- Gary, M., McAfee, R., Wolf C.L. (eds) (1972). *Glossary of Geology*. Am Geol Inst.
- Holcomb, R.T. (1981). U.S. Geol. Stnv. Open-File Rep. 81-354.
- Hon, K., Kauahikaua, J., Denlinger, R., and Mackay, K. (1994). *Geological Society of America Bulletin*, v. 106, p. 351-370.
- Kauahikaua, J., Cashman, K.V., Mattox, T.N., Heliker, C.C., Hon, K.A., Mangan, M.T., and Thornber, C.R. (1998). *Journal of Geophysical Research*, v. 103, no. B11, p. 27,303-27,323.
- Miller, James A.; Whitehead, R. L.; Oki, Delwyn S.; Gingerich, Stephen B.; Olcott, Perry G. (1997), in Ryder P.D., Ardis A.F., eds. *Hydrology of the Texas Gulf Coast Aquifer Systems*. Denver, CO : U.S. Dept. of the Interior, U.S. Geological Survey : 2002.; 1998.
- Peterson, D.W., and Tilling, R.I. (1980). *Journal of Volcanology and Geothermal Research*, v. 7, p. 271-293.
- Rossi M.J., Gudmundsson A. (1996). *Journal of Volcanology and Geothermal Research* 72:291-308.
- Walker, G.P.L. (1991). *Bulletin of Volcanology*, v. 53, p. 546-558.
- Walker, G.P.L. (2008). In Thordarson, T., et al., eds., *Studies in volcanology; the legacy of George Walker: IAVCEI Special Publication 2*: London, Geological Society of London, p. 17-32.

## Hydrothermal Systems and Soda Dam

Sky Beard

Hydrothermal systems are formed when ground water is heated by magma (or impacts) resulting in hot springs (hydrothermal water mixed with ground water), fumaroles (emitting steam and other gasses), geysers (eject water and steam after being held under pressure), and mineral deposits (precipitation of minerals when going to a lower energy state). Hydrothermal outflow plumes must have convective upflow above a deep reservoir of heat, and lateral flow into a permeable layer next to the region of upflow. To have fluid convection, active faulting is needed to facilitate channels for fluid flow (Heasler et al. 2009)

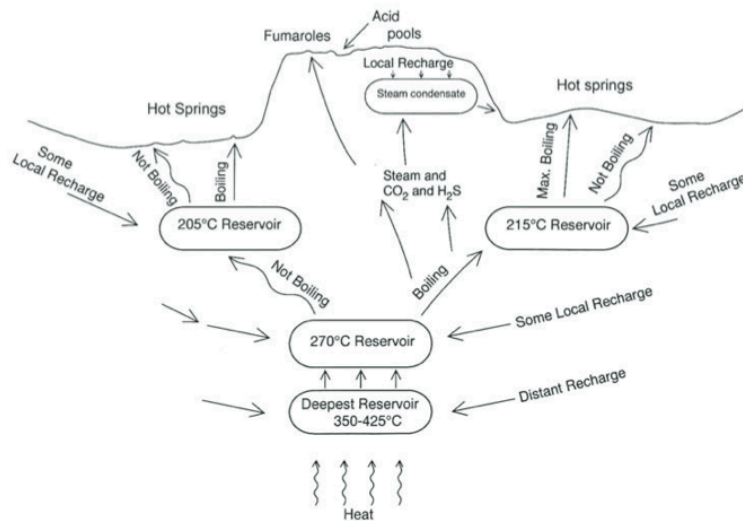


Figure 1. Subsurface geologic flow in a volcano-related hydrothermal system. Deep waters, which have been recharged from distant sources, rise and either conductively cool, boil, and or mix with more local cold waters, as they make their way to the land surface. At the surface, hot spring, geysers, mud pots, and fumaroles can form. Modified from Fournier et al. 1996 in Heasler et al. 2009.

Soda Dam is a carbonate taverntine deposit originating from hot springs that were originally produced by the Valles geothermal system ~1.12 Ma, and represents the most recent spring/tavertine deposit of a long lived hot spring system in the area. Travertine is limestone deposited by mineral/hot springs and forms from rapid precipitation of calcium carbonate. It generally forms from geothermally heated alkaline waters, that when surfaces, degasses  $CO_2$  and increases its pH. Carbonate solubility decreases with increased pH and is therefore precipitated out of solution. Large tavertine deposits can be found 215 meters above the present springs along the west wall of the San Diego Canyon. These deposits have been used to try and unlock clues to the evolution of the hydrothermal system, such as the age and the fluctuations in size and temperature, using U-Th disequilibrium techniques and stable isotope analysis (Goff and Shevenell 1987).

Soda Dam discharges along the Jemez River through the San Diego Canyon (Paleozoic and Precambrian rock) which was filled with hundreds of meters of Bandelier Tuff at 1.12 Ma. The Valles hydrothermal system dates to at least 1.0 Ma, which is roughly as old as the caldera itself. The basic hydrology of the system is

thought to be practically unchanged since the time of formation, though studies of the travertine ages show occasional pulses in travertine deposition from 1.0-0.48 Ma, 0.107-0.058Ma, and from 0.005 Ma to present (Goff and Shevenell 1987).

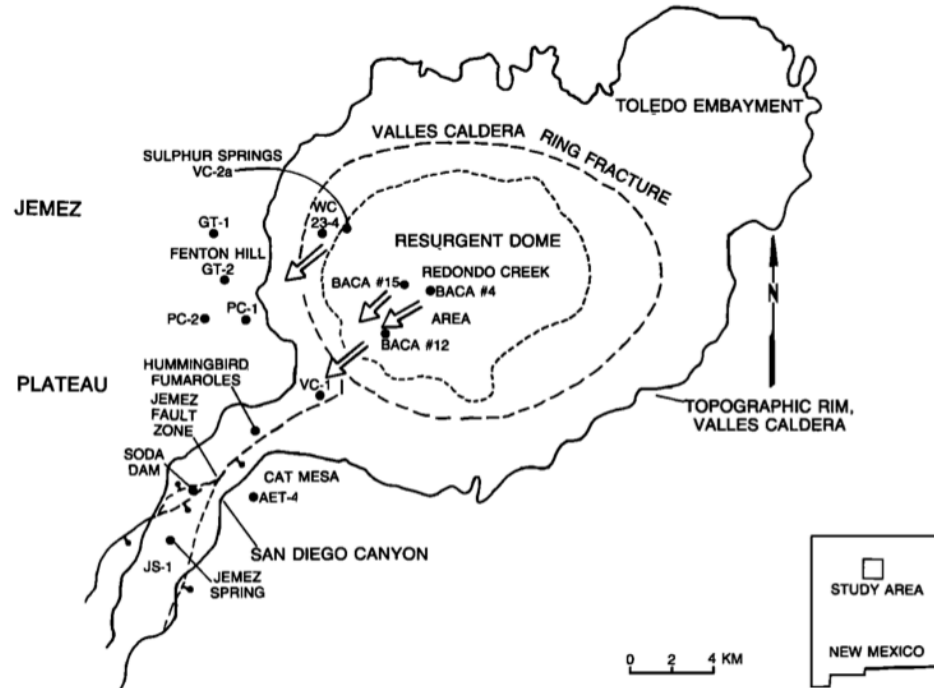


Fig. 1. Sketch map showing the locations of 12 geothermal wells in the Valles caldera region; the short-dashed line outlines the border of the resurgent dome within Valles caldera. Large arrows show the two source reservoirs and direction of lateral flow of the Valles caldera hydrothermal plume.

Figure 2, above, from Goff et al. 1988.

Volumes of these deposits show that Soda Dam was once larger than it is today, perhaps up to 5-10 times as much discharge of fluid ( $Na-HCO_3-Cl$ ). Stable isotope studies of the travertines show that although Soda Dam was larger in the past, the temperature was never more than  $10^{\circ}C$  higher than what is seen today ( $\sim 48^{\circ}C$ ). Incision rates by the Jemez River through the tuff are implied to be relatively rapid because of the similar ages of the caldera system and large scale deposition of travertine from hydrothermal circulation (cut through  $\sim 400$  m of tuff in 100,000 years or less).

Geologic data (geophysical, chemical, and drill hole) indicate the waters of Soda Dam originate from a lateral outflow plume from the  $200-300^{\circ}C$  hydrothermal system of the caldera. This water flows along the Jemez fault zone while mixing and diluting with ground water. Finally the water emerges at the surface between  $32-48^{\circ}C$ . There are 20 hot springs and hot seeps in the area presently. The total discharge of the system has varied from 400 L/min to 1,500 L/min over the past 80 years (as of 1987, Trainer 1987).

The Valles hydrothermal system was originally very hot, with fluid temperatures estimated to be  $300^{\circ}C$  at just 400 meters depth (at 1 Ma). Today, these fluid temperatures are found at 2-3km depth, where the flow system originates next to

magma pockets (Grigsby 1982, Goff et al. 1992). The fluid convectively rises for 500-600 meters and then heads laterally toward the caldera wall, which is why most of the hot-springs and fumaroles are around the perimeter of the caldera.

Chemically, the waters of Soda Dam are predominantly  $Na-HCO_3-Cl$ , with concentrations of 1500mg/kg of  $HCO_3$ , 1500 mg/kg  $Cl$ , and 4600 mg/kg in total dissolved solids. The water also has significant amounts of  $Ca$  and  $Mg$  which is thought to indicate that the hydrothermal fluids are dissolving the paleozoic limestone. The concentrations of  $Na$  and  $Cl$  are about 25% less in the Soda Dam than in other local hydrothermal areas, which is caused by dilution in the ground water.

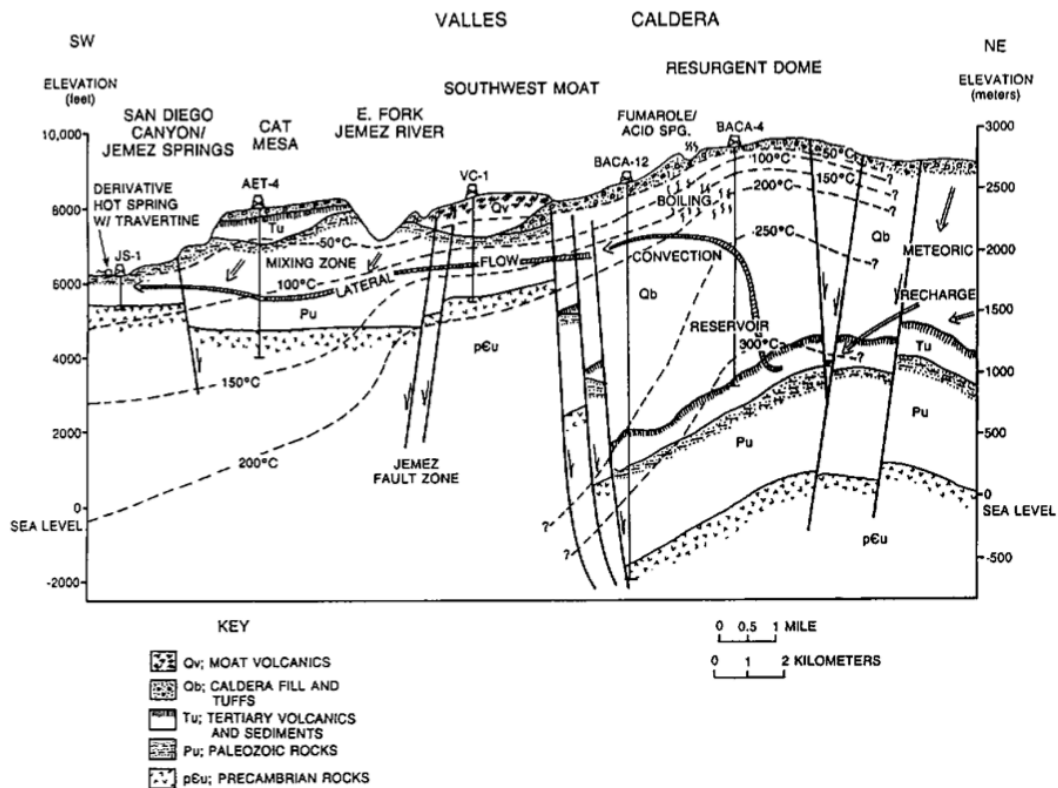


Fig. 6: Cross-section of southwest margin, Valles caldera showing general configuration of the active hydrothermal system (modified from Goff et al., 1988). Surface geology, wellbore data, geophysics and fluid geochemistry provide tight constraints on this model.

Figure 3, above, shows a cross section of the caldera along with prominent flow paths of fluids in the system, from Goff et al. 1992

Soda Dam itself is a formation of travertine that extends across a narrow gorge of the Jemez River. The travertine extends for 100m in length and is 25 m wide. Depending on the flow rates, there are several points along and around Soda Dam where thermal water issues, including from an interesting 1m tall travertine mound inside a cave to the southeast (Grotto Spring). Soda Dam use to have fresh deposits of calcite from a central fissure, which has since been destroyed when the highway

department blasted a notch in the dam, altering the flow (~1965), and without replenishment of calcite, Soda Dam is disintegrating.

There are three older deposits (Fig 4) of travertine around Soda Dam, extending to about 1 km southwest of and up to 215 meters higher in elevation than Soda Dam (7000 ft asl). Deposit A is primarily porous tufa and massive travertine layers (up to 2m thick) that contain calcite “dikes” and “sills” that were possibly feeder conduits for ancient springs.

Episodic behavior of travertine deposition is implied from dating techniques, though it is possible that some travertines have been destroyed through erosion (though there are no signs to indicate this). Factors that influence travertine deposition include the amount of precipitation, magmatic activity, and hydrology of the caldera. The Bandalier magma chamber that formed the Valles caldera is the heat source driving hydrothermal activity. There have been post-caldera rhyolite dome eruptions that inject heat into the shallow crust at ~100,000 year intervals, which would likely cause fluctuations in hydrothermal activity (Goff and Shevenell 1987).

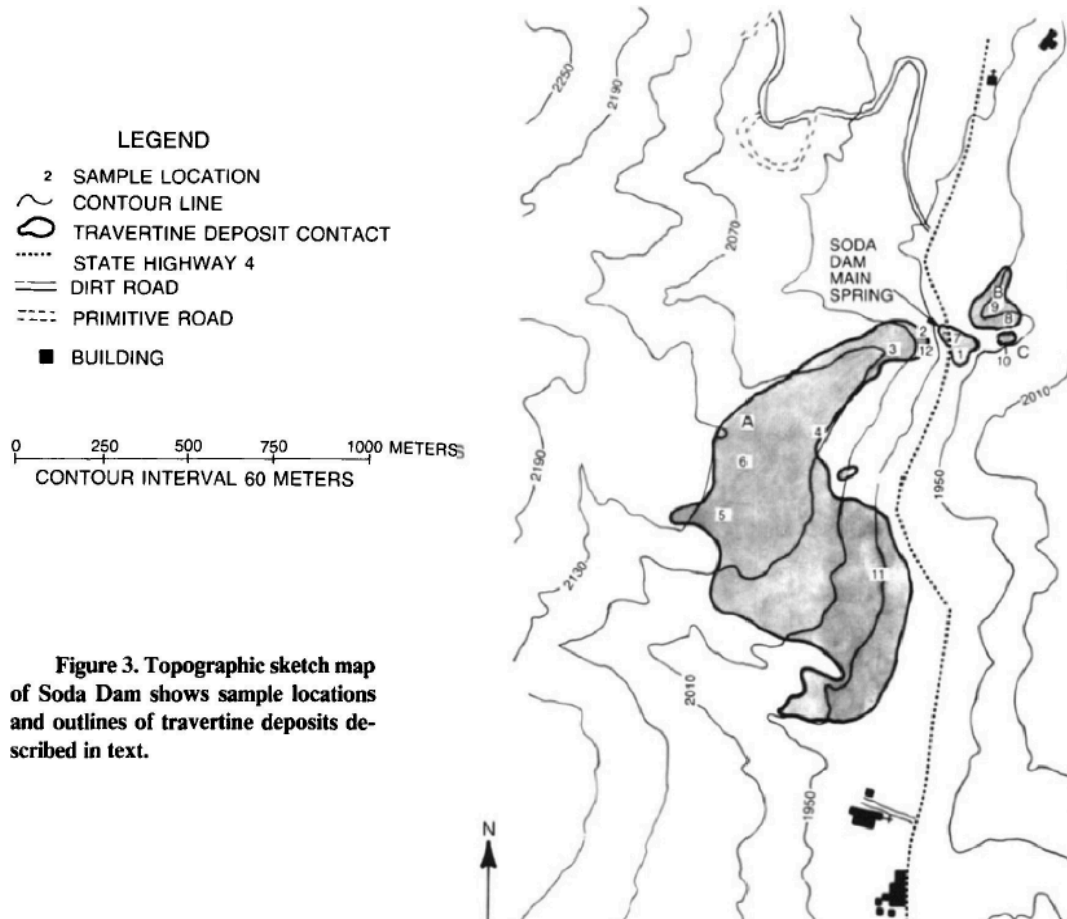


Figure 4, above, from Goff and Shevenell 1987.

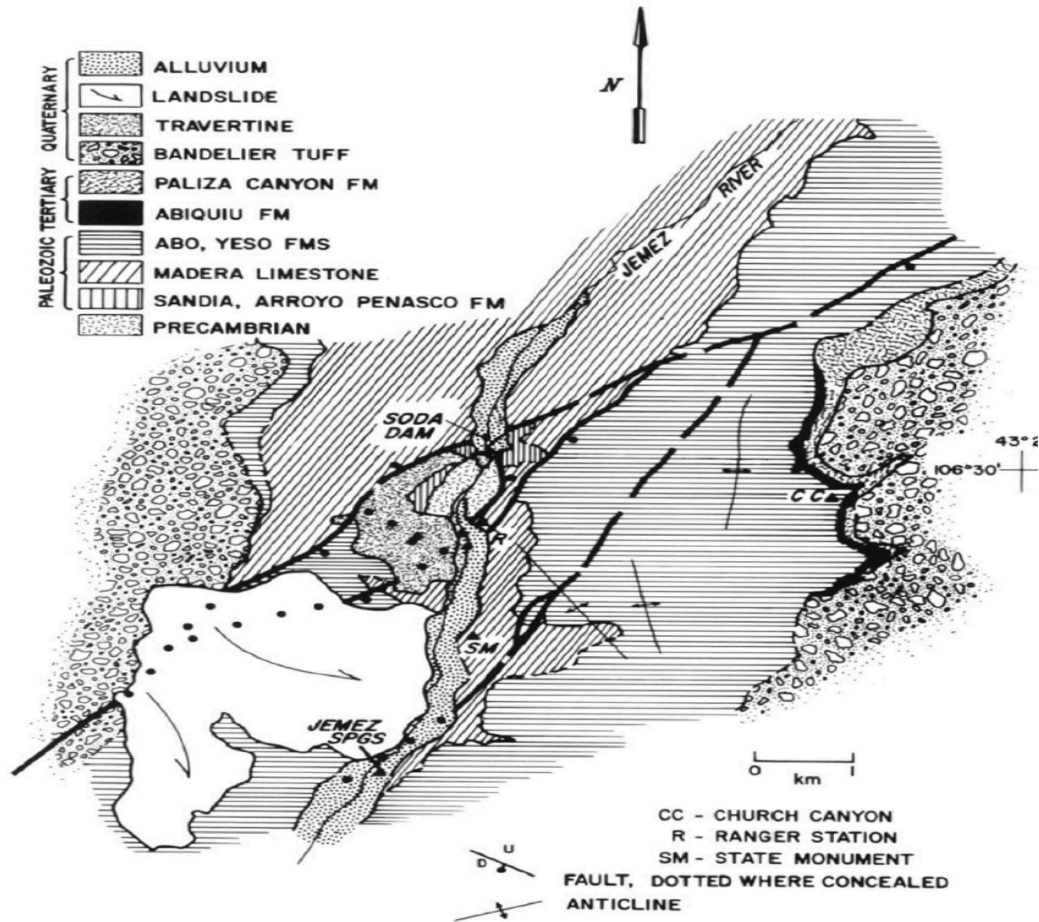


Figure 5: Geologic context surrounding Soda Dam.

### Hydrothermal Systems from Impacts:

Hydrothermal systems can also be formed due to impacts. High velocity impacts, capable of producing craters, in presence of water at or near the surface of earth will disrupt the local hydrosphere (if there is one). This happens by interaction of ground water with the hot, impact generated rocks or shock generated melt. The extent of the disruption depends on the magnitude of the impact and the particulars of the cooling mechanisms. This interaction can dissolve, transport, and precipitate various minerals, and can contribute to regolith modification and soil development. One terrestrial example is the Haughton impact structure (~24km) in arctic Canada (75N), where hydrothermal alteration was recognized within impact breccias in the central portion of the structure and in localized pipes in the concentric fault system (impact induced). Breccia alteration at this location showed three forms of fracture filling dominated by sulfide with the presence of carbonate, carbonate, or sulfate alone. Minor constituents include celestite, barite, fluorite, quartz, marcasite, and selenite. These and other components will precipitate at different temperatures and can help us understand its hydrothermal history. Osinski et al 2001, proposed three stages of evolution including an early stage (>200), main stage (200-100), and a late stage (<100). They also estimate “that it took several tens of thousands of years to cool below 50C following impact.” (Fig. 6).

The time estimation comes from necessary cooling rates to deposit specific minerals, for example, Fournier, 1985 showed that quartz precipitation generally occurs at temperatures below 200-340°C, and rapid cooling will deposit amorphous silica, which has not been observed at Haughton.

During the impact, the water table would be disrupted and not reequilibrate until after the crater modification ended. At this point water will be rising from depth and also flow in laterally. In the hot breccia lens, the water would be boiled off and this region of the hydrothermal system would be vapor dominated (Fig. 7). Deeper down, there is a transition zone to a vapor+liquid dominated region. The vapor migrates upwards while the liquid phase travels laterally (for up to several km) away from the boiling zone, where it can interact with cooler ground water or discharge in hot springs or fumeroles (Osinski et al. 2001).

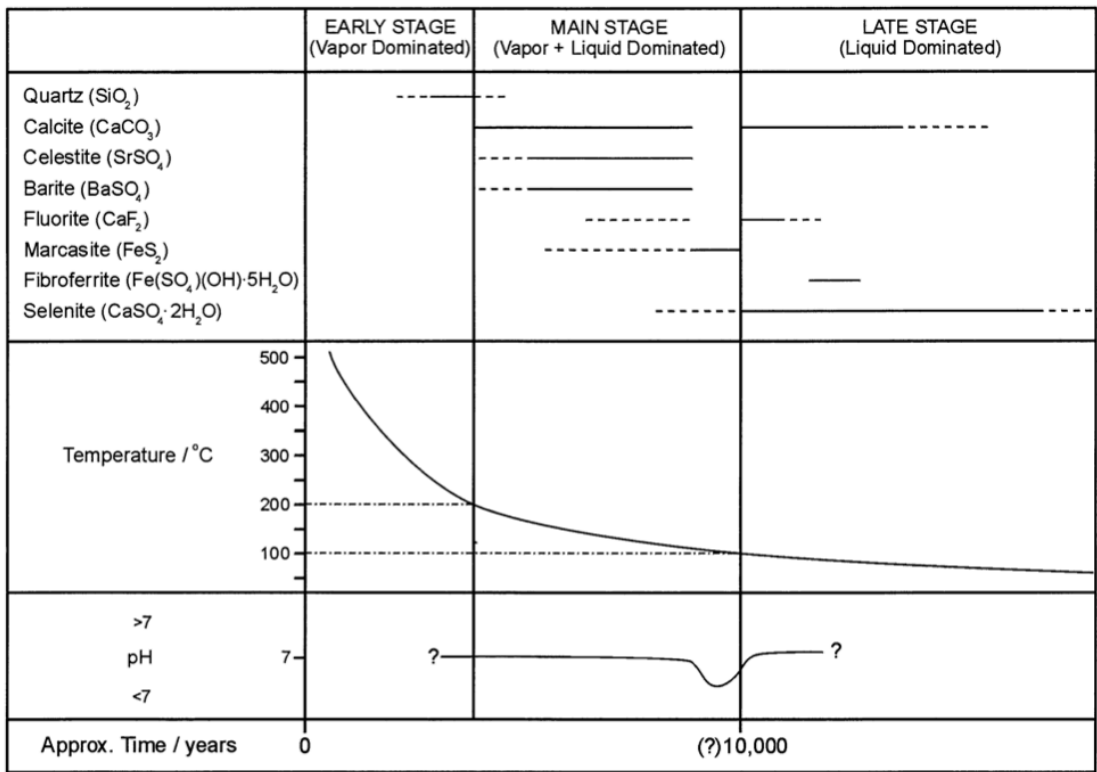


Figure 6: Hydrothermal mineralization sequence for breccia mineralization at Haughton crater. Quartz was the first to be precipitated from hydrothermal solutions at temperatures of 200-340 C. Calcite precipitation followed and continued into the late stages. As pH decreased, deposition of marcasite crystals began forming. Precipitation of selenite in the lower reaches of the poynict impact breccias was also in the late-stage event. Temperature, pH, and duration estimate are further discussed in the text of Osinski et al. 2001

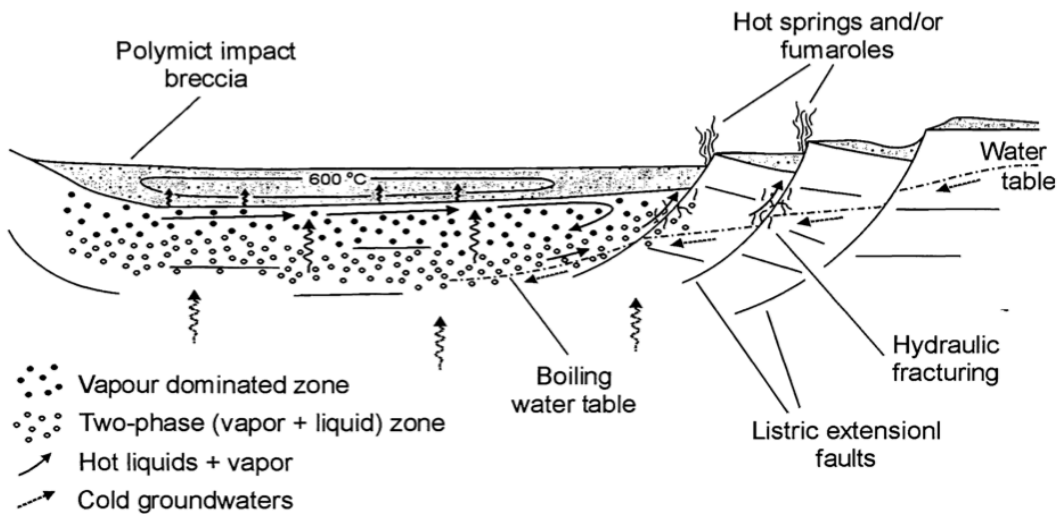


FIG. 5. Schematic model of the early stage of hydrothermal activity within the Houghton impact structure. Trapped pore waters and groundwaters interact with the hot polymict impact breccias. Impact-generated faults act as fluid pathways enabling hot liquids and steam to migrate and possibly discharge, forming hot springs and/or fumaroles at surface.

Figure 7, from Osinski et al. 2001

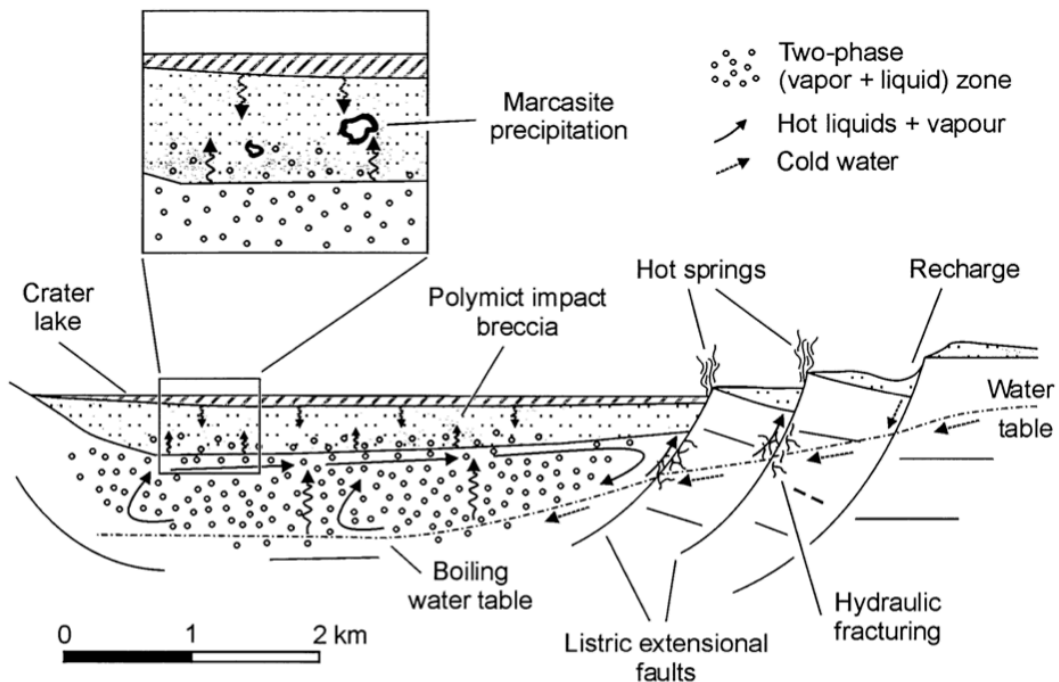


FIG. 6. Schematic model of the main stage of hydrothermal activity showing the development of a simple convection system. Progressive cooling of the polymict impact breccias, the development of a crater lake and boiling of the hydrothermal fluids led to precipitation of a series of alteration mineral assemblages.

Figure 8, from Osinski et al. 2001

# Hot Springs Astrobiology

**extremophile** -- an organism that lives in "extreme" conditions which are harmful to many other terrestrial species. Most extremophilic species are microbes, commonly Archaeans.

- *thermophiles* - thrive at temperatures  $>45^{\circ}\text{C}$ 
  - *hyperthermophiles* - optimum temperatures  $80\text{-}122^{\circ}\text{C}$
- *acidophiles* - pH optimum at 3 or less

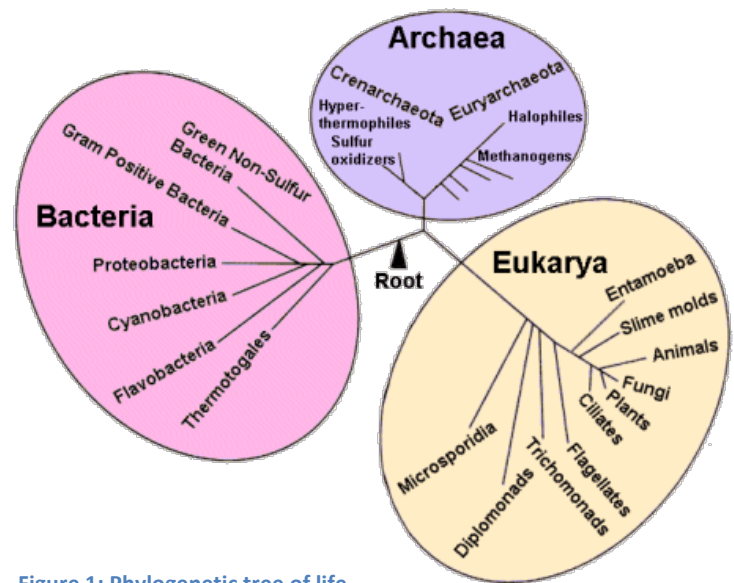


Figure 1: Phylogenetic tree of life.

Hot springs are an example of an environment with extreme temperatures and sometimes extreme pH levels, and can contain abundant extremophilic diversity. These organisms can be autotrophic or heterotrophic, and have a range of metabolic chemistries. Metabolism is fundamentally oxidation-reduction (redox) reactions:

electron donor (oxidized)  $\rightleftharpoons$  electron acceptor (reduced)

Laboratory and environmental studies suggest that thermophiles and hyperthermophiles can metabolize using a range of electron donors ( $\text{H}_2$ ,  $\text{Fe}^{2+}$ ,  $\text{H}_2\text{S}$ ,  $\text{S}$ ,  $\text{S}_2\text{O}_3^{2-}$ ,  $\text{S}_4\text{O}_6^{2-}$ , sulfide minerals,  $\text{CH}_4$ , various mono-, di-, and hydroxy-carboxylic acids, alcohols, amino acids, and complex organic substrates) and electron acceptors ( $\text{O}_2$ ,  $\text{Fe}^{3+}$ ,  $\text{CO}_2$ ,  $\text{CO}$ ,  $\text{NO}_3^-$ ,  $\text{NO}_2^-$ ,  $\text{NO}$ ,  $\text{N}_2\text{O}$ ,  $\text{SO}_4^{2-}$ ,  $\text{SO}_3^{2-}$ ,  $\text{S}_2\text{O}_3^{2-}$ , and  $\text{S}$ ) (Amend & Shock 2001).

## Terrestrial Case Studies:

- Tiberias hot springs, Israel - possibly the first hot spring from which a thermophile was isolated (Figure 2); taxonomy unknown, but optimal growth at  $50^{\circ}\text{C}$ . No growth observed at  $T < 37^{\circ}\text{C}$  (Kahan 1961).
- Yellowstone National Park - known for abundant geothermal springs and diverse microbiology
  - Acidothermophile isolated which survives in temperatures from  $45\text{-}70^{\circ}\text{C}$  and at a pH as low as 2. Capable of oxidizing either iron or sulfur (Brierley & Brierley 1972).
  - *Chromatium tepidum* sp. nov. (Figure 3) – new species of obligate photosynthetic purple bacteria found in a hot spring microbial mat (See Figure 4 for typical mat structure); optimum temperature for growth was  $49^{\circ}\text{C}$ . Pigmentation due to bacteriochlorophyll *a* and carotenoids (Madigan 1986).

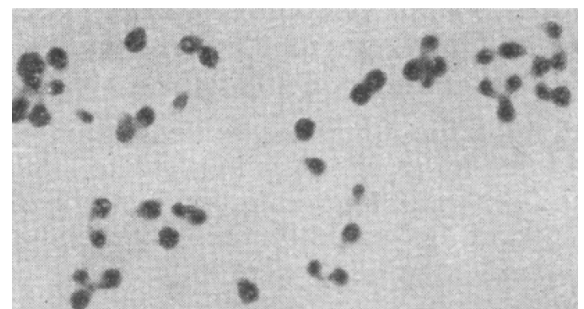


Figure 2: Micrograph of thermophilic isolate, Kahan 1961.

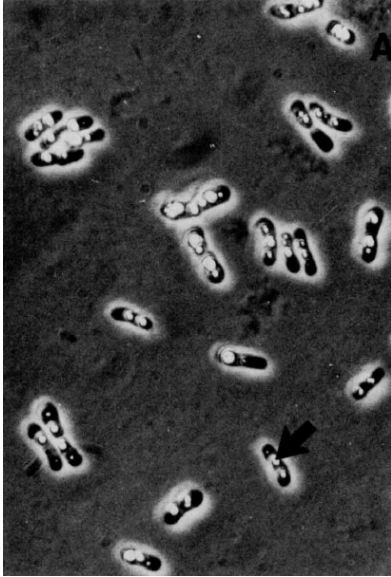


Figure 3: Micrograph of *C. tepidum*; white spots are sulfur in actively-metabolizing cells. From Madigan 1986.

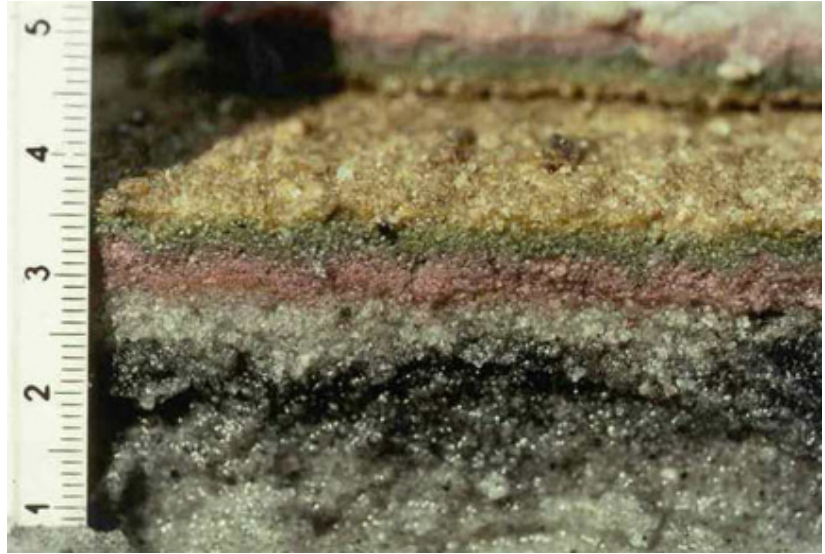


Figure 4: Microbial mat stratification; different pigments imply different chlorophyll types and photosynthetic wavelengths.

- Northwestern Great Basin, tectonically-driven water heating and circulation;  $T > 73^{\circ}\text{C}$ . Contained an abundance of uncultivable species, so metabolisms difficult to determine (Costa et al., 2009)
- Northern Nevada hot springs (4 sites) found archaea at temperatures between  $40\text{-}84^{\circ}\text{C}$  and pHs from 6.0-9.2 (Pearson et al 2004).

### Microbiology of New Mexico Hot Springs

Hot springs in New Mexico, including the Soda Dam hydrothermal area and nearby regions, have been the focus of several microbiology studies:

- Anoxygenic phototroph<sup>1</sup>, mildly thermophilic (optimal temperature  $\sim 42^{\circ}\text{C}$ ), nonsulfur purple bacterium isolated from a Soda Dam microbial mat. Strain of *Rhodospseudomonas*, which contains bacteriochlorophyll *b*, (Resnick & Madigan 1989).
- A microbiological and geochemical study (Rzonca & Schulze-Makuch 2003) of 11 hydrothermal sites in the Rio Grande Rift and Valles caldera identified three chemical groups with differing biomass and diversity. Figure 6 shows the locations of these sample

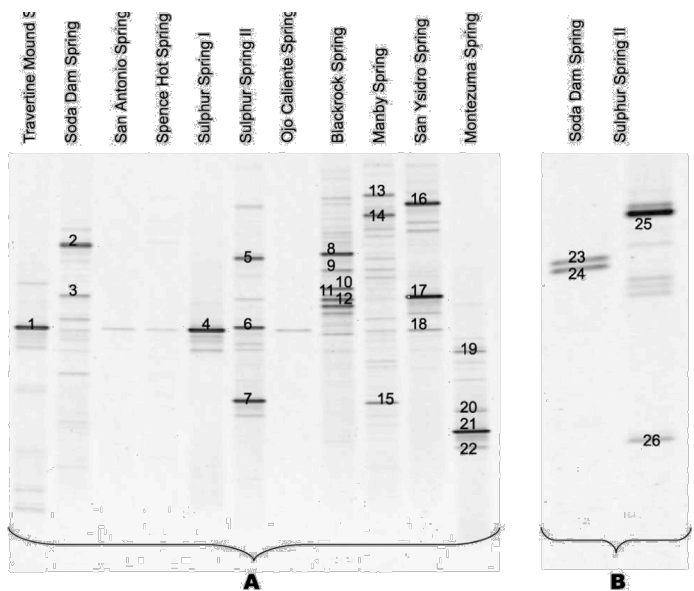


Figure 5: DGGE showing biodiversity of hydrothermal sites from Rzonca & Schulze-Makuch 2003. A=bacteria; B=archaea

<sup>1</sup> Anoxygenic photosynthesis doesn't use water as the reducing agent (therefore doesn't produce oxygen); a common alternate electron donor is sulfur (for sulfur bacteria), whereas non-sulfur bacteria typically use  $\text{H}_2$ .

sites as well as their chemical compositions; note the divisions into deep thermal/derivative waters, acid sulfate waters, and thermal meteoric waters. Acid sulfate waters mostly contained thermophilic microbes and had high biomass, whereas deep geothermal waters had high diversity but low biomass. Thermal meteoric waters had low biomass and low diversity (Figure 5).

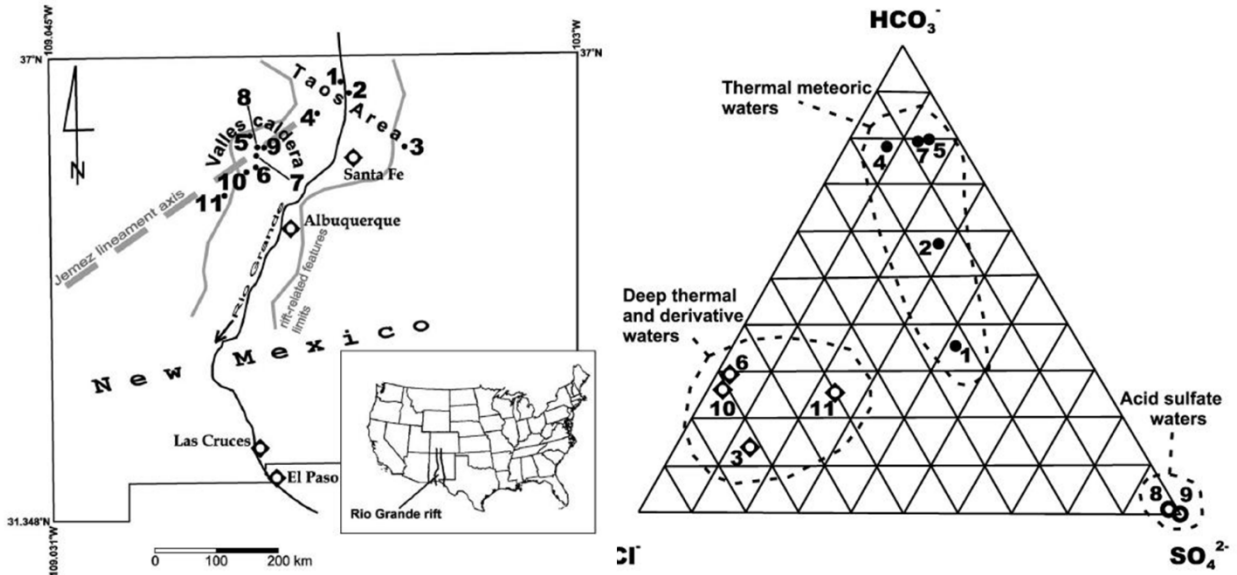


Figure 6: Northern New Mexico sample sites and chemical compositions from Rzonca & Schulze-Makuch (2003).

### Hydrothermal Springs on Mars: Implications for Life

- Hydrothermal systems associated with impact craters (Figure 7) could have created transient habitable areas near the surface, even under cold climactic conditions, as long as sufficient water was present (Rathburn & Squyres 2002). Although it's been argued that only very large impacts could produce extensive hydrothermal systems, so they may have only been relevant during periods with high cratering rates (Noachian) (Pope et al 2006).

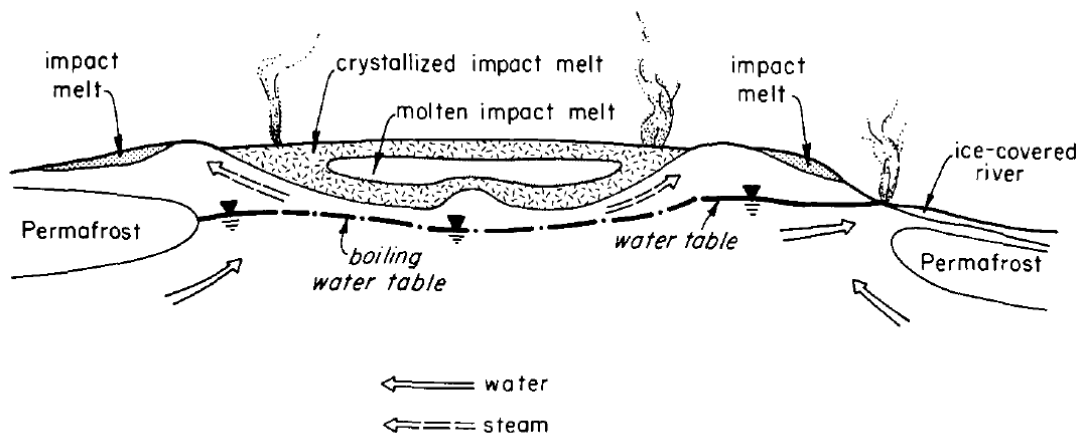
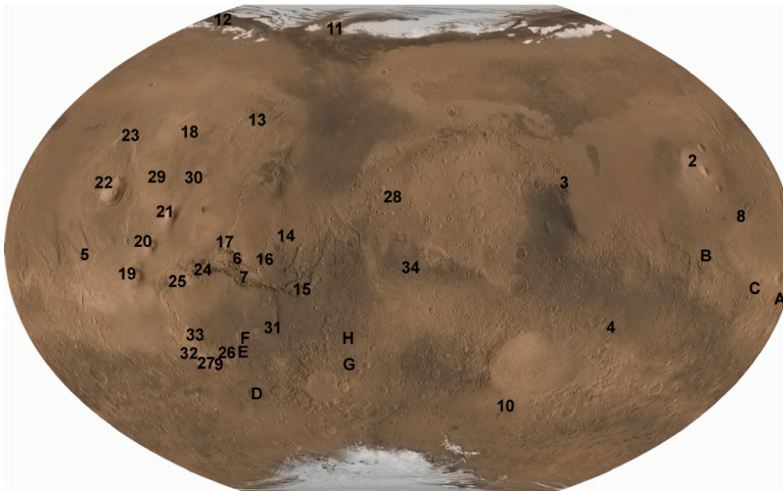


Figure 4. Illustration of impact-related hydrothermal system on Mars, showing hot-spring locations around melt-sheet fringes. Modified from Newsom (1980).

Figure 7: Impact-generated hydrothermal systems; from Breckenridge et al. (1985).

- Vernal Crater, Arabia Terra - contains structures best explained by ancient subsurface fluid movement and spring activity (Allen & Oehler 2008).
- Nili Patera caldera, Syrtis Major – observations of silica deposits consistent with late-stage (post-Early Hesperian), volcanically-driven hydrothermal system (Skok et al 2010).
- Schulze-Makuch, et al (2007) also identified several candidate hydrothermal targets on Mars based on a range of geomorphologic, stratigraphic, topographic, and compositional observations (Figure 8).

Since life on Earth may have emerged in hydrothermal systems (most likely marine), and because these types of environments are known to preserve terrestrial biosignatures and microfossils, potential sites of hydrothermal activity on Mars are of high astrobiological significance.



**Figure 8: Potential hydrothermal sites from Schulze-Makuch et al (2007). Numbers correspond to endogenic sources (e.g. volcanic or tectonic), and letters correspond to candidate large impact basins.**

## References

- Allen, C.C. & D.Z. Oehler (2008). *Astrobiology* 8:1093-1112.
- Amend J.P., E.L. Shock (2001). *FEMS Microbiology Reviews* 25:175-243.
- Brakenridge G.R., H.E. Newson, V.R. Baker (1985). *Geology* 13:859-862.
- Brierley C.L. & J.A. Brierley (1972). *Canadian Journal of Microbiology* 19:183-188.
- Costa K.C., J.B. Navarro, E.L. Shock, C.L. Zhang, D. Soukup, B.P. Hedlund (2009). *Extremophiles* 13:447-459.
- Kahan D. (1961). *Nature* 192:1212-1213.
- Madigan M.T. (1986). *International Journal of Systematic Bacteriology* 36:222-227.
- Pearson A., Z. Huang, A.E. Ingalls, C.S. Romanek, J. Wiegel, K.H. Freeman, R.H. Smittenberg, C.L. Zhang (2004). *Applied Environmental Microbiology* 70:5229-5237.
- Pope K.O., S.W. Kieffer, D.E. Ames (2006). *Icarus* 183:1-9.
- Rathburn J.A. & S.W. Squyres (2002). *Icarus* 157:362-372.
- Resnick S.M. & M.T. Madigan (1989). *FEMS Microbiology Letters* 65:165-170.
- Schulze-Makuch D., J.M. Dohm, C. Fan, A.G. Fairen, J.A.P. Rodriguez, V.R. Baker, W. Fink (2007). *Icarus* 189:308-324.
- Skok J.R., J.F. Mustard, B.L. Ehlmann, R.E. Milliken, S.L. Murchie (2010). *Nature Geoscience* 3:838-841.

# Supervolcanoes & the Valles Caldera Eruptions

## Ning Ding

### Supervolcanoes

A supervolcano is capable of producing a volcanic eruption with ejecta greater than  $1,000\text{km}^3$ , eruptions that are thousands of times larger than most historic volcanic eruptions. Supervolcanoes can occur when magma in the Earth rises into the crust from a hotspot but is unable to break through the crust. Pressure builds in a large and growing magma pool until the crust is unable to contain the pressure, causing a monumental explosion<sup>[1]</sup>.

**Tamu Massif** is the Earth's largest volcano, and it lurks beneath Pacific Ocean<sup>[2]</sup>. Shatsky Rise is a large plateau with a volume of  $\sim 2.5 \times 10^6 \text{ km}^3$ , and total area similar to Japan or California.

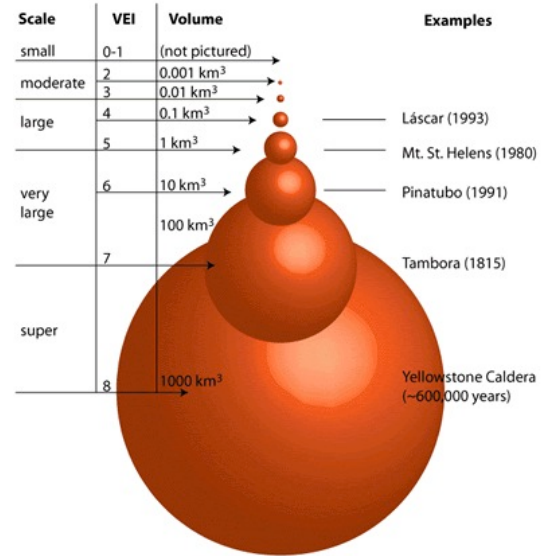


Fig.1 Volcanic eruptions are classified using the **Volcanic Explosivity Index—VEI**<sup>[3]</sup>.

### Caldera

Calderas are the huge depressions created after the supervolcanic eruption<sup>[3]</sup>. A collapse is triggered by the emptying of the magma chamber beneath the volcano, usually as the result of a **large volcanic eruption**. If enough magma is ejected, the emptied chamber is unable to support the weight of the volcanic edifice above it. A roughly circular fracture, the ring fault, develops around the edge of the chamber. Ring fractures serve as feeders for fault intrusions which are also known as ring dykes.

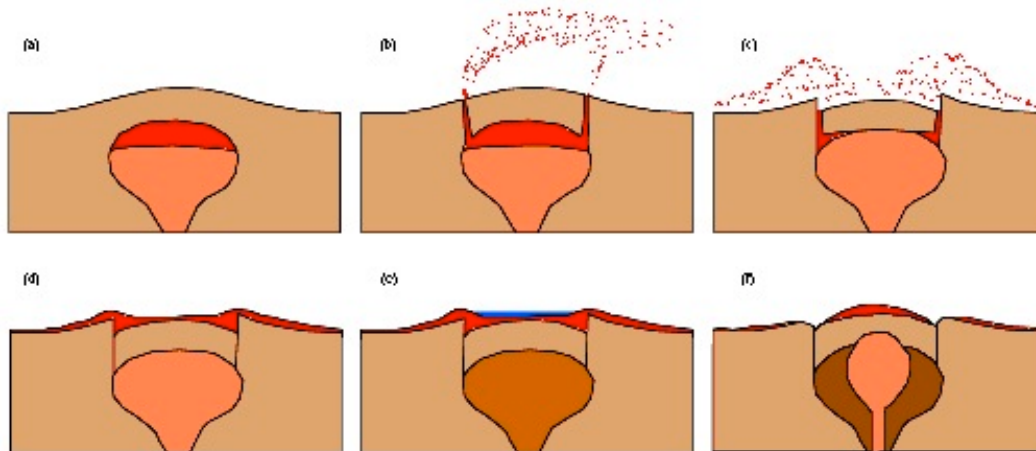


Fig.2 Formation model of Valles caldera of New Mexico<sup>[4]</sup>.

## **Valles Caldera**

Valles Caldera (or Jemez Caldera) is a 22.0 km wide volcanic caldera in the Jemez Mountains of northern New Mexico. Valles Caldera is one of the smaller volcanoes in the supervolcano class (VEI-7)<sup>[5]</sup>. The caldera only measures 22.0 km across as opposed to the **Yellowstone caldera** which is 72 km wide and 55 km long. The Valles Caldera is the younger of two calderas known at this location, having collapsed over and buried the **Toledo Caldera**, which in turn may have collapsed over yet older calderas. It last exploded 1.47 Myr and 1.15 Myr ago, piling up 625 km<sup>3</sup> of rock and blasting ash as far away as Iowa. Many of the formations in Bandelier National Monument were created by ash deposits from Valles Caldera<sup>[6]</sup>. Seismic investigations show that a low-velocity zone lies beneath the caldera, and an active geothermal system with hot springs and fumaroles exists today<sup>[5]</sup>.

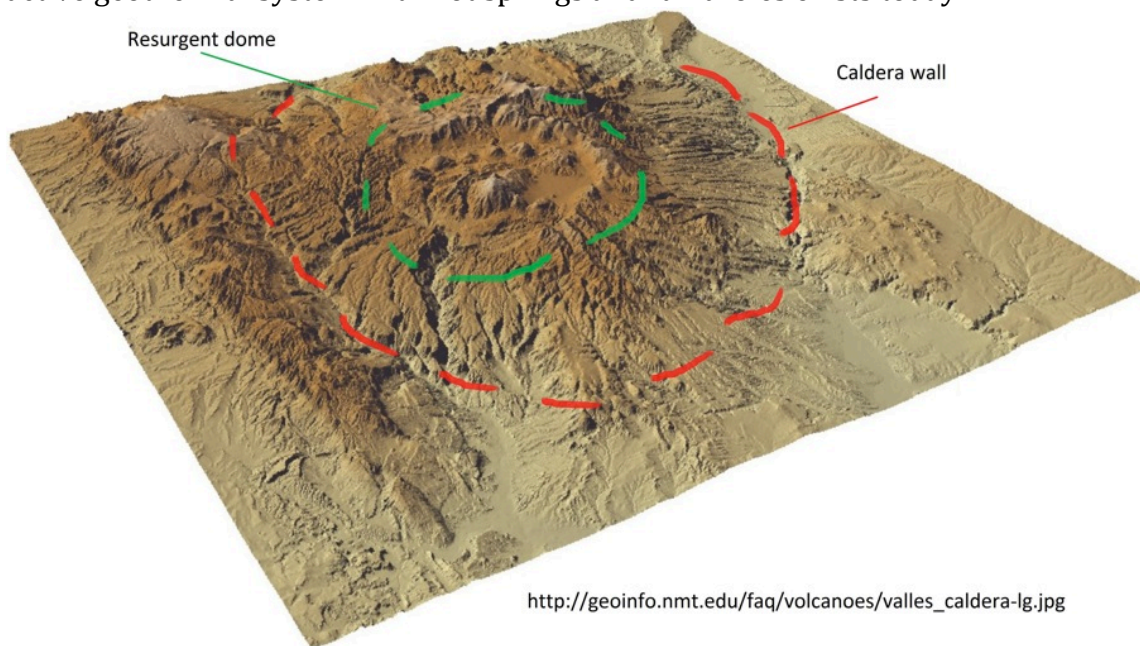


Fig.3 View of the Jemez Mountains, Sierra Nacimiento, and the Valles caldera from the southwest<sup>[7]</sup>.

Supervolcanoes are on a much bigger scale than normal volcanoes and an eruption would have global consequences<sup>[3]</sup>. Supervolcanoes like Valles Caldera have been blamed for mass extinctions throughout Earth's history, increased greenhouse gasses, and even a change in the circulation of the Earth's oceanic currents.

## **Reference**

[3] <http://en.wikipedia.org/wiki/Supervolcano>

[8] Sager W.W. et al., 2013. An immense shield volcano within the Shatsky Rise oceanic plateau, northwest Pacific Ocean. Nature Geoscience. DOI: 10.1038/NGE01934

[7] <http://www.hinchingbrookeschool.co.uk/geography/GCSERestlessEarth5.html>

[2] <http://astro.if.ufrgs.br/solar/valles.htm>

[5] [http://en.wikipedia.org/wiki/Valles\\_Caldera](http://en.wikipedia.org/wiki/Valles_Caldera)

[6] <http://seethesouthwest.com/2402/valles-caldera-new-mexicos-supervolcano/>

[1] <http://volcano.oregonstate.edu/calderacollapse>

# Resurgent Domes

Catherine Elder

## 1 Postcollapse magmatism and resurgent domes

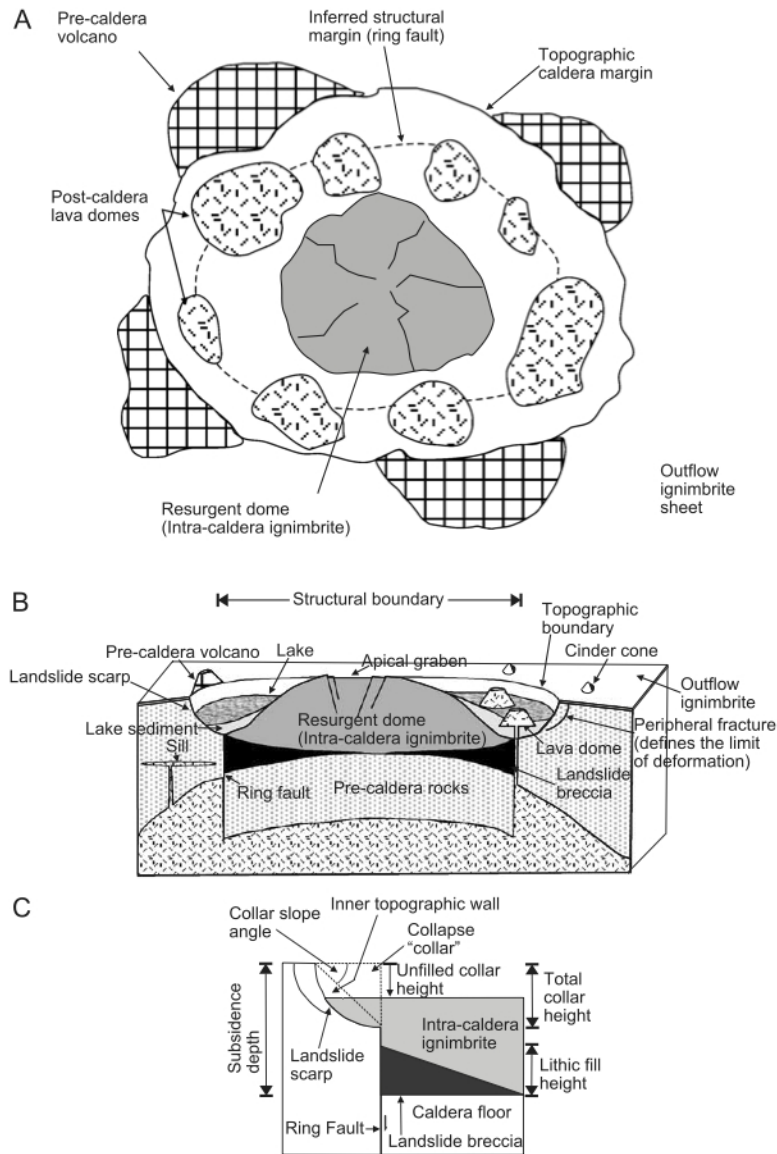


Figure 1: A) map, B) block diagram, and C) terminology of a piston-type caldera. Not all calderas will have all of the labeled features (Cole *et al.* 2005).

- Postcollapse magmatism can continue intermittently for millions of years (Lipman 1999). It can be caused by the upward resurgence of magma into the magma chamber or post-caldera sill emplacement (Cole *et al.* 2005).

- Volcanism after caldera formation can be randomly scattered within the caldera or localized along regional structural trends (Cole *et al.* 2005).
- Thermal modeling suggests that heat loss by hydrothermal convection is so great that shallow caldera-related magmatic systems cannot survive more than a few hundred thousand years without replenishment by additional magmatism, but long histories of postcollapse volcanism at many calderas suggests that replenishment must be common (Lipman 1999).
- The renewed rise of magma can also uplift calderas by doming or block uplift of the core of the caldera or it could affect the region and uplift one or more calderas in adjacent portions of the volcanic field (Lipman 1999).
- Broad uplift is detected in some young volcanic fields by regionally high topography, slight tilting of volcanic strata away from central parts of the field, and extensional structures between individual calderas. This is interpreted to be broad resurgence of an underlying batholithic magma body that is larger than any individual caldera (Lipman 1999)
- Faults created during the caldera formation can be reactivated in the opposite sense as part of the caldera is forced upwards. New faults can also be created and are often exposed in the resurgence dome (including at Valles Caldera). Post-caldera sediments can provide a record of the resurgence process (Cole *et al.* 2005).
- Resurgent calderas are more common within continental crust than in young volcanic arcs within ocean basins (Lipman 1999).

## 2 Valles Caldera and Redondo peak



Figure 2: Redondo peak, Valles Caldera (Price 2010).

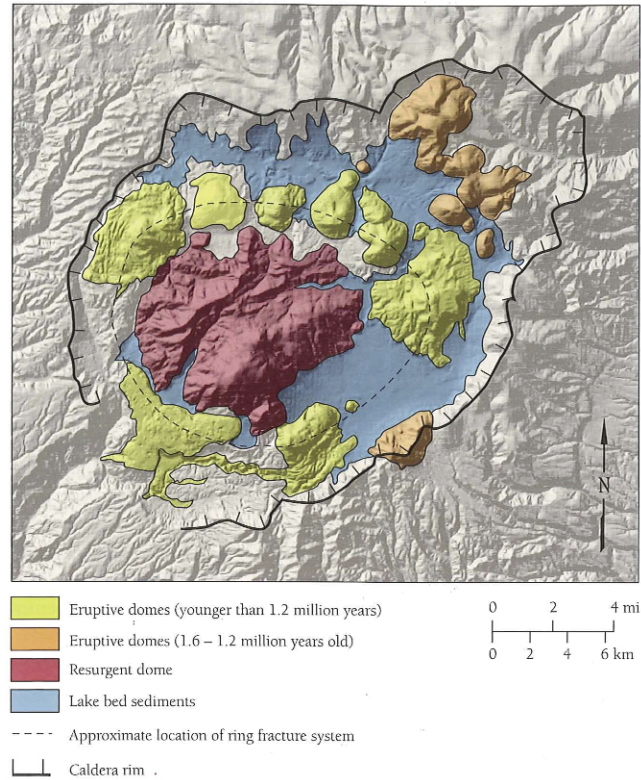
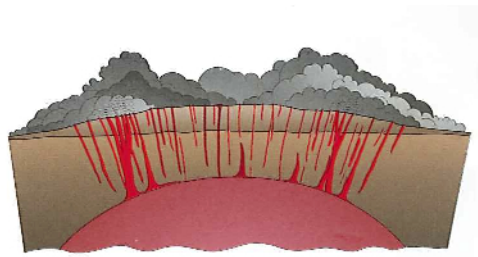
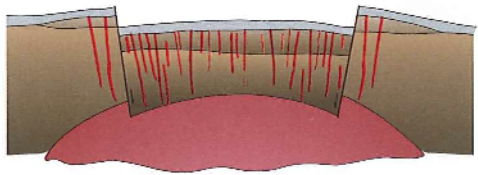


Figure 3: Map of Valles caldera which shows Redondo Peak (the resurgent dome) and younger eruptive domes (Price 2010).

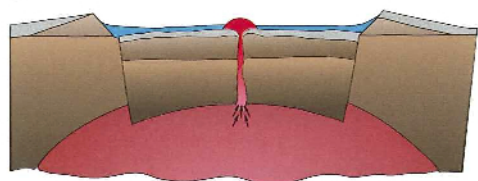
- Valles Caldera is one of the best studied 'Rhyolitic' calderas, and it is the first place resurgence was fully studied (Cole *et al.* 2005).
- Redondo Peak is composed mostly of Bandelier Tuff which formed the floor of the caldera after the 1.2-million-year-old eruption (Price 2010).
- Resurgence of more than 1 km occurred during the 100 ka after initial collapse and formed Redondo Dome (Cole *et al.* 2005). It might have occurred in as little as 40,000 yrs (Price 2010). A lake formed during the same time and deposited sediments in a 'moat' surrounding the resurgent dome (Cole *et al.* 2005).
- The eruptive domes inside the caldera started forming soon after the uplift of Redondo Peak. These formed by the passive eruption of viscous magma. The circular arrangement of the domes suggests the presence of a large fault or ring fracture that formed when the caldera formed (Price 2010).



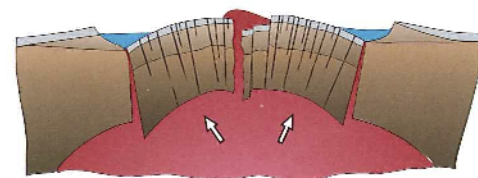
Stage 1—Final stage of eruption



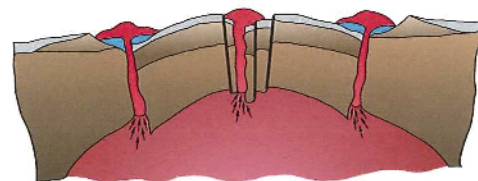
Stage 2—Post-eruption (caldera collapse)



Stage 3—Eruptive domes & lakes



Stage 4—Structural resurgence (resurgent dome)



Stage 5—Post-resurgent eruptive domes

Figure 4: The evolution of Valles caldera (Price 2010).

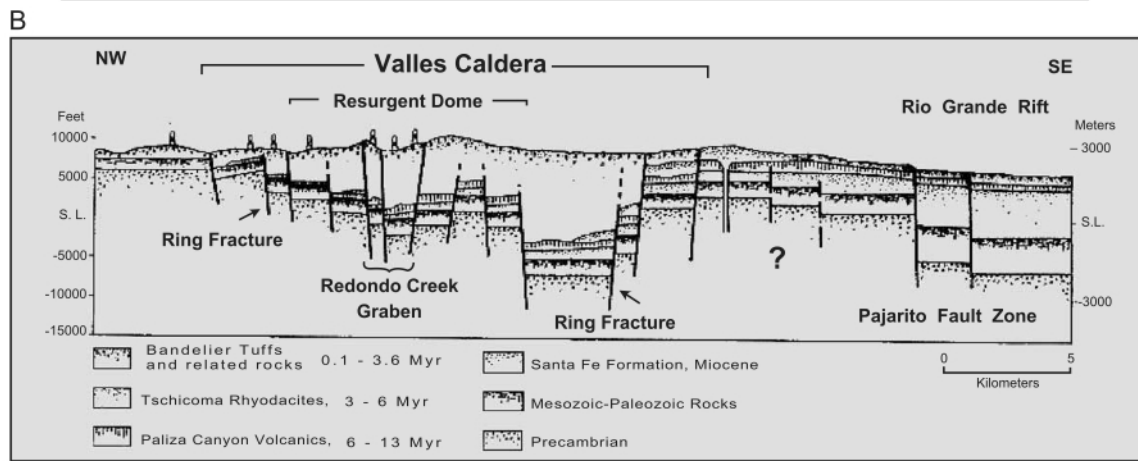
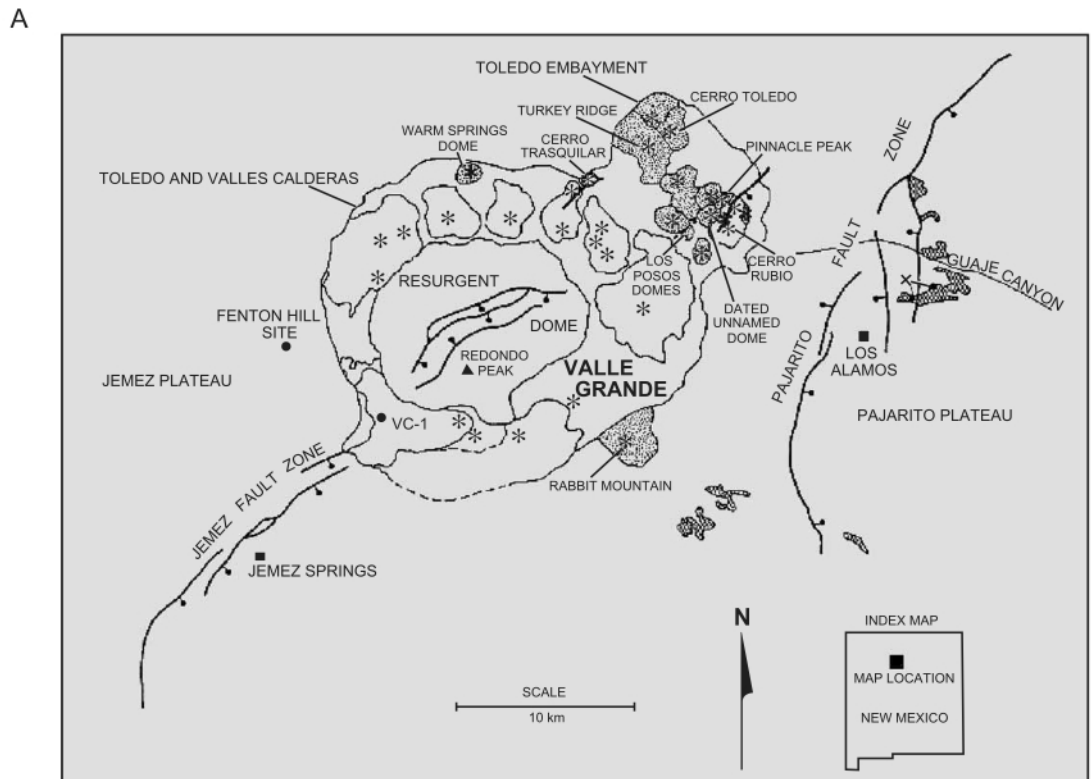


Figure 5: A) Map of Valles and Toledo calderas. Asterisks are vent locations for intracaldera domes and flows. Stippled pattern indicates rhyolite domes associated with the Toledo caldera. B) Cross-section of Valles caldera and Pajarito Fault Zone based on drill holes and gravity data (Cole *et al.* 2005).

## References

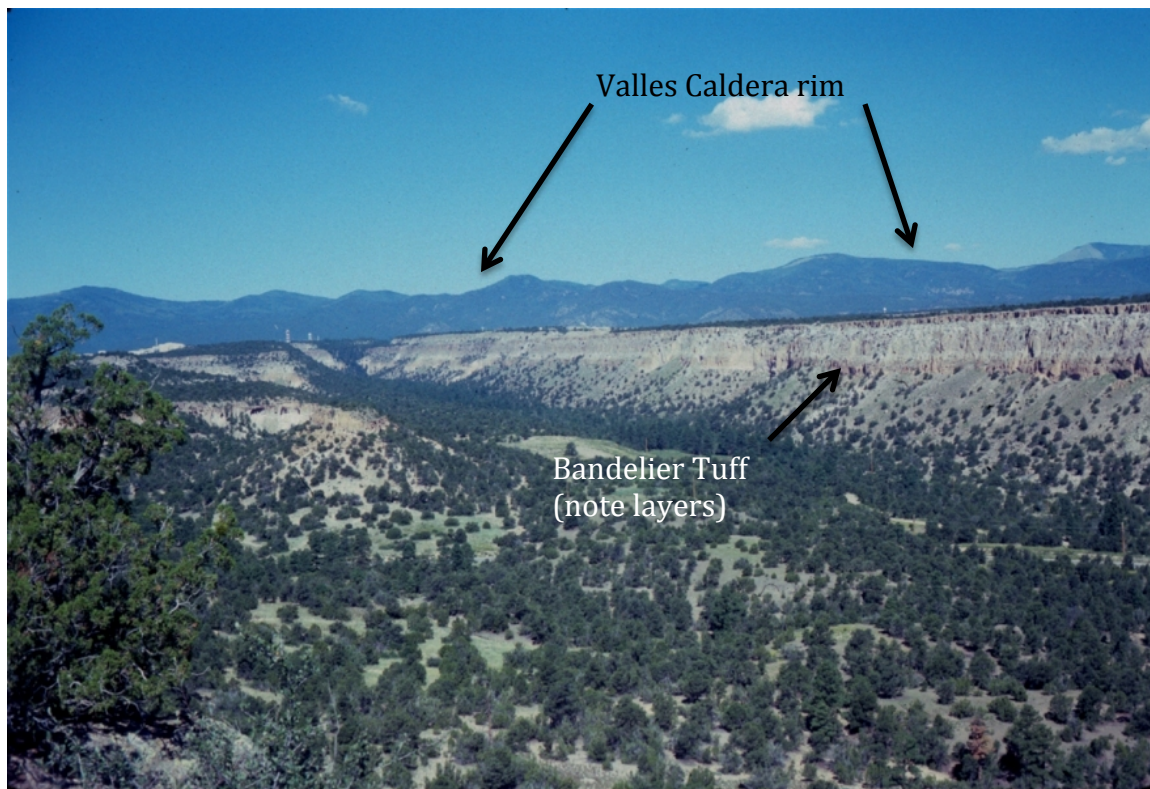
- Cole, J., D. Milner, and K. Spinks 2005. Calderas and caldera structures: a review. *Earth-Science Reviews* 69(12), 1 – 26.
- Lipman 1999. *Encyclopedia of Volcanoes*, Chapter Calderas. Elsevier Science.
- Price, L. 2010. *The Geology of Northern New Mexico's Parks, Monuments, and Public Lands*. New Mexico Bureau of Geology and Mineral Resources.

# Bandelier Tuff and Ash Fall vs. Flow Deposits

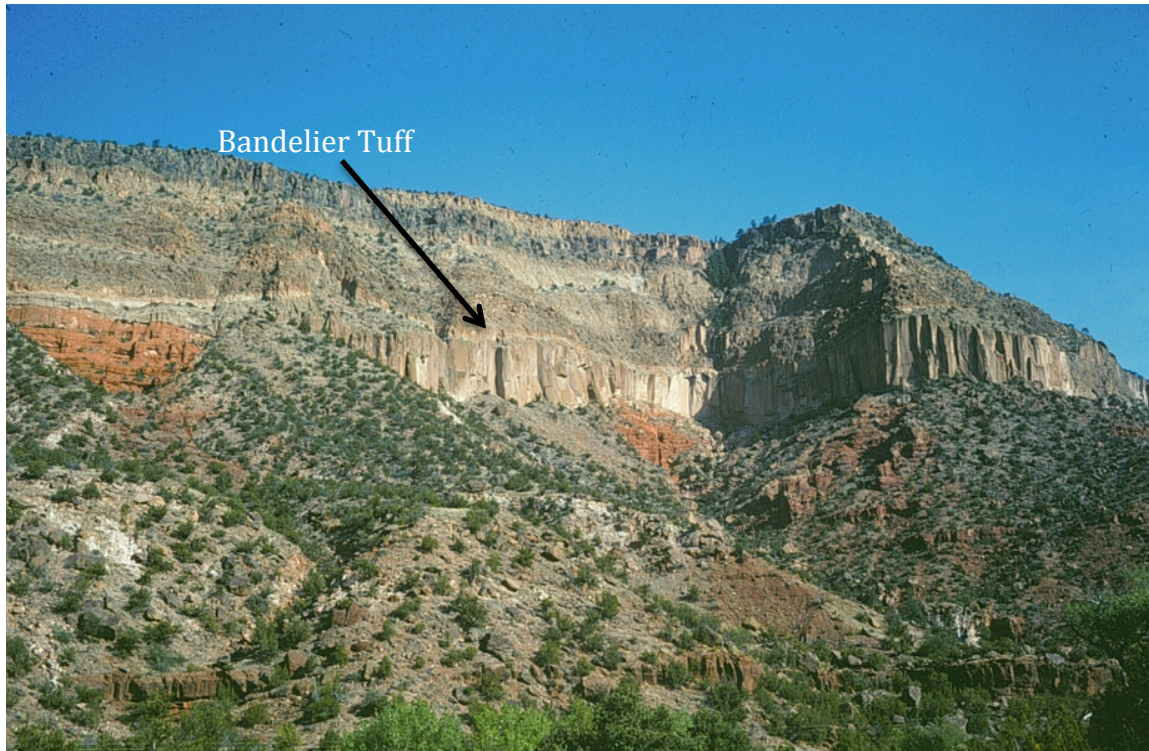
## Ingrid Daubar

### Bandelier Tuff

- Ash-flow tuff (see below for definitions)
- Source = Valles Caldera. Erupted ~ 1.14 million years ago.
- Flows > 100 km/hr. Traveled 25-35 kilometers from source.
- Average several hundred meters thick. Thin far from the caldera, much thicker in canyons.
- Varies in hardness from obsidian-like to crumbly. Center cools more slowly than the top and bottom → welded, cliff-forming vs. shallow slopes formed by top and bottom.
- Layers ~ two major eruptions, different cooling rates in each deposit.
- Above, below, and beyond the Bandelier are ash-fall tuffs. Air-fall ash from Valles Caldera recognized as far away as Iowa.



**Bandelier Tuff** (Image credit: A. Treiman)



**Bandelier Tuff, Jemez Canyon.** (Image credit: A. Treiman)

## Ash Fall vs. Ash Flow Deposits

**Fall deposits** – Material has traveled through the air as some kind of projectile during a volcanic eruption (“tephra”). Fall deposits follow the lay of the topography, covering hill tops as well as valleys (“mantle bedding”). Deposits are well-sorted.

**Flow deposits** – Flows form when hot fragmenting material is made buoyant by hot gas and begins to flow as a fluid. The flow is a density current in highly heated (~500-700°C) mixture of volcanic gases and ash. Fluidization occurs when the hot gasses accompanying the ejecta, together with trapped air and gas being released by the ejecta as it vesiculates, forms an air cushion around each particle preventing it from coming into contact with adjacent particles. Thus, the whole mass behaves like a fluid with low viscosity, enabling it to travel great distances down slopes and, in many instances, up relatively steep slopes.

The ash flow itself can also be called a **nueé arente, pyroclastic flow, or glowing avalanche.**

Formation mechanisms:

- Cloud spills over the lip of a volcano, flows downslope as a density current
- Eruption cloud/column collapses due to a lack of momentum & heavy load of pyroclastics
- Material piles up on the upper slopes of the volcano and collapses

Deposits:

- Include pumice, scoria, and blocks, abundant fine-grained ash in the matrix
- Relatively thick, poorly sorted, with little to no bedding
- Slight differences in size of fragments in different layers give an irregular and indistinct stratification to some deposits
- Flat fragments near base strongly oriented parallel to depositional surfaces
- Inverse grading (largest pumice fragments at the top of the flow; denser lithic fragments at the base) ← caused by buoyant rise during flow
- Maximum sizes of fragments decrease with distance from source

### Distinguishing flow deposits from fall deposits:

- Fall deposits are very well sorted compared to flow deposits
- Falls coat topography ~evenly; flows thicker in low-lying areas (e.g. fill canyons)
- Flow structures (alignment of clasts, etc.)
- Impact of bombs/blocks dropped in falls produce bedding sags, while in flows larger fragments are moved into place so do not form sags

**Surge Deposit** = Compositionally ≈ flow deposits, but more lithic clasts. Relatively thin, better sorted than flow deposits, with or without abundant matrix fines, and well bedded to cross bedded (wavy-, lenticular- or low angle cross bedding is characteristic).

## Definitions

**Ash** = Small (0.025 - 4 mm diameter), jagged pieces of rocks, minerals, and volcanic glass the size of sand and silt. Produced from explosive eruptions (magma + gas or water).

- Extremely abrasive and mildly corrosive (→ acid rain)
- Conducts electricity when wet
- Last material to settle after eruption
- Ash clouds can travel thousands of miles, even circle the Earth
- Ash can remain in the stratosphere for days-weeks after an eruption

**Ignimbrite** = rock formed from deposition of an ash flow or fall. Ranges from **welded tuffs** (high temperatures of emplacement) to nonwelded, unconsolidated ash deposits. Rich in pumice and glass shards.

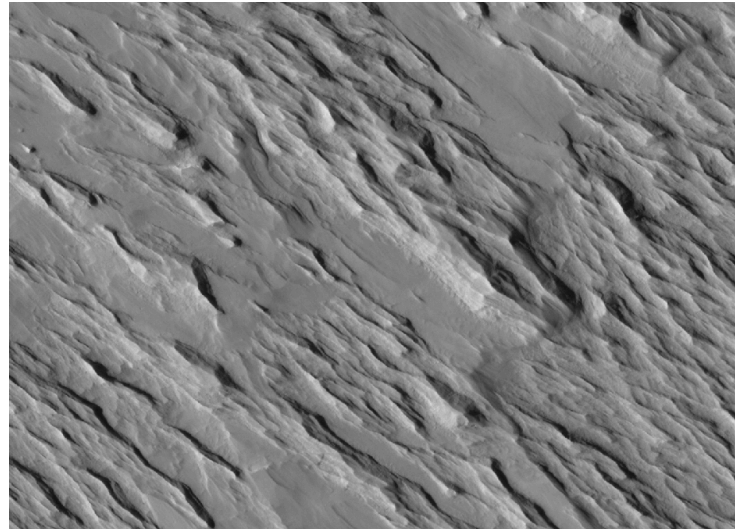
**Welded Tuff** = glass-rich pyroclastic rock, indurated by the welding together of its glass shards under the combined action of the heat retained by particles, the weight of overlying material, and hot gases. Composed of silicic pyroclasts. Appears banded or streaky. sometimes bedded in layers representing eruption phases.

### Tephra Classifications:

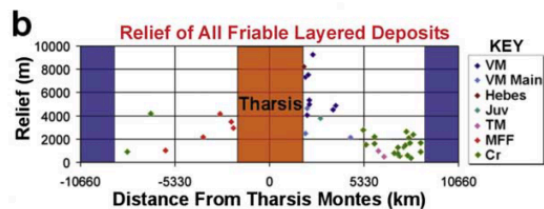
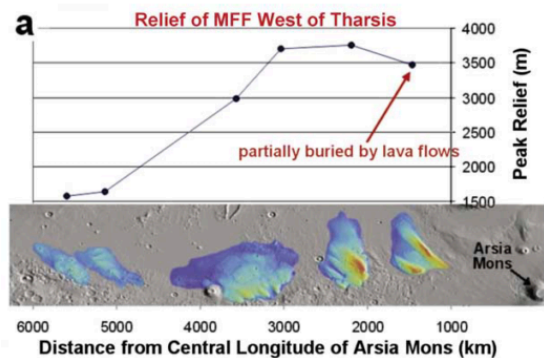
<b>&gt; 32 mm</b>	blocks, bombs
<b>4 mm-32 mm</b>	lapilli, pumice, scoria, etc.
<b>0.025 mm-4 mm</b>	ash
<b>&lt;0.025 mm</b>	fine ash, dust

## Planetary connection

**Medua Fossae Formation** – formed by volcanic ash flows and air fall from Tharsis eruptions? (Other explanations have also been proposed.)



(above) Medusa Fossae formation: finely layered, indurated, fine-grained material, eroded by wind into yardangs. HiRISE image ESP\_028702\_1875, 7.331°N, 199.0°E.



(left) Thinning of deposits with distance from Tharsis → source of pyroclastics? [Hynek et al. 2003]

## References

- El-Baz, F., et al. (1979) "Eolian features in the Western Desert of Egypt and some applications to Mars." JGR 84, 8205-8221. DOI: 10.1029/JB084iB14p08205
- Fisher, R.V. (1997) "Deposits Of Pyroclastic Sediment Gravity Flows." Technical report. <http://volcanology.geol.ucsb.edu/deposits.htm>, retrieved 9/20/13.
- Hynek, B.M. (2003), "Explosive volcanism in the Tharsis region: Global evidence in the Martian geologic record." JGR 108, 5111. DOI: 10.1029/2003JE002062
- Kanen, R.A. (2001) "Pyroclastic Deposits." <http://www.geologynet.com/pyro.htm>, retrieved 9/20/13.
- Kenedi, C. A. et al. (2000) "Volcanic Ash Fall—A 'Hard Rain' of Abrasive Particles." USGS Fact Sheet 027-00. <http://pubs.usgs.gov/fs/fs027-00/>
- Lanagan, P. (2000) "Eruption and Deposition of Ass – I mean 'Ash' – Flows." Planetary Geology Field Practicum PTYS 594a, p. 17.
- Treiman, A. (2003) "The Great Desert: Geology and Life on Mars in the Southwest." <http://www.lpi.usra.edu/science/treiman/greatdesert/workshop/index.html>, retrieved 9/20/13.
- Wikipedia: "Volcanic ash." [http://en.wikipedia.org/wiki/Volcanic\\_ash](http://en.wikipedia.org/wiki/Volcanic_ash), retrieved 9/20/13.

# Environmental Effects from Large Volcanic Eruptions

Sarah Peacock



## ASH FALLOUT AND DEPOSITS

Ash fallout is airborne for anywhere between a few hours to days. Depending on location, the effects from super eruptions can be felt across a whole hemisphere or even globally. Ash from the super-eruptions of Yellowstone caldera is known to cover much of North America, while ash from Mount St. Helens eruption was found as far as Oklahoma (over 3000 km away).

- While erupting, airborne ash is a hazard to anything in flight, such as birds and planes
- More than 1 cm of ash can cause disruption to agricultural production (if it falls during the growing season)
- There can be chemical and filtration problems associated with water supplies including drinking water and waste disposal

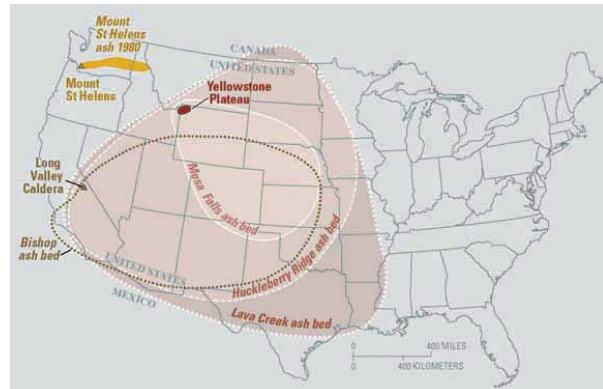


Figure 1: Ash beds from Yellowstone and Mount St. Helens eruptions



Figure 2: This house was damaged by a heavy load of ash that accumulated on the roof during the eruption of Rabaul Caldera in 1994

- Thin layers of fallen ash (< 1 cm) can cause roof collapse, especially if the ash is wet. Dry ash has a weight of 400-700 kg/m<sup>3</sup> and rainwater can increase

## PYROCLASTIC FLOWS AND DEPOSITS

A pyroclastic flow is a fast moving (up to ~700 km/h) current of hot gas and rock. Due to their temperature and mobility, they can be very destructive and deadly. Some effects they can have include:

- Burial of objects on the ground
- Fires
- Secondary mudflows (lahars) along river valleys and streams after rainfall on fresh volcanic deposits. Lahars can flow tens of meters per second, be 140 m deep, and destroy anything in their path
- If the volcano is near a coast, pyroclastic flows can cause a tsunami



Figure 3: A lahar from the 1982 eruption of Galunggung



Figure 4: The pyroclastic flows entering the sea from the 1883 eruption of the island volcano of Krakatoa caused a tsunami that killed thousands of people

## Gas and Aerosols

The most widespread effects come from volcanic gases, sulphur gases being particularly important. This gas is converted into sulphuric acid aerosols in the stratosphere and layers of aerosol can cover the global atmosphere within a few weeks to months. These remain for several years and affect atmospheric circulation causing surface temperature to fall in many regions.

- Climate change
  - mainly cooler temperatures for a few years after the eruption
    - This can change agricultural yields
  - Some areas may experience warming (in high latitude regions)
  - Changes in rainfall patterns could lead to flooding in certain areas

- Dry fog and acid aerosol air pollution
  - Dry fog in the lower atmosphere composed of sulfur dioxide gas and sulfuric acid aerosols could completely cover a hemisphere
  - sulfur and halogens (Cl, F and perhaps Br) released from the magma cause significant changes to the normal atmospheric concentrations of these gases or of their acids H<sub>2</sub>SO<sub>4</sub>, HCl and HF
- Ozone depletion
  - Stratospheric aerosols will serve to catalyse ozone loss, permitting higher UV-B flux to the ground in high-mid-latitude regions

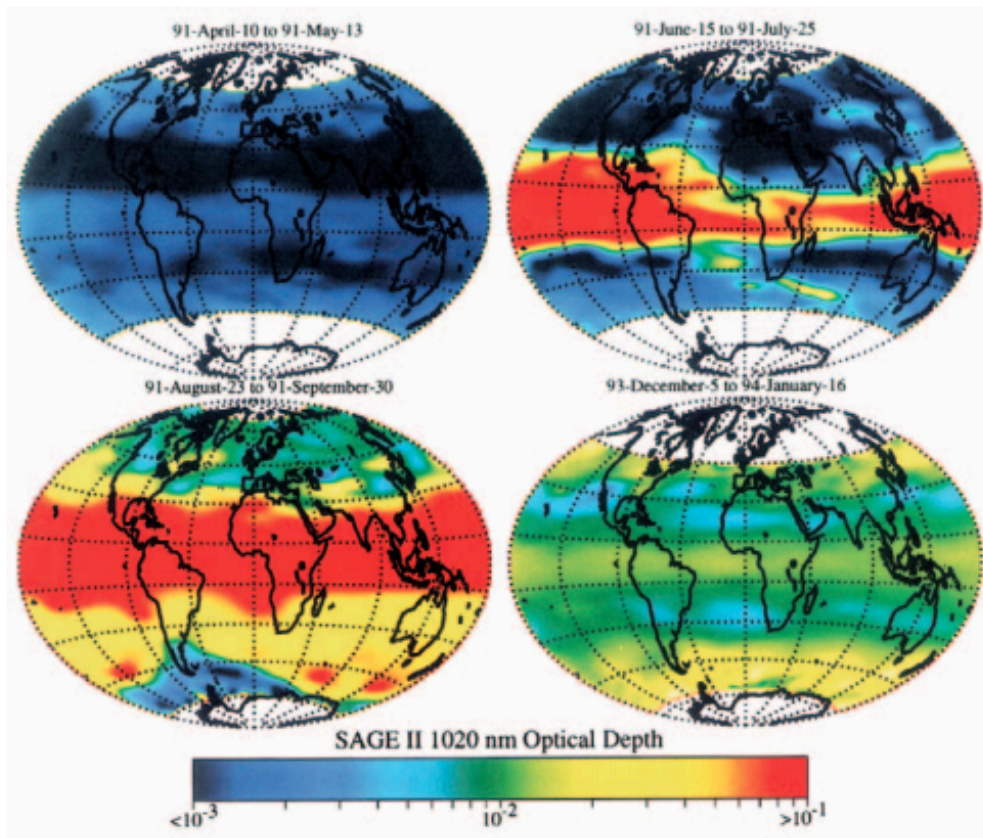


Figure 5: Spread of Pinatubo's sulfate aerosol cloud; the top-left panel shows the situation before the 1991 eruption; other panels show the situation to January 1994. Colors represent the optical depth of the aerosol cloud, with blue being background values and red being the highest concentrations. Note the global coverage by aerosols within a few months of eruption (from McCormick et al. 1995)

References:

- McCormick MP, Thomason LW, Trepte C (1995) Atmospheric effects of the Mt Pinatubo eruption. *Nature* 373: 399-404.
- Self, S., and S. Blake (2013) Deep Carbon Emissions from Volcanoes, *Reviews in Mineralogy and Geochemistry* 75(1) 323-354.
- Self, S. (2006) The effects and consequences of very large explosive eruptions. *Philos Trans R Soc A* 364:2073-2097.

# Rio Grande Rift

Youngmin JeongAhn

The Rio Grande rift is the region of Cenozoic extension stretching from the central Colorado to the north of Chihuahua, Mexico. There are three major basins: San Luis, Espanola, and Albuquerque basins from north to south. The rift forms the border between the Colorado Plateau and the Great Plains. It extends from the southern Rocky Mountain region in the north and becomes wider and less distinct in the south; it is joined to the Basin and Range.

The subduction of Farallon and Kula plates under North America plate triggered the Laramide orogeny and compressional stress was exerted until about 40 mya. The Rocky mountains in the north were mainly

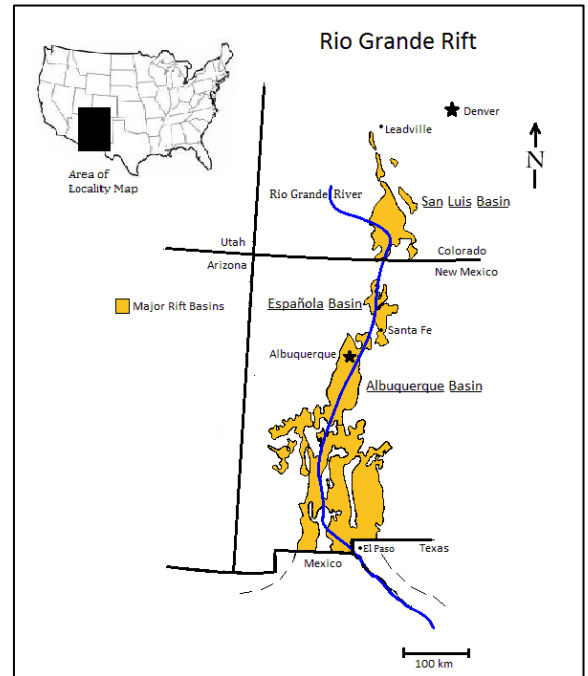


Figure 1 Rio Grande rift area (by utdlabrador)

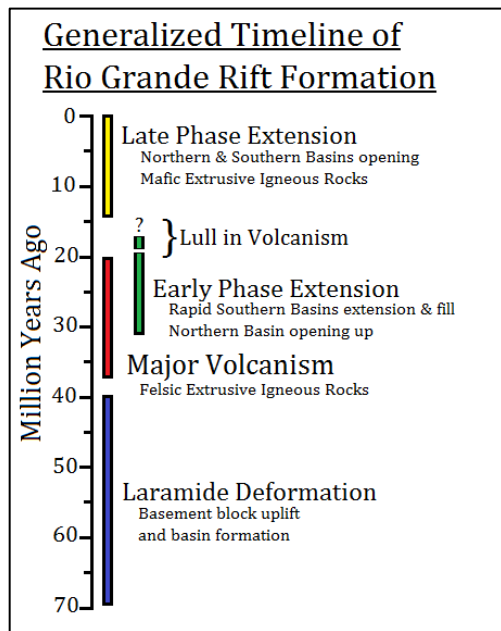


Figure 2 Timeline of Rio Grande rift formation (by utdlabrador)

formed during this period. Deformation under this compressional stress might have weakened the crust making it vulnerable to the following extensional events.

The early phase of extension occurred from the mid-Oligocene (30 mya) to the early Miocene (18 mya). The early rift basins are found in the southern New Mexico along with thick sequence of basaltic andesite flows. Low-angle normal faults are developed and the orientation of early phase extension is NE-SW direction. The amount of extension is 30% in average and 100% in some area.

The late phase extension mainly achieved during late Miocene (10 to 5 myr) after a quiet period in volcanism.

Basins are narrow and typically half-graben (bounded along one side only). Vertical motions are dominant than the rotating movements and faults are spaced widely.

The crust thickness of Rio Grande is about 30-35km, which is thinner than the Colorado Plateau (40-45km) and the Great Plains (50km). The Southern part of the rift is thinner due to large amount of extension. The intervening lithospheric mantle is absent or little beneath the rift.

The Rio Grande (river) is developed along the rift axis by cutting through the

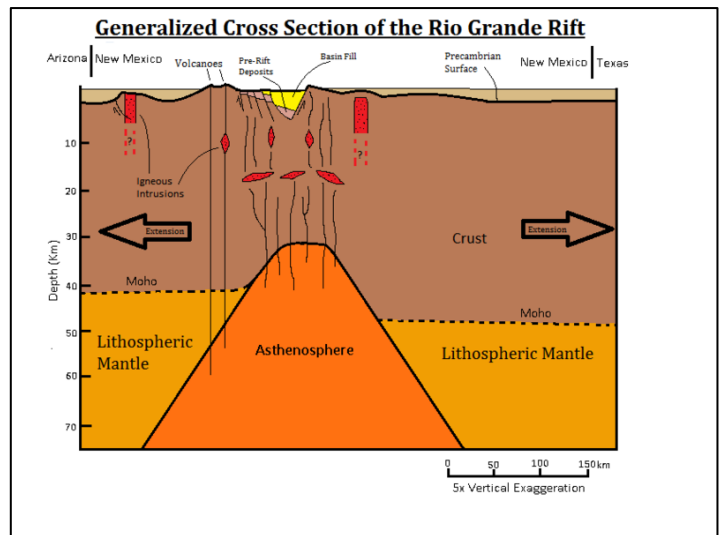


Figure 3 a cross section of Rio Grande rift (by utdlabrador)

basins. The river flows into the Gulf of Mexico and the watershed covers 472,000 km<sup>2</sup>.



Figure 4 Rio Grande drainage basin (by Kmusser)

### Planetary Connection

The bands on Europa crisscrossing ridged plains are formed by extensional stress. Liquid material rising through the crack forms unique ridges.

Extensional features can be seen also on the Moon, Mars, Venus, Ganymede, and many more.

### References

Morgan P., Seager, W.R., and M.P. Golombek 1986. JGR 91:6263-6276

Perry, F.V., Baldrige, W.S., and D.J.

DePaolo 1987. JGR 92:9193-9213

Russel, L.R., and S. Snelson 1994. GSA 291:83-121

# K-T Layer Structure & the Double Layer in the Raton Basin

By Xianyu Tan

## Global structure of the K-T layer

Four groups of sites: (see Fig. 1)

- **< 500 km** from Chicxulub: impact deposits are quite thick. A >100-m-thick impact-breccia sequence, and 1-m- to >80-m-thick ejecta-rich deposits are present in the surrounding Central American region.
- **500 – 1000 km** from Chicxulub and around the northwestern Gulf of Mexico: the K-T boundary is characterized by a series of cm- to m-thick ejecta spherule-rich, clastic event beds indicative of high-energy sediment transport, for example, by tsunamis and gravity flows.
- **1000 – 5000 km** from Chicxulub: the K-T boundary deposit consists of a 2- to 10-cm-thick spherule layer topped by a 0.2 to 0.5cm-thick layer anomalously rich in platinum group elements with abundant shocked minerals, granitic clasts, and Ni-rich spinels.
- **> 5000 km** from Chicxulub: a reddish, 2- to 5-mm-thick clay layer rich in impact ejecta material is usually present at the K-T boundary.

A thin layer (known as the fireball layer) of a few mm exists in all four groups, which consists Iridium, Ni-rich spinels, ejecta spherules.

## The double layer in the Raton Basin

Raton Basin is in the intermediate distance (1000 – 5000 km) from Chicxulub.

Upper layer:

- 3-mm thick, laminated claystone.
- Iridium-spike, shocked mineral grains.
- Altered spherules.
- Thought to be equivalent to the global fireball layer.

Lower layer:

- 1-2 cm thick, kaolinitic claystone.
- No enhanced Iridium, few shocked minerals (no projectile component).

Note: the two layers are distinct bands with a sharp contact between them. The upper layer correlates to the global boundary layer and rests sharply on top of the lower layer. Not a single season of leaves is found between them.

What is the possible way to form this double layer?

*Ejecta deposit and atmosphere interaction:*

- First, a very rough process of an impact in airless condition: Rocks vaporize in high pressure and material (mixture of target and projectile) squirts or jets outwards at high velocity. The vapor plume or fireball expands upward and

outward. Material of the target is excavated, and the ejecta form an ejecta blanket around the crater up to certain distance. Both vapor plume and ejecta curtain materials finally fall back and deposit ballistically.

- Then consider the atmosphere of the Earth (e.g., Goldin & Melosh 2007):
  - Case of distal fireball layer (without terrestrial ejecta): the particles fall through the upper atmosphere and accumulate a dense layer at ~50 km altitude. The deceleration of particles heats the atmosphere, causing expansion of the atmosphere, creating a boundary between atmosphere below and above the particles (Fig. 2 left a b c).
  - Case forming double layer (including terrestrial ejecta) (Fig. 2, right panel): The compression of the atmosphere by the terrestrial material alters the structure of the atmosphere causing the fireball material to fall separately and resulting in the deposition of two distinct layers. Deposition of the lower terrestrial layer on the ground begins at ~80 minutes and that of the upper fireball layer begins at ~130 minutes.

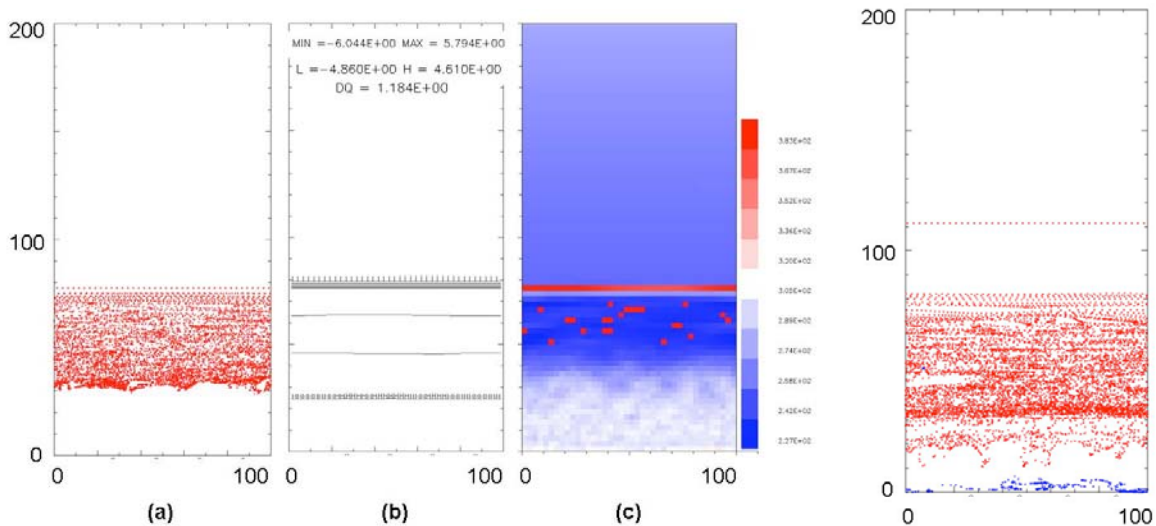


**Fig. 2 Left:** (a) the positions of injected liquid tracers (fireball spherules), (b) log pressure contours where pressure is measured in bars, and (c) temperature contours in Kelvin after 80 minutes (assuming simple black body thermal radiation) for the distal fireball layer model. Injection angle is 45 degrees and all axes are labeled in kilometers. **Right:** 90 minutes after impact, ejecta curtain (blue) begin to deposit, distinct from the fireball material (red) which will form the upper layer.

*Reference:*

Smit, J. "The global stratigraphy of the Cretaceous-Tertiary boundary impact ejecta." *Annual Review of Earth and Planetary Sciences* 27.1 (1999): 75-113.

Goldin, T. J., and H. J. Melosh. "Interactions Between Chicxulub Ejecta and the Atmosphere: The Deposition of the K/T Double Layer." *Lunar and Planetary Institute Science Conference Abstracts*. Vol. 38. 2007.

Schulte, Peter, et al. "The Chicxulub asteroid impact and mass extinction at the Cretaceous-Paleogene boundary." *Science* 327.5970 (2010): 1214-1218.

De Pater, Imke, and Jack J. Lissauer. *Planetary sciences*. Cambridge University Press, 2010.

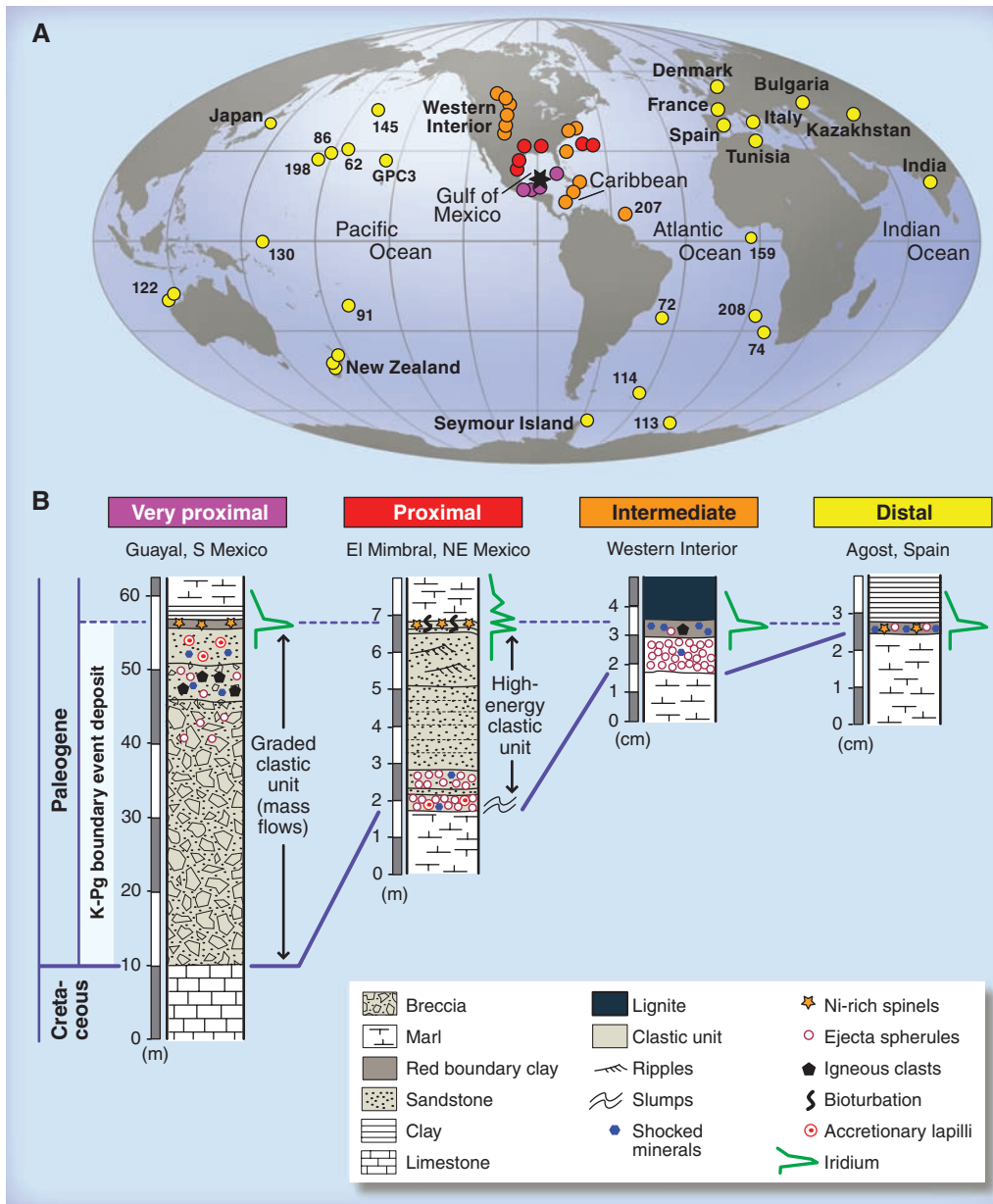
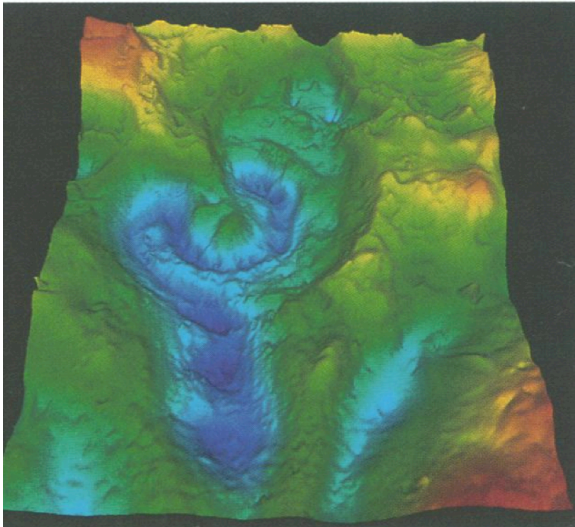


**Fig 1. (Peter Schulte et al. 2010)** (A) Global distribution of key K-T boundary locations. Deep-Sea drill sites are referred to by the corresponding Deep Sea Drilling Project (DSDP) and ODP Leg numbers. The asterisk indicates the location of the Chicxulub impact structure. Colored dots mark the four distinct types of K-T boundary event deposit related to distance from the Chicxulub crater: magenta, very proximal (up to 500 km); red, proximal (up to 1000 km); orange, intermediate distance (1000 to 5000 km); and yellow, distal (>5000 km). Schematic lithologies of the four groups of K-T boundary event deposits (B) highlighting high-energy event beds (clastic unit) proximal to the crater and the depositional sequence of different materials that originated in one single impact in proximal to distal sites.

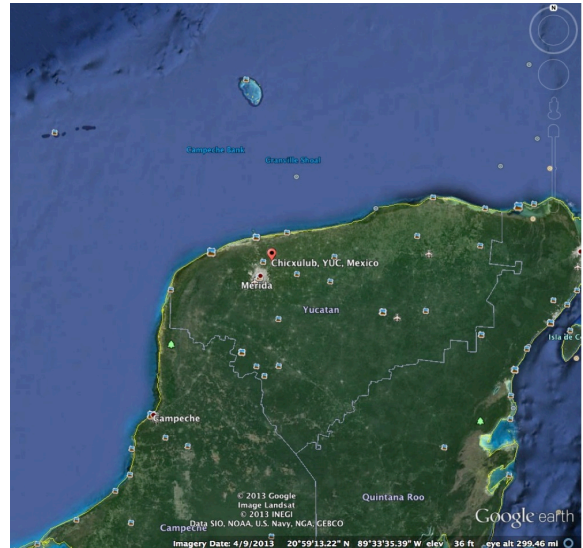
## The Chicxulub impact crater and large impact events

### Chicxulub impact vital statistics

- Diameter (current) ~165km (Morgan et al 1997)
- Morphology: multi ring basin
- Target material: shallow water and continental crust
- Ejecta volume: ~50,000 km<sup>3</sup>
- Impact energy: 0.7-3.4x10<sup>24</sup> J (1.7- to 8.1x10<sup>8</sup> megatons TNT) (Pope et al 1997)
- Other >150-km-diameter terrestrial structures: Vredefort (South Africa), Sudbury (Ontario, Canada)



Gravity anomaly data collected by Sharpton et al. (1993) shows a distinct impact feature as well as several potential ring structures. Gravity anomaly values range from -14.6 mgal to +53.6 mgal over the Sharpton et al. (1993) study region.

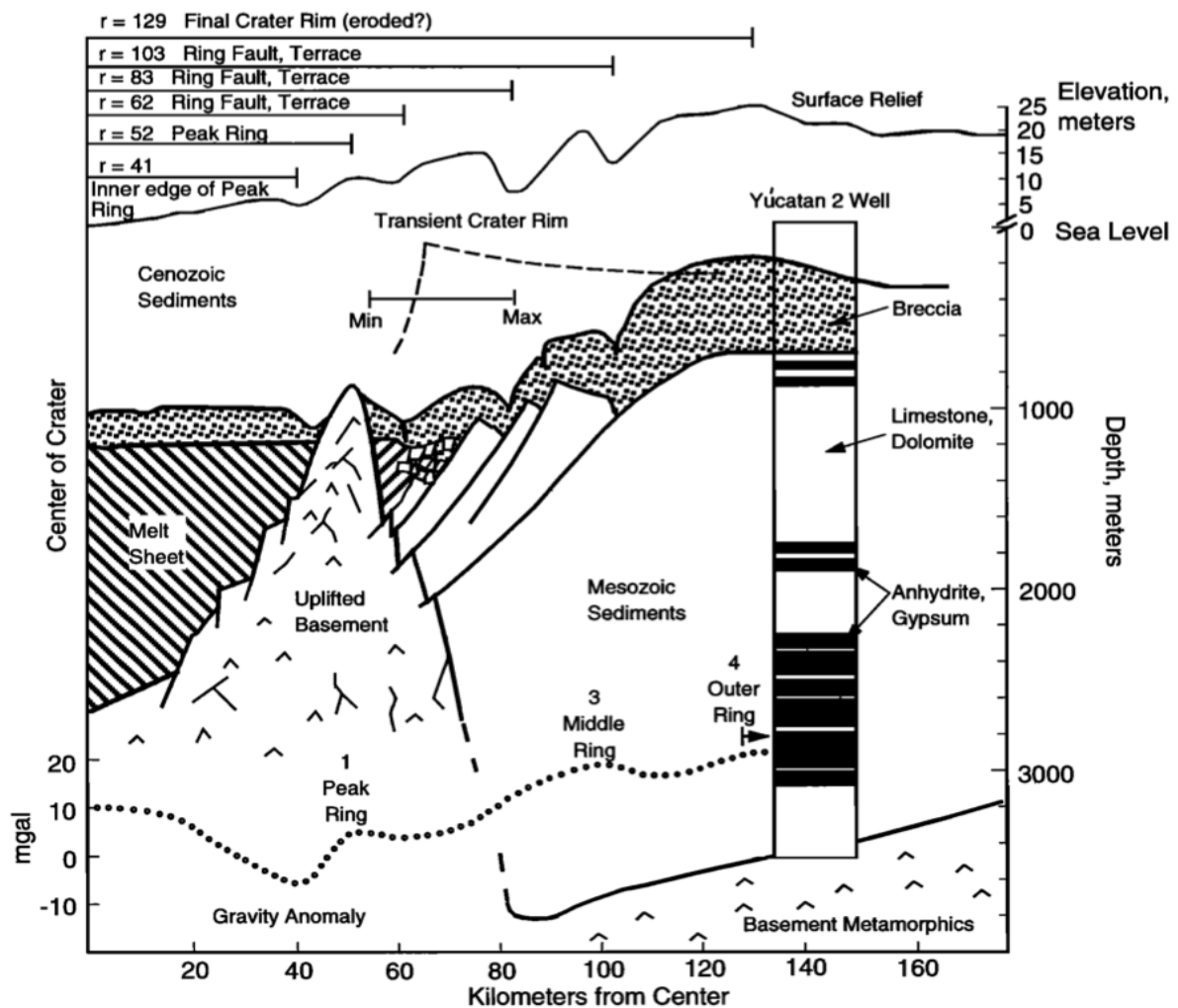


A Google Earth view of the Yucatan Peninsula shows the site of the Chicxulub impact event (center roughly shown with orange marker and extends to reef to the north).

### Identification and Discovery

- Was identified as an unusual structure by oil surveys in the 1950s
- Alvarez et al (*Science*, 1982) identify high levels of iridium in the drilling site similar to the iridium content in the K/T boundary
- Hildebrand et al (1991) published a study suggesting that the structure was of impact origin—called “the smoking gun” by a reviewer
- <sup>40</sup>Ar/<sup>39</sup>Ar analysis gives an age of ~64 million years before present as

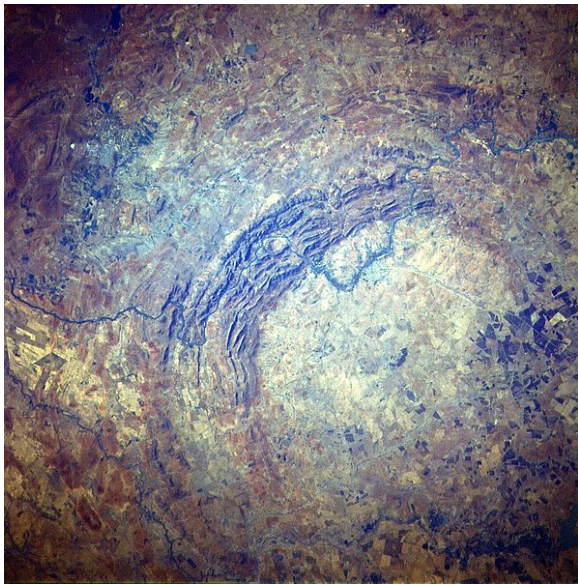
- impact time (Sharpton et al 1992, Swisher et al 1992) which is also consistent with age of the K/T boundary structure
- So, the Chicxulub crater is identified as the source of the iridium and the K/T extinction event as well as a tsunami and other environmentally catastrophic side effects throughout the Americas



The diagram of the Chicxulub crater structure from Pope et al. (1997) is shown above. Note the sea level mark on the depth axis, as most of this impact structure is now submerged.

### Large impact processes

- High shock pressures
- Crater is formed within minutes, even with a multi-ring basin
- Shocked metamorphic phases of minerals including quartz are often used to identify impact structures
- Unique features of large impact craters
  - Large central dome from rebound of target after impact
  - Multiple rims or rings in the basin
  - Follow a non-bowl shaped structure
- Chemical analysis of the impact melt can also be used to identify sites
- Vredefort (South Africa) was identified as an impact structure through geochemical and geomorphological analysis confirming the presence of shocked quartz and zircon as well as high meteoric content in the impact melt (Leroux et al., 1994; Kamo et al., 1996; Koeberl et al., 1996)



The Sudbury impact structure in Ontario, Canada, is shown as the ellipse at the center of the NASA Challenger orbital image. It is approximately 1.9 Gya old and is heavily eroded.

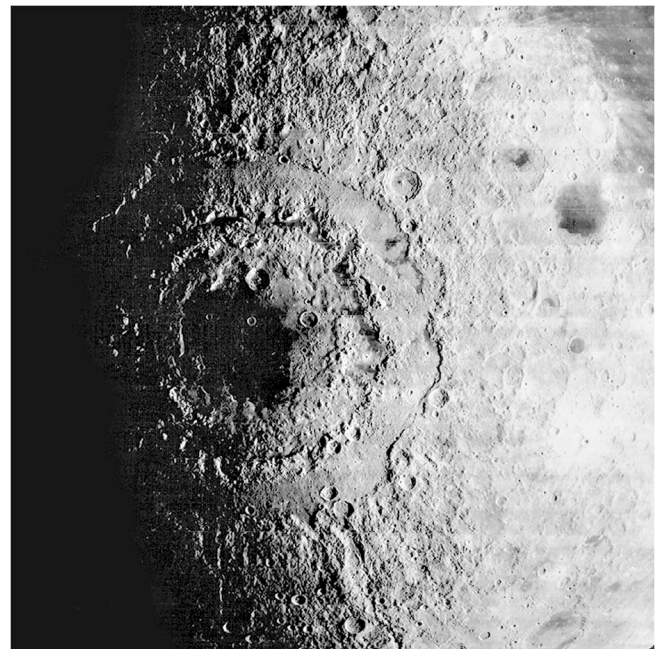
The Vredefort impact structure in South Africa as seen from space. It is approximately 2.0Gya old. Image: NASA STS51I-33-56AA.

#### Other examples of multi-ring basins

- Orientale Basin, Moon
- Valhalla basin, Callisto

#### References

- Alvarez, W., F. Asaro, H. Michel, and L. Alvarez (1982). "Iridium Anomaly Approximately Synchronous with Terminal Eocene Extinctions." *Science* 216, 886-888.
- Hildebrand, A.R., Penfield, G.T., Kring, D.A.M., Pilkington, A., Carmargo, Z., Jacobsen, S.B., and Boynton, W.V., (1991). "Chicxulub crater: A possible Cretaceous/Tertiary boundary impact crater on the Yucatan Peninsula, Mexico". *Geology* 19, 867-871.
- Kamo S.L., Reimold, W.U., Krogh, T.E., Colliston, W.P. (1996). "A 2.023 Ga age for the Vredefort impact event and a first report of shock metamorphosed zircons in pseudotachylitic breccias and Granophyre." *EPS Letters* 144, 369-387.
- Koeberl, C., Reimold, W. and Shirey, S. (1996). "A Re-Os isotope and geochemical study of the Vredefort Granophyre: clues to the origin of the Vredefort structure, South Africa." *Geology* 24, 913-916
- Leroux, H., Reimold, W., Doukhan, J.C. (1994). "A TEM investigation of shock metamorphism in quartz from the Vredefort dome, South Africa." *Tectonophysics* 230, 223-239.
- Morgan, J., Warner, M., et al. (1997). "Size and Morphology of Chicxulub impact crater." *Nature* 390, 472-476
- Pope, K., K. Baines, A. Ocampo, B. Ivanov (1997). "Energy, volatile production, and climatic effects of the Chicxulub Cretaceous/Tertiary impact". *JGR*, 102 21645-64
- Sharpton, V., Dalrymple, G.B., Marin, L.E., et al. (1992). "New links between the Chicxulub impact structure and the Cretaceous /Tertiary boundary." *Nature* 359, 819-821
- Sharpton, V., Burke, K., et al. (1993). "Chicxulub Multiring Impact Basin: Size and Other Characteristics Derived from Gravity Analysis." *Science* 261, 1564-7.
- Swisher, C.C., Grajales-Nishimura, J.M., et al. (1992). "Coeval <sup>40</sup>Ar/<sup>39</sup>Ar Ages of 65.0 Million Years Ago from Chicxulub Crater Melt Rock and Cretaceous-Tertiary Boundary Tektites." *Science* 257, 954-958.



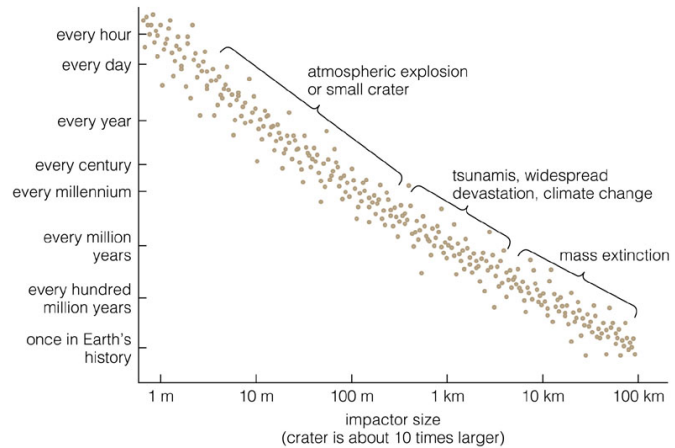
1967 Orbiter IV image of the Orientale Basin on the Moon, an example of a multi-ring basin on another planetary body.

# Environmental Changes and Extinctions from Large Impacts

Xi Zhang

## What did impacts do?

- Created the moon?
- And its face
- Brought the water to Earth?
- And global Firestorms
- Produce acid rains?
- And Diamonds
- Make the planet dusty?
- Hotter or cooler?
- Induce volcanoes?
- ...
- Brought the life to Earth?
- And killed it---**Mass Extinctions!**



From *Wiki*: “The impact of a sufficiently large asteroid or comet could have caused food chains to collapse both on land and at sea by producing dust and particulate aerosols and thus inhibiting photosynthesis. Impacts on sulfur-rich rocks could have emitted sulfur oxides precipitating as poisonous acid rain, contributing further to the collapse of food chains. Such impacts could also have caused megatsunamis and/or global forest fires...”

## What will a 10-km asteroid do?

Produces explosion that is equivalent to an earthquake of magnitude 12.4 on the Richter scale. Left a 150-kilometer diameter crater. If it hits any deep point in the Pacific (the largest ocean), it produces a megatsunami along the entire Pacific Rim, half-kilometer high tsunami over 1000 km distance from the center....

## Did the mass extinction happen before? *Five times.*

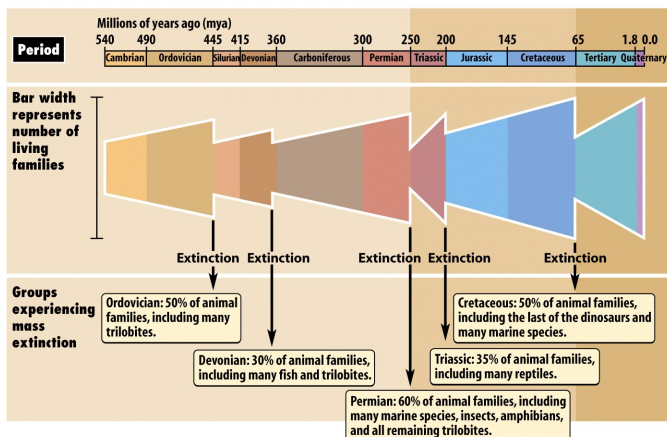
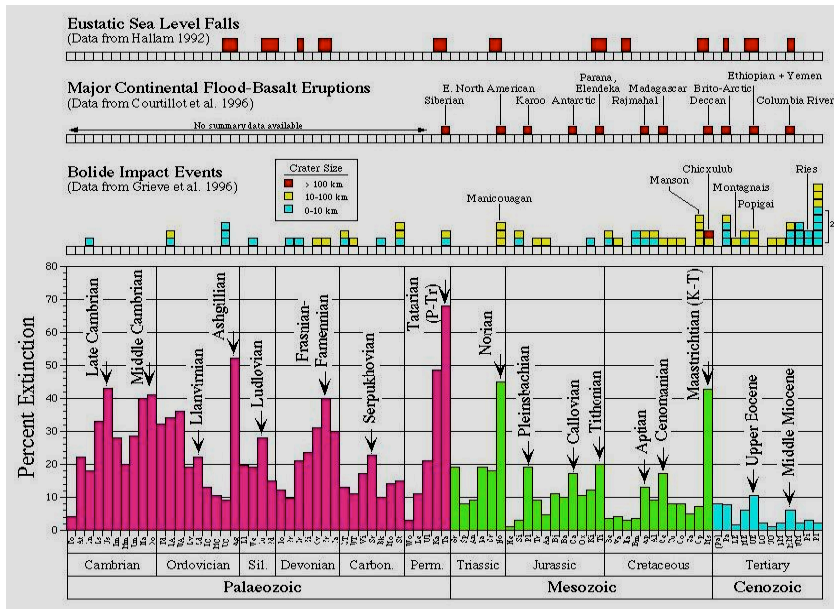


Figure 19-8 Discover Biology 3/e  
© 2006 W. W. Norton & Company, Inc.

## Possible Causes (e.g., Macleod, 2001)



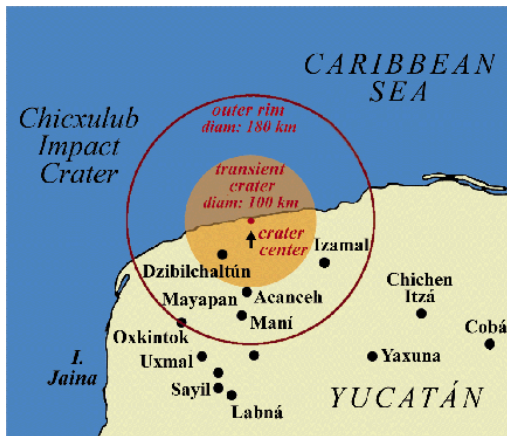
## The K-T Extinction (The story of dinosaurs)

66 Ma, also called the Cretaceous–Paleogene (or K-Pg) extinction event in place of Cretaceous-Tertiary. About 17% of all families, 50% of all genera and 75% of all species became extinct. In the seas it reduced the percentage of sessile animals to about 33%. The majority of non-avian dinosaurs became extinct during that time. Mammals and birds emerged as dominant land vertebrates in the age of new life. There was considerable stratigraphic evidence that marine and continental extinctions looked like they might be synchronous.

In 1980, Nobel laureate Luis Alvarez, his geologist son Walter Alvarez, nuclear chemist Frank Asaro, and paleontologist Helen Michael (from right to left), published on their discovery of high levels of the element Iridium in a clay layer separating marine sediments of Cretaceous and Tertiary age (now has been found worldwide at 100 different sites). It could come from (1) supernovae, (2) volcanic eruption (Kilauea Volcano in Hawaii), or (3) a large impact. But they did not find the evidence for another element Plutonium (Pu244), which should be also produced by a supernovae. They proposed an *impact winter* scenario to explain the mass extinction. Anomalies in chromium isotopic ratios found within the K-T boundary layer also strongly support the impact theory because they are similar to the chromium isotopic ratios found in carbonaceous chondrites. Later, Bohor



and Izett in 1986 discovered shocked quartz at K-T boundary, therefore they excluded the volcanic eruption hypothesis.



But where is the impact site? The impact structure, discovered buried beneath the shore of the Yucatan Peninsula (Chicxulub) of Mexico in 1978 by geophysicists Antonio Camargo and Glen Penfield, turns out to be 180 km wide, possibly the largest impact known in the world and said by some to be the largest known in the solar system. Camargo and Penfield did not publish their work in a "flashy" enough journal, so their work was basically ignored until "rediscovered" by Alan Hildebrand and William Boynton in 1990. In recent years, several other

craters of around the same age as Chicxulub have been discovered, all between latitudes 20°N and 70°N, such as the disputed Silverpit crater in the North Sea and the Boltsh crater in Ukraine. This has led to the hypothesis that the Chicxulub impact may have been only one of several impacts that happened nearly at the same time. However, in late 2006, Ken MacLeod conducted his analysis approximately 4,500 km from the Chicxulub Crater to control for possible changes in soil composition at the impact site. The analysis revealed there was only one layer of impact debris in the sediment, which indicated there was only one impact.

Some critics argue that such an impact would have killed frogs as well as dinosaurs, yet the frogs survived the extinction event. Some argues that recent core samples from Chicxulub prove the impact occurred about 300,000 years before the mass extinction, and thus could not have been the causal factor. On the other hand, the possible mechanism is still under debate. For example, the Chicxulub bolide struck a thick deposit of marine limestone ( $\text{CaCO}_3$ ) and underlying marine calcium sulphate ( $\text{CaSO}_4$ ). This probably put large amounts of  $\text{CO}_2$  and sulfuric acid into the atmosphere within minutes. The  $\text{CO}_2$  would have produced a large greenhouse effect (but the sulfuric acid would result in global cooling). That might be the real cause of the mass extinction.

In 2007, a hypothesis was put forth that argued the impactor belonged to the Baptistina family of asteroids. In 2010, another hypothesis was offered which implicated the newly discovered asteroid *P/2010 A2*, a member of the Flora family of asteroids, as a possible remnant cohort of the Chicxulub impact. Shiva hypothesis proposes that periodic gravitational disturbances cause comets from the Oort cloud to bombard earth every 26 to 30 million years.

The dinosaur story never ends...

# Impact Hazards and Impact Rates for the Terrestrial Planets

Christa Van Laerhoven

## I. Populations of small bodies in the solar system

- Near-Earth Objects (NEOs): small bodies whose orbits are in near-Earth space (i.e. closer to the Sun than the Main Belt Asteroids).
- Main Belt Asteroids (MBAs): population of mostly rocky bodies most of which have semi-major axes between about 2.1 and 3.3 AU.
- Jupiter Family Comets (JFCs): cometary bodies that are dynamically controlled by Jupiter
- Centaurs: small bodies that are in and among the giant planets.
- Kuiper Belt Objects (KBOs): small rocky/icy bodies whose orbits lie beyond Neptune's.
- Oort Cloud Comets (OCCs): bodies that were flung out far enough for galactic tides to be important, have a roughly isotropic distribution.

The NEO, JFC and centaur populations are unstable. The NEO population is resupplied from the Main Belt. The JFC and centaur populations are resupplied from the Kuiper Belt. The Oort Cloud supplies the super long-period comets.

The current NEO population is: >90% asteroidal (former MBAs), <10% former JFCs, 4-5% Long-Period Comets (combination of former OCCs and KBOs) (Bottke et al 2002, Bottke et al 2008).

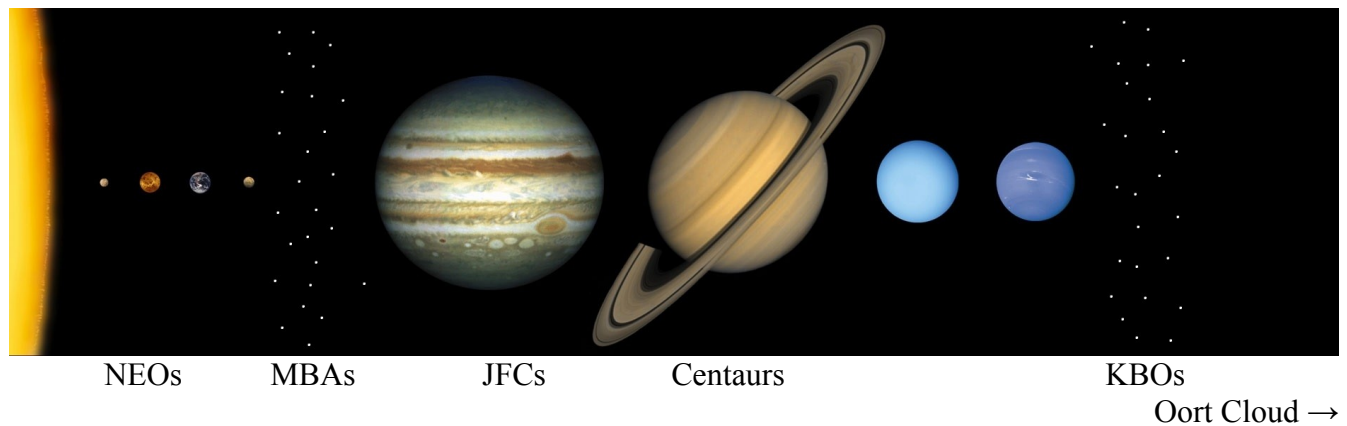
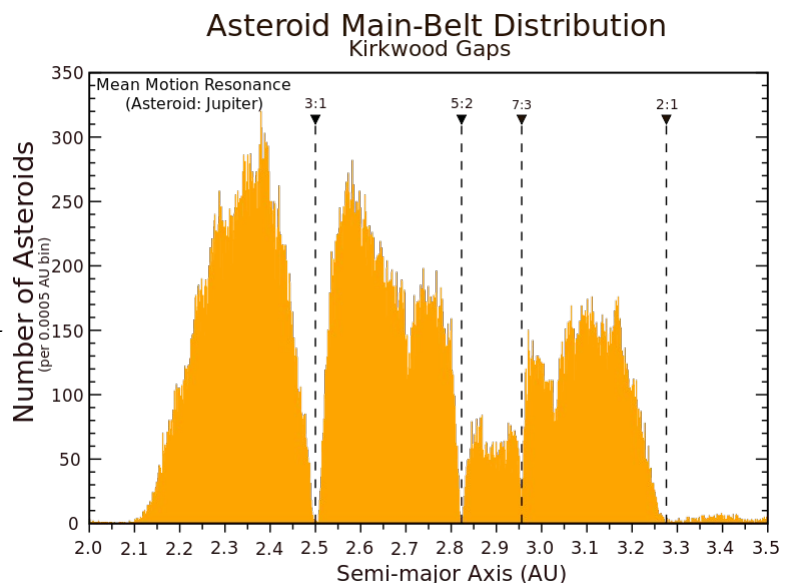


Figure 1 (above): Schematic of small body populations in the solar system.

Figure 2 (right): Number of asteroids versus their semi-major axes. The areas around mean-motion resonances are unstable. Also, the  $\nu_6$  secular resonance is unstable, defining the inner edge of the belt.



## II. From MBA to NEO

There are several unstable regions in the vicinity of the Main Belt. In particular, mean-motion resonances with Jupiter carve away the Kirkwood Gaps and the inner edge of the belt is carved by the  $\nu_6$  secular resonance (Figure 2). The  $\nu_6$  secular resonance depends on all of  $a$ ,  $e$ , and  $i$  (as opposed to  $a$ , with a smaller contribution from  $e$ , for the mean-motion resonances). As a result, the inner edge of the disk is not sharp, as seen in Figure 2. An MBA will reach near-Earth space via one of these unstable regions. Earth crossers are primarily delivered via the 3:1 mean-motion resonance or the  $\nu_6$  secular resonance.

### II.A Yarkovsky Drift

How does an MBA reach one of these unstable regions? → Orbital evolution from Yarkovsky drift. Yarkovsky drift arises from the fact that light carries energy and momentum. See Figures 3 and 4.

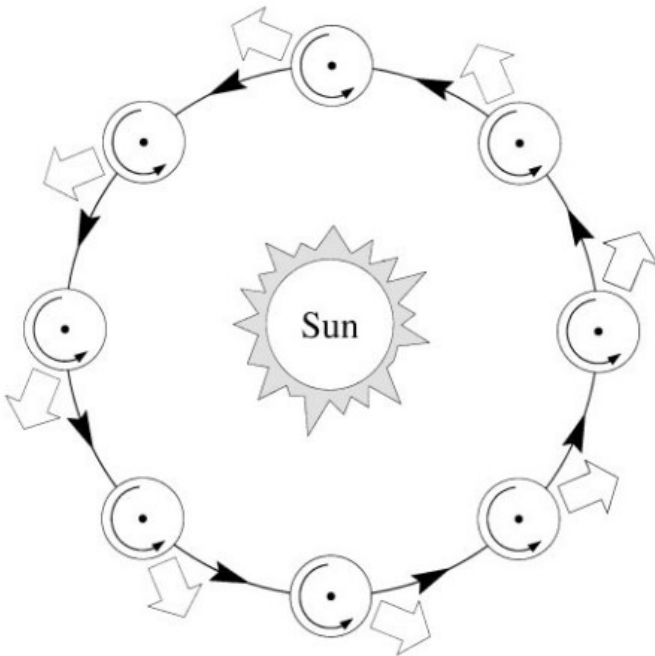
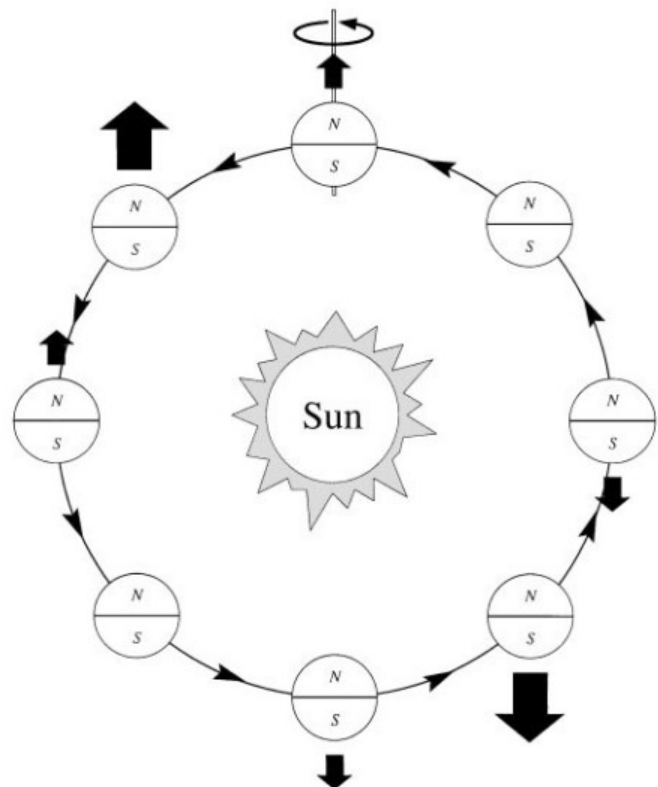


Figure 3 (left): From Bottke et al (2000): “The diurnal Yarkovsky effect is shown for a rotating body at various places along its circular orbit. The asteroid spin axis is perpendicular to the orbital plane. A fraction of the solar insolation is absorbed only to be later radiated away, yielding a net thermal force in the direction of the wide arrows. Since the thermal reradiation in this prograde-rotation example is concentrated at about 2 PM on the spinning asteroid, the radiation recoil force is always oriented at about 2 AM. In this case, the along-track component causes the object to spiral outward. Retrograde rotation causes the orbit to shrink.”

Figure 4 (right): From Bottke et al (2000): “The seasonal Yarkovsky effect at various points along a circular orbit for an asteroid whose spin axis lies in the orbital plane as shown at the top of the figure. Seasonal heating and cooling of the “northern” and “southern” hemispheres give rise to a thermal force which lies along the spin axis. The strength of the reradiation force varies along the orbit as a result of thermal inertia; the maximum resultant radiative forces are applied to the body somewhat after their most asymmetric (N vs S) energy absorption has occurred. The net effect over one revolution always causes the object to spiral inward.”



## II.B The K/Pg Impactor

The K/Pg impactor probably originated from the disruption of the Baptistina family about 160 Myr ago (Bottke et al 2007). That said, the age of the Baptistina family is uncertain, so further work may indicate a different asteroid family is responsible.

Figure 5 (right): hehe.

Figure 6 (below): Observed members of the Baptistina family. Note the locations of the 7:2 mean-motion resonance with Jupiter and 5:9 mean-motion resonance with Mars. Conversion from absolute magnitude to diameter is done assuming an albedo of 0.04 (Bottke et al 2007).

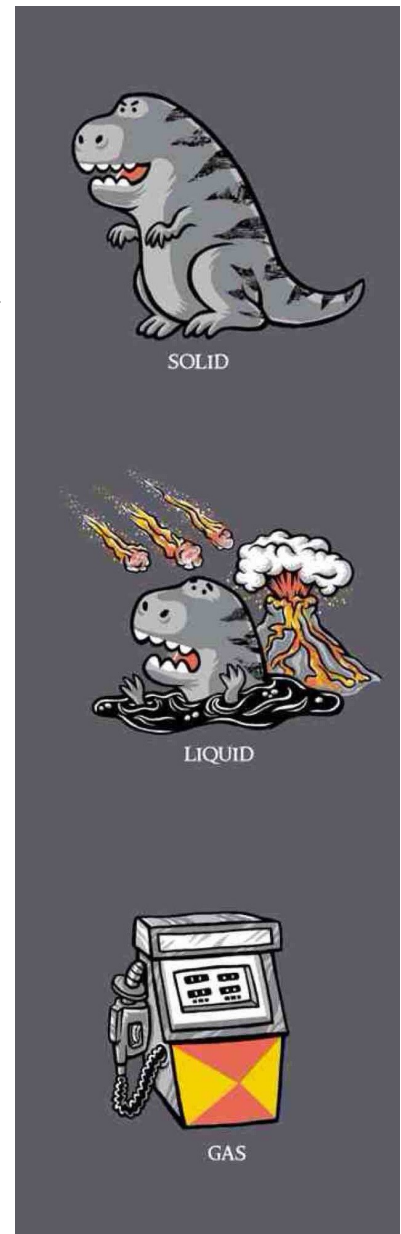
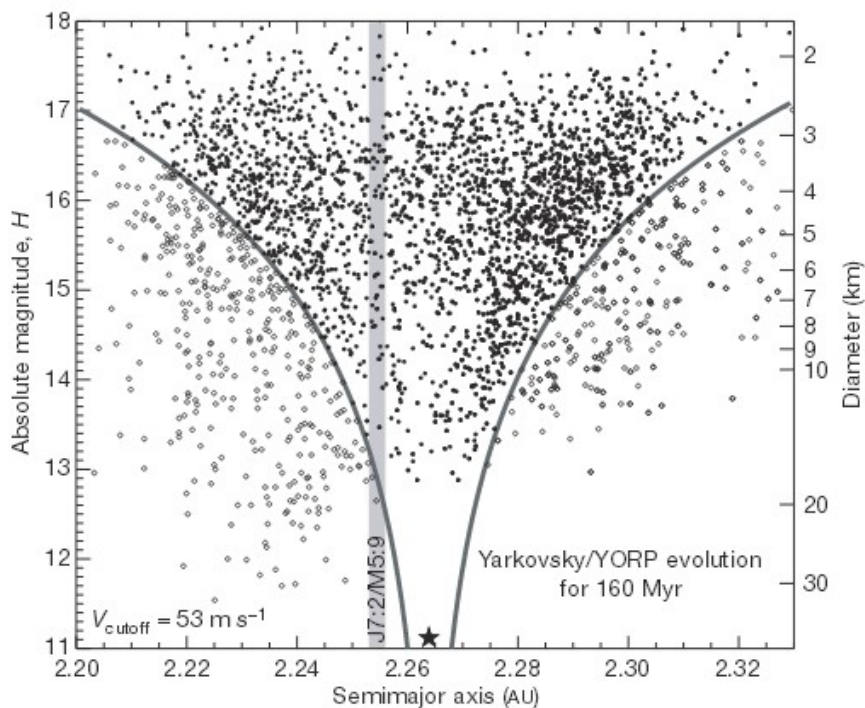
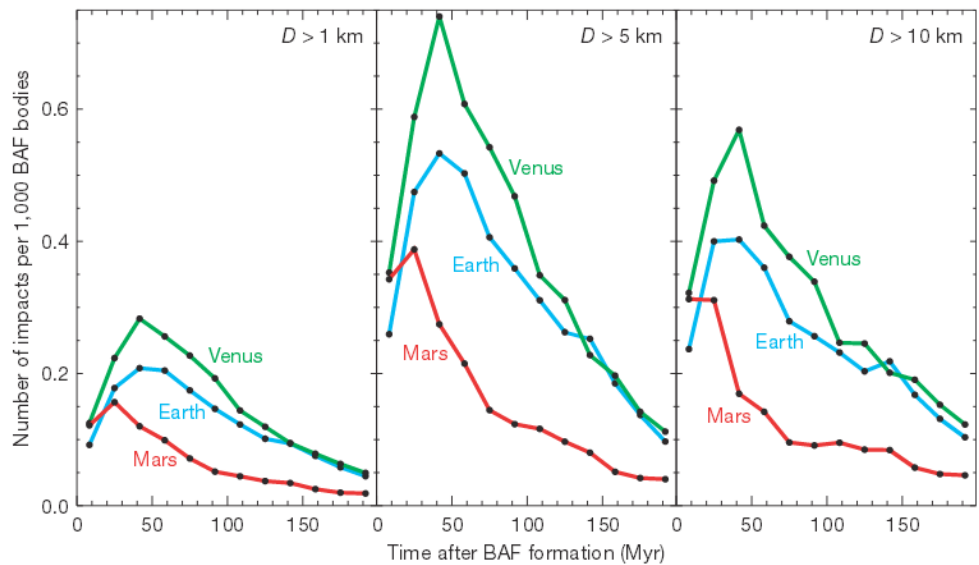


Figure 7: Impacts on the terrestrial planets resulting from the disruption of the Baptistina family (Bottke et al 2007).



### III. Jupiter Family Comets

JFCs typically have orbits with periods of about 20-30 years and are dynamically coupled to Jupiter.

When meeting their demise, JFCs tend to get suddenly flung out of the solar system or in to the Sun. They tend to not spend much time in the terrestrial planet region, though as mentioned above, former JFCs do make up some portion of the NEO population.

### IV. Oort Cloud Comets

Galactic perturbations will send OCCs on hyperbolic orbits towards the inner solar system. These comets only make one pass through the inner solar system (unless they encounter a planet and get their orbit changed).

### V. Current Impact Rates for Earth

Stony asteroid impacts that generate an airburst

<b>Impactor diameter</b>	<b>Kinetic energy at atmospheric entry</b>	<b>Airburst energy</b>	<b>Airburst altitude</b>	<b>Average frequency</b>
4 m (13 ft)	3 kt	0.75 kt	42.5 km (139,000 ft)	1.3 years
7 m (23 ft)	16 kt	5 kt	36.3 km (119,000 ft)	4.6 years
10 m (33 ft)	47 kt	19 kt	31.9 km (105,000 ft)	10.4 years
15 m (49 ft)	159 kt	82 kt	26.4 km (87,000 ft)	27 years
20 m (66 ft)	376 kt	230 kg	22.4 km (73,000 ft)	60 years
30 m (98 ft)	1.3 Mt	930 kt	16.5 km (54,000 ft)	185 years
50 m (160 ft)	5.9 Mt	5.2 Mt	8.7 km (29,000 ft)	764 years
70 m (230 ft)	16 Mt	15.2 Mt	3.6 km (12,000 ft)	1900 years
85 m (279 ft)	29 Mt	28 Mt	0.58 km (1,900 ft)	3300 years

Stony asteroids that impact sedimentary rock and create a crater

<b>Impactor diameter</b>	<b>Kinetic energy at atmospheric entry</b>	<b>Impact energy</b>	<b>Crater diameter</b>	<b>Average frequency</b>
100 m (330 ft)	47 Mt	38 Mt	1.2 km (0.75 mi)	5200 years
130 m (430 ft)	103 Mt	31 Mt	2.0 km (1.2 mi)	11000 years
150 m (490 ft)	159 Mt	71.5 Mt	2.4 km (1.5 mi)	16000 years
200 m (660 ft)	376 Mt	261 Mt	3.0 km (1.9 mi)	36000 years
250 m (820 ft)	734 Mt	598 Mt	3.8 km (2.4 mi)	59000 years
300 m (980 ft)	1270 Mt	1110 Mt	4.6 km (2.9 mi)	73000 years
400 m (1,300 ft)	3010 Mt	2800 Mt	6.0 km (3.7 mi)	100000 years
700 m (2,300 ft)	16100 Mt	15700 Mt	10 km (6.2 mi)	190000 years
1,000 m (3,300 ft)	47000 Mt	46300 Mt	13.6 km (8.5 mi)	440000 years

Both tables using impactor density =  $2600\text{kg/m}^3$ , impact speed =  $17\text{km/s}$ , impact angle = 45 degrees, from Marcus et al (2010).

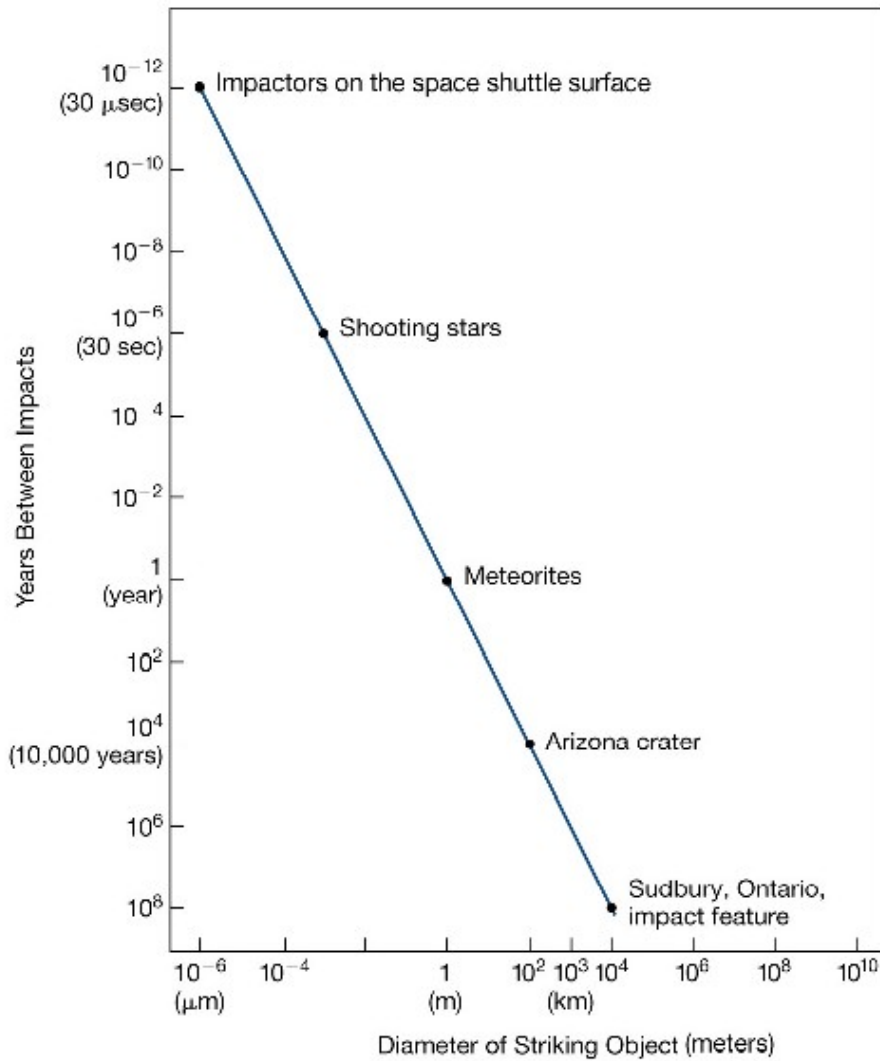
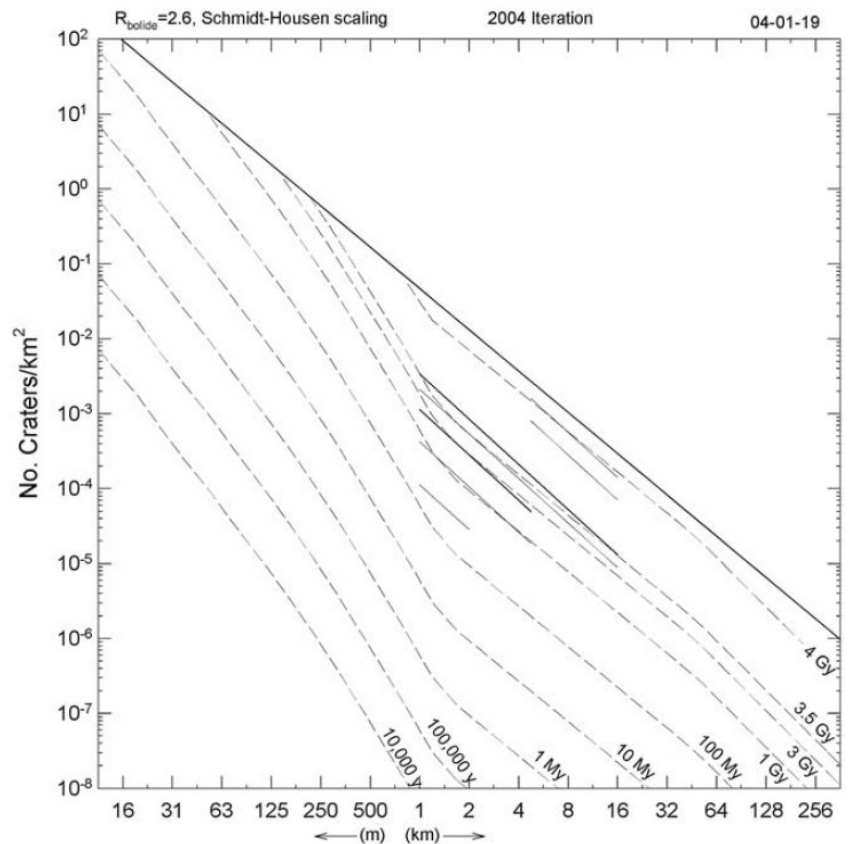


Figure 8: graph of impact rates versus impactor size and impact energy.

## VI. Impact Rates for Mars

Figure 9: Impact isochrons for Mars. Each line denotes the cumulative number of craters in a log diameter for a given age. From Hartmann (2005): "Heavier short lines ( $1\text{km} < D < 16\text{km}$ ) mark divisions of Amazonian, Hesperian, and Noachian eras; lighter nearby solid lines mark subdivisions of eras – all based on definitions by Tanaka (1986). Uncertainties on isochron positions are estimated at  $\pm$  factor  $\sim 2$ , larger at the smallest  $D < 100\text{m}$  (total uncertainties in final model ages, derived from fits at wide range in  $D$ , including uncertainties in counts, are estimated  $\pm$  factor  $\sim 3$ ."



## References

W. Bottke, D. P. Rubincam, J. A. Burns (2000). "Dynamical evolution of Main Belt meteoroids: numerical simulations incorporating planetary perturbations and Yarkovsky thermal forces". *Icarus* 145, 301-331.

W. Bottke, et al. (2002) "Debiased orbital and absolute magnitude distribution of the Near-Earth Objects" *Icarus* 156, 399-433.

W. Bottke, D. Vokriuhlicky, D. Nesvorny (2007). "An asteroid breakup 160 Myr ago as the probably source of the K/T impactor". *Nature* 449, doi:10.1038.

W. Bottke, H. Levison, A. Morbidelli (2008). "Early solar system impact bombardment". Workshop on the early solar system impact bombardment, LPI Contribution No. 1439, 19-20.

W. Hartmann (2005). "Martian cratering 8: isocron refinement and the chronology of Mars". *Icarus* 174, 294-320.

R. Marcus, H. J. Melosh, and G. Collins (2010). "Earth Impact Effects Program". Imperial College London / Purdue University.





### LPL Faculty Word Search: Hardest

M Y Z P C  
M A T F C Z  
L L Q N S O  
N H Q B U

R Y J C X  
A U J X R X  
X W S R Y  
A B L S Y  
T H I N E

L Q F W L  
I L Y L C  
Z Z E Q S  
B T Y Q E  
I P M G N

C M L R J  
U G A W K  
Q P H E S  
E G T L S

W K C C I  
B E I T C  
S Y H Q A  
O X H R C  
U Q S D Z

A J H G  
X Y R Z  
E I S Y  
F F B C P  
D S S O M

Q J C A M  
M P I W U  
M E I U J  
G V M R L

G B C T B  
T G S A N  
O R D E E  
X H D A  
F R Y V M

G F B P P E  
M I R R P V  
T P H A V  
S U C L E  
B E

Y F A Z O  
D A E H P  
O G L A V  
A A M W Z  
M G M V J

W M G R I  
R H L G Z  
I D A F C  
F R L G R K  
T R B Z K

J J T Q E  
E B Q R Q  
E Q G R I  
Z O K T U  
W I S A

T U S R R  
L B L E Q  
Z B K Q  
A N K N F  
E J Z T X

Y L H O P  
G E D U H  
B O L K G  
C D V L K  
I X J F E

S R T G U T  
T R E J  
U L H N F  
M D F B Y  
G Q W X W

O J L I E  
C A L N H  
E H R P K  
N Y A L J  
B Q A K I

B H H M T  
S P A J J A  
M A J V Z  
L Q O V Z  
J A F O D

A N K O A  
R U E P U  
L Q K K O  
F I X P V  
X U N H K

W O X B I  
S X N P I  
R J I Z A  
O K R D X  
O Q A K C

T Q E Q K  
G T W J F  
Q B Y X T  
H S Z L S  
O N E G Z

G M E M F  
C A D E F  
L Q H U K  
S R B S G  
F B C L J

N G W R D  
Q L T I N  
B G W E Q  
C Q J K H  
H M I E M

U M B D D E  
A B R M M  
S L X P T  
D P W Q P  
P A P U

P C B T R  
O O S M L L  
W V A A N  
G N U S P  
U W V S C

G D Q K D  
M G S K T  
Q K I E O  
J B G A I C  
A K Z O C

E U S W J  
C I Z K J  
H E R L T  
Z H G V K  
Y N J X

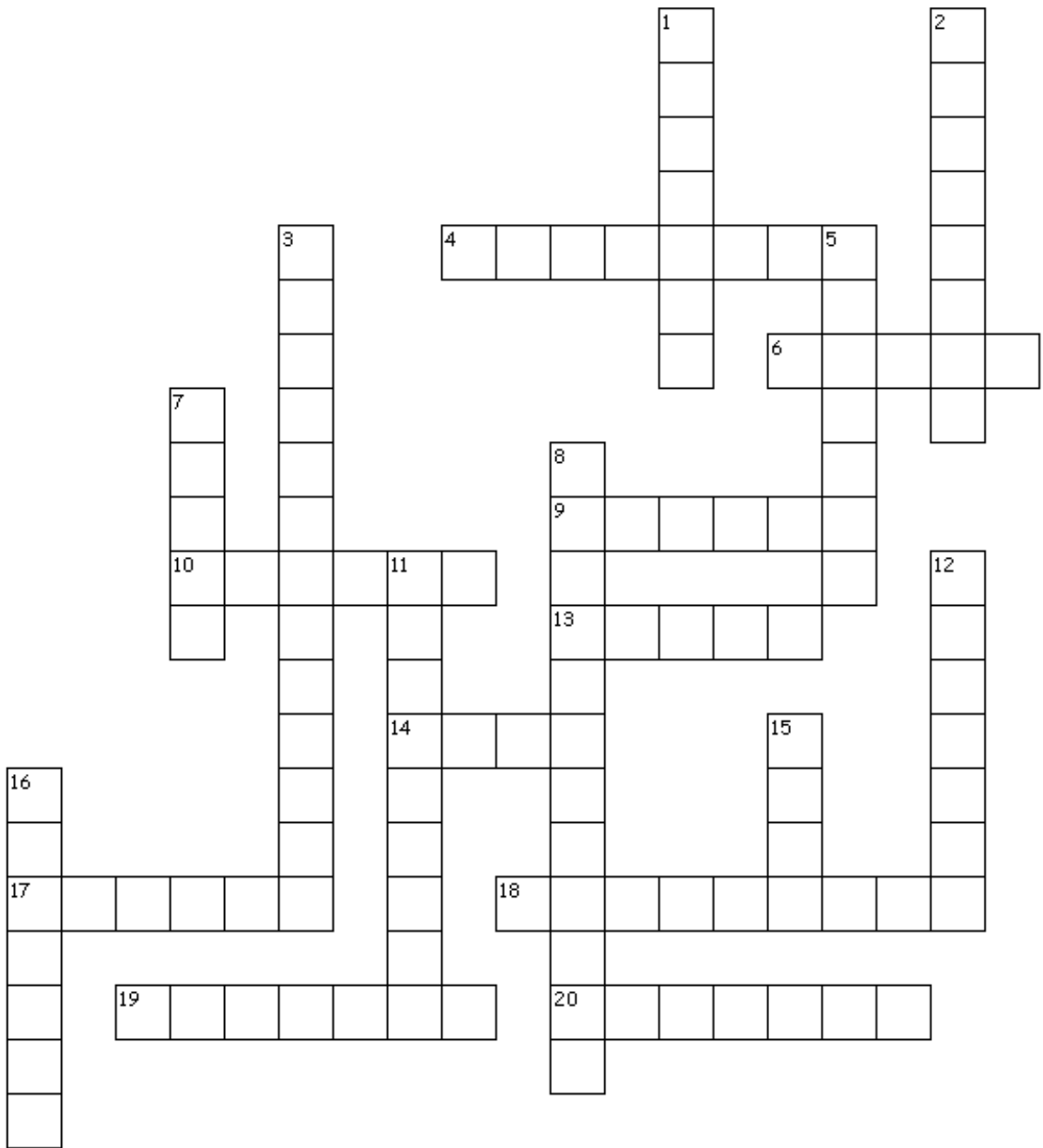
R A E I B  
H Z Y D R  
V E O P O  
R O H F W  
J A K O N

G V H J U  
V J J T S  
W F V Z D  
Q Y M A W T  
B I C X L

K X F F E S  
E N A C V H  
C J G V H  
D E C Q X

- APAI
- BARMAN
- BROWN
- BYRNE
- GIACALONE
- GREENBERG
- GRIFFITH
- HUBBARD
- JOKIPII
- MALHOTRA
- MATSUYAMA
- PELLETIER
- RIEKE
- RUSSELL
- YELLE
- ZEGA

# What's in a name?



## Clues

### Across

4. Christopher, \_\_\_\_\_ is the home of actor John Malkovich. The state is also the home of the world's first skyscraper, the first McDonalds, and the home of Superman.
6. Although actor Shane Byrne is best known for his role in *Shane of the Dead*, actor John Bernthal is best known for his role as Shane \_\_\_\_\_ in *The Walking Dead*.
9. Baseball player Josh Hamilton plays for the \_\_\_\_\_.
10. Christopher Nolan is famous for his movies involving what superhero?
13. David Byrne is the lead singer from the popular New Wave band Talking \_\_\_\_\_, which was active from the 1970s to the early 1990s.
14. In 2011, Rose Byrne played the role of Moira MacTaggert, an expert genetic mutations, in what popular comic book franchise?
17. The Hamilton Watch Company is now owned by what internationally popular Swiss watch brand?
18. The Byrne name traces back to a clan whose motto is "Certavi et vici," or "I have fought and \_\_\_\_\_" for those of us who don't speak Latin. (Hint: Veni, vidi, vici...)
19. In what state is Hamilton College located?
20. This European country has had three kings by the name of Christopher.

### Down

1. Byrne is the \_\_\_\_\_ most common last name in Ireland.
2. Shane's Rib Shack is a BBQ chain located in eleven states. Their humble beginnings in 2002 included a tin roof shack next to a(n) \_\_\_\_\_.
3. Christopher Robin is a character from which popular children's book?
5. In Anthony Burgess' novel *Byrne*, the main character is a descendant of survivors of the \_\_\_\_\_ Armada.
7. When he's not riding motorcycles, killing zombies with his friend Tom, or moonlighting as a planetary science professor, Shane Byrne has been known to enjoy some Irish TV. In April 2012, Shane Byrne was featured in an episode of the Irish TV show *Come Dine with Me* for his participation in what sport?
8. The Hamilton is a restaurant with live music that aims to provide "a contemporary dining experience that's as eclectic as the talent in our music hall." It is located in which city (the same that the widow of number 11 died in!).
11. Although an impressive statesman, \_\_\_\_\_ Hamilton is perhaps equally well-known for his duel with Aaron Burr.
12. The motto for jewelry company Shane Co. is "Your friend in the \_\_\_\_\_ business."
15. Christopher was one of the twenty most popular names in England from nineteen forty until nineteen ninety- \_\_\_\_\_.
16. What genre is the 1953 film *Shane*?

## Northern New Mexican food

New Mexican food is a fusion of Spanish, Mexican, and Pueblo Native American foods. It is similar, but not the same as Mexican. Many New Mexicans are descendants of local Native Americans and Spanish colonists who arrived in New Mexico in the 1500s.

E F G Y L R G K X N H N Z A X T M I S G X J Z B L  
T I Y Y J H E W B R P H A O E H T O E R C J J H A  
A I P R K L S D P O S O L E Z D P L C E U G R C A  
X C Y O J R P K G I B E V A H A R U U E I Y I O A  
S H W W T K A R M R L G Z W I Q D G M N Z V E W K  
Z Y L H P I K L P I E S D P U U D O R C E F Z N T  
D Y E J A L R N W C V E I R Y L D D Q H N V K R W  
Q G H B A N F F F U O L N G Y P M V F I U D J O P  
Z W M S N S W B K R L H T O M J Z W T L Q Y Y C E  
X V M I I Y C U L A O P H Y R I P N V E E Z Z E R  
S T U N N O N I P O D C E C E C U S U S D S S U P  
J F S F D M W G Y O P I S H U H H N R T R P W L C  
K X U Z X E X A W S O M I I D A B R Z E M M M B M  
R Z D D A I M J H K H Q B L L O Q U I W F Q S Y U  
Z N D R J I S X J A C R Z E V T W I M S H G M A R  
D W Y W H U K Z T C O Y E E I Q R O W E T W S G Q  
B V J C H C S C Y F V L B D B U A D U G G M Z V K  
G R E E N C H I L E C H E E S E B U R G E R A Z I  
H Z R G T Z W J S R J P E V G O X M J M T I Z S P  
A D E N C Q P W M Q N K C G P T X L A X I S Q C N

**Chile** – In NM, chile means chile pepper, or powder or sauce made from that pepper. Although spelled chili in many parts of the US, Senator Pete Domenici of NM made the state’s spelling (chile) official by entering it into the Congressional Record in 1983.

**Red, Green or Christmas?** – If you order something with chile on it in a restaurant in NM, the server will ask you if you want it “red, green, or Christmas” which means red chile, green chile, or half and half.

**Chimayo** – The NM town with the best red chile.

**Hatch** – The NM town with the best green chile. Most varieties grown here have been cultivated by New Mexico State University over the past 130 years.

**Posole** – A thick stew made with hominy corn.

**Sopaipilla** – puffed, fried bread. Eaten with butter and honey as a dessert or stuffed with veggies or meat and beans and eaten as an entre.

**green chile stew** – A stew usually made with green chile, potatoes and beef or pork.

**green chile cheeseburger** – A hamburger topped with green chile and cheese. Most restaurants claim to have the best in the state, but the winner is actually determined annually at the NM state fair.

**pinon nuts** – pine nuts. A traditional food of local Native Americans which is harvested from pinyon pine trees.

**frito pie** – Fritos, covered in red chile and cheese traditionally served in the frito bag. Sometimes also topped with pinto beans, meat, lettuce, and or tomato. The exact origin of the frito pie is unknown, but New Mexicans claim it originated at the Woolworths in Santa Fe in the 1960s.

**blue corn** – a variety of corn grown in Mexico and the southwestern US. It is ground into blue corn meal and often used to make tortillas in NM food. It has a sweeter, nuttier taste than yellow or white corn and contains more protein.

## **Congressional speech by a NM Senator**

"New Mexicans consume mass quantities of this magical and life-giving fruit from birth, and labels on chile products, descriptions of dishes at New Mexican restaurants and billboards and advertisements all reinforce the fact that chile is spelled with an 'e' and not an 'i,'" Domenici said in the speech, entered into the *Congressional Record*. "A naivete exists among native New Mexicans who wrongly assume that everyone spells it with an 'e.'"

"Even the dictionary makes the error," Domenici waxed on. "Knowing that criticizing the dictionary is akin to criticizing the Bible, I nevertheless stand here before the full Senate and with the backing of my New Mexican constituents state unequivocally that the dictionary is wrong.

"that inedible mixture of watery tomato soup, dried gristle, half-cooked kidney beans, and a myriad of silly ingredients that is passed off as food in Texas and Oklahoma. The different tabascos and jalapeno sauces added to the mixture do little good and in most cases simply cause a casual visitor to suffer great gastrointestinal distress."

Contrast this to New Mexico, where ordering a bowl of chile is a delightful experience," Domenici said. "Hospitable as we are to all visitors, we have chile that is mild enough to make a baby coo in delight, or hot enough to make even the strongest constitutions perspire in a sensual experience of both pleasure and pain.

"I could go on and on about the wonders of red and green chile, but in reality, all I wanted to do was inform Congress on the correct way to spell the word."

*Domenici, P. 1983. The correct way to spell chile. Congressional Record 129 (149) (Nov. 3).*

Welcome to our world of fun trivia quizzes and quiz games: [New Player](#) → [Play Now!](#) →

## The Real Land of Enchantment

Created by **sassy111**

[Fun Trivia](#) : [Quizzes](#) : [New Mexico](#)



"I had a lot of fun making this quiz about my home state. I hope you have fun taking it!"

15 Points Per Correct Answer - No time limit

### 1. What vegetable is Hatch, New Mexico famous for?

- Pinto Beans
- Lettuce
- Corn
- Green Chilis

### 2. What is Roswell best-known for?

- Ghosts
- Their military academy
- A rare species of lizard
- Aliens

### 3. What animal is Capitan best known for?

- A fox
- A bear

- A rabbit
- A wolf

#### 4. What is Ruidoso Downs famous for?

- Horse races
- Skiing
- Dog races
- Golf

#### 5. What is Carlsbad famous for?

- Petroglyphs
- Aztec Ruins
- White Sands
- Caverns

#### 6. What year was New Mexico admitted to the Union?

- 1947
- 1911
- 1913
- 1912

#### 7. Believe it or not, the population of the entire state of New Mexico is a little over 1 million people-the amount that most states have in a single city. About 1/3 of the people in New Mexico live in which city?

- Clovis
- Las Cruces
- Albuquerque
- Santa Fe

**8. Which of the following celebrities resided in Roswell at one point?**

- Demi Moore
- Peter Hurd
- John Denver
- All of these

**9. Which state borders New Mexico to the north?**

- Montana
- Colorado
- Wyoming
- Arizona

**10. The world's first Atomic Bomb was tested in New Mexico. Where was it manufactured?**

Answer:  *(Two words)*

**11. What's the state flower of New Mexico?**

Answer:  *(One word)*

**12. What is the longest river that runs through New Mexico?**

- Pecos
- Canadian
- Gila
- Rio Grande

**13. What is the HIGHEST point in NM?**

Answer:  *(Two words)*

**14. What is the LOWEST point in NM?**

- Bottomless Lakes
- Elephant Butte
- Red Bluff Lake
- Conchas Lake

**15. What is the name of the outlaw that resided in Lincoln county New Mexico?**

Answer:  *(Billy Joel sang a song about him)*

Submit my Answers!

Copyright, FunTrivia.com. All Rights Reserved.  
[Legal / Conditions of Use](#)

Compiled Jun 28 12

Welcome to our world of fun trivia quizzes and quiz games: [New Player](#) → [Play Now!](#) →

## The Jemez Mountains

Created by CellarDoor

[Fun Trivia](#) : [Quizzes](#) : [New Mexico](#)



"The Jemez Mountains of north-central New Mexico are a place of long history and great beauty. Let me take you on a journey there, through space and time . . ."

15 Points Per Correct Answer - No time limit

**1.** About 1.6 million years ago, the Jemez Mountains as we now know them were formed in a cataclysmic volcanic eruption that released some 50 cubic miles of ash. Is the region still geologically active?

- Yes
- No

**2.** Many, many years passed. Flowing water easily carved caves and canyons in the soft volcanic rock that coated the surrounding mesas. What is the name for this type of rock, made up of compacted ash?

- pumice
- basalt
- obsidian
- tuff

**3.** In the eastern part of the Jemez Mountains, one of the mightiest Western rivers flows through a deep rift valley. What is the U.S. name of

**this river, which begins in Colorado and forms the border between Texas and Mexico?**

- Jemez River
- Pecos River
- Colorado River
- Rio Grande

**4. From the eastern foothills of the Jemez Mountains, the traveler is treated to a spectacular view over much of north-central New Mexico. Looking east, you can see mountains towering over Santa Fe; they're a range of the Rockies. What name does this mountain range have, given in tribute to its glorious red color during some sunrises and sunsets?**

- Red Mountains
- Sangre de Cristo Mountains
- Grand Teton Mountains
- Scarlet Mountains

**5. The Jemez Mountains were once home to an ancient people whose cliff dwellings are found all over the Southwest. Although they were probably the ancestors of the modern Pueblo peoples, we don't know what this ancient group called themselves, so we commonly call them by what name given to them by ancient Navajos?**

- Anasazi
- Zuni
- Hohokam
- Mogollon

**6. These ancient cliff-dwellers left behind a large number of pictures carved into the rock. In some cases, these pictures stand out dramatically: the artists pecked through the dark patina of volcanic rock to reveal the lighter stone underneath. What is this type of art called?**

- lithograph
- pictograph
- geoglyph
- petroglyph

**7.** Some of the best-preserved, most accessible archaeological sites in New Mexico are found in a 33,000 acre national monument centered on Frijoles Canyon in the Jemez Mountains. Paved trails running along the cliffside take visitors through cliff dwellings and to a "ceremonial cavern" with a reconstructed kiva. What is the name of this monument, named for a 19th-century anthropologist?

- Chaco Culture National Historical Park
- Santa Fe National Forest
- Petroglyph National Monument
- Bandelier National Monument

**8.** In the southern Jemez Mountains lies the Jemez Pueblo, a sovereign indigenous nation with about 3,400 tribal members. This pueblo, whose roots in the region go back to the late 1200s, is one of how many federally recognized pueblos in the state of New Mexico?

- 1
- 103
- 19
- 7

**9.** Despite the beauty of the Jemez Mountains, this region is strongly associated with one of the most destructive moments of human history: the development of the atomic bomb. In 1943, Oppenheimer, Fermi, Teller, and other scientists of the Manhattan Project moved their operations here, in hopes that the remote location would improve security and secrecy. The laboratory they founded outlasted the war, and still conducts scientific research for the government to this day.

**What is the name of this lab?**

- Sandia National Laboratory
- Fermi National Accelerator Laboratory
- Lawrence Livermore National Laboratory
- Los Alamos National Laboratory

**10.** In the year 2000, Congress purchased 89,000 acres of ranchland in the volcanic caldera in the center of the Jemez Mountains. This land now comprises the beautiful Valles Caldera National Preserve, where herds of elk roam and where visitors can hike, fish, cycle, or even ride horseback. But what happened to the cattle who grazed there in the summer?

- Without summer grazing, they had to be sold to ranchers and other concerns across the country.
- Nothing: by law, the National Preserve remains a working ranch.
- Summer grazing is now found about 200 miles to the northeast.
- It was agreed that summer grazing in the National Preserve should be phased out by 2020.

Submit my Answers!

Copyright, FunTrivia.com. All Rights Reserved.  
[Legal / Conditions of Use](#)

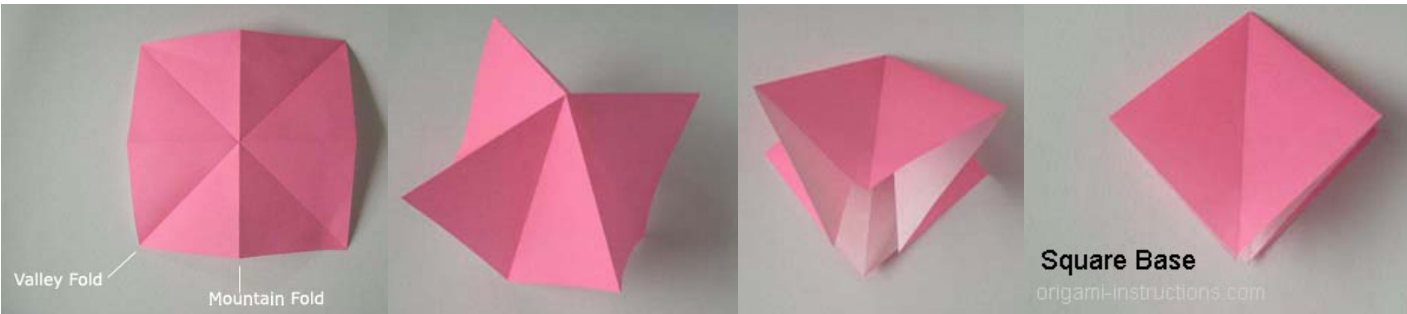
Compiled Jun 28 12

# How to make an Origami Dinosaur (pt.1)

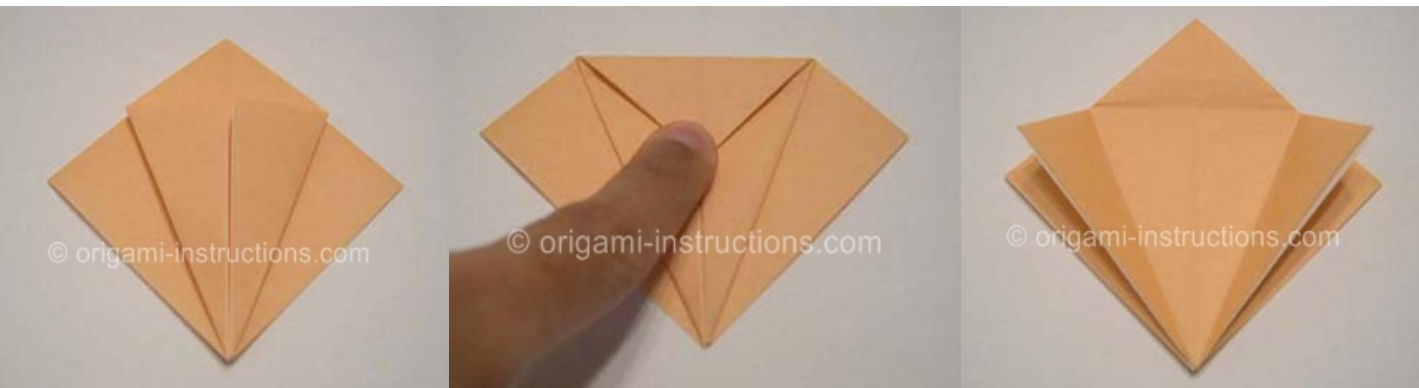
Follow the instructions below, and you can turn the attached piece of colored paper into a dinosaur! To start, rip out the colored paper and cut it into a square.

This follows instructions from: <http://www.origami-instructions.com/origami-square-base.html>

Fold the square along the diagonals, as well as on the North-South and East-West.  
Collapse the square along these folds to make



Fold the corners of this square base in toward the center. Make sure that the creases are good.



Now open up the upper-most layer of the well-creased square, folding the tip upward and flattening.

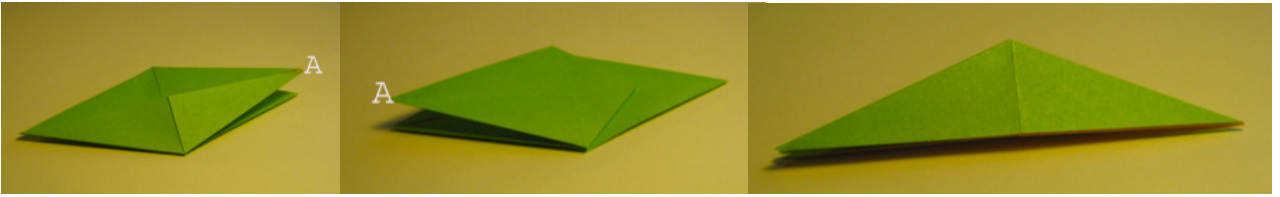


Flip the whole assembly over, and repeat the previous step for the other side of the origami.

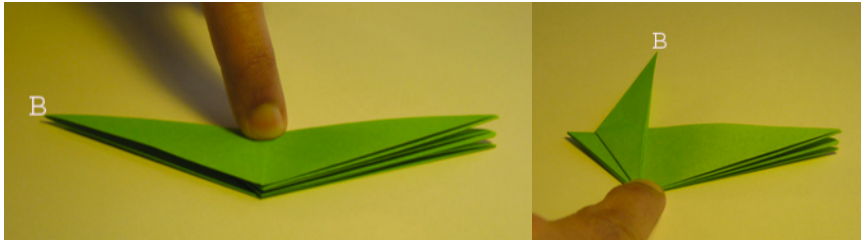


# How to make an Origami Dinosaur (pt.2)

Fold corner A of the "bird base" to the left, as shown below. Then fold the assembly in half along the long axis.



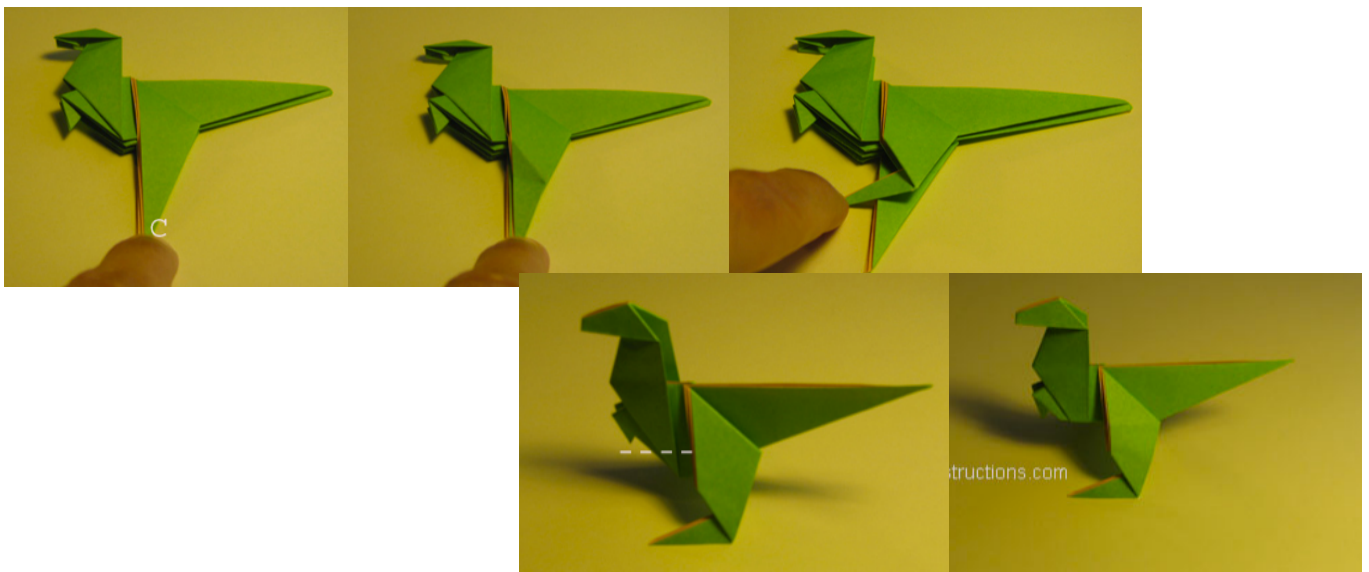
Rotate the assembly 180 degrees, and then do a reverse fold to create the dinosaur's neck.



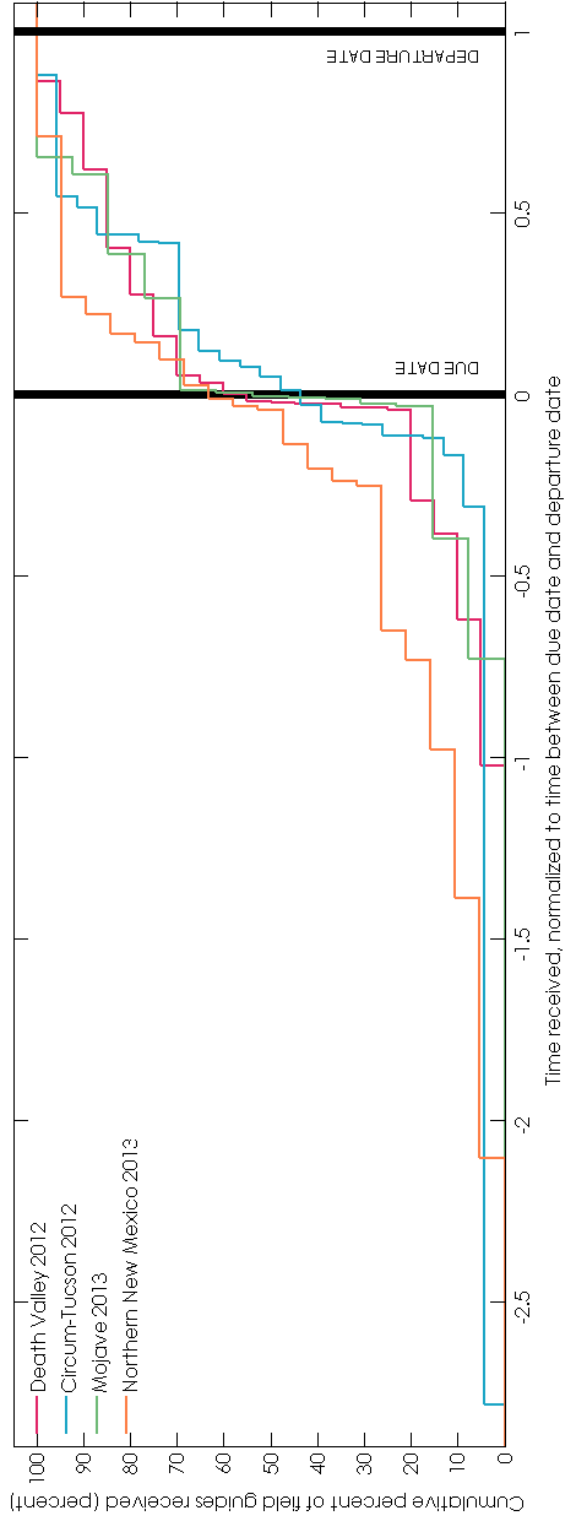
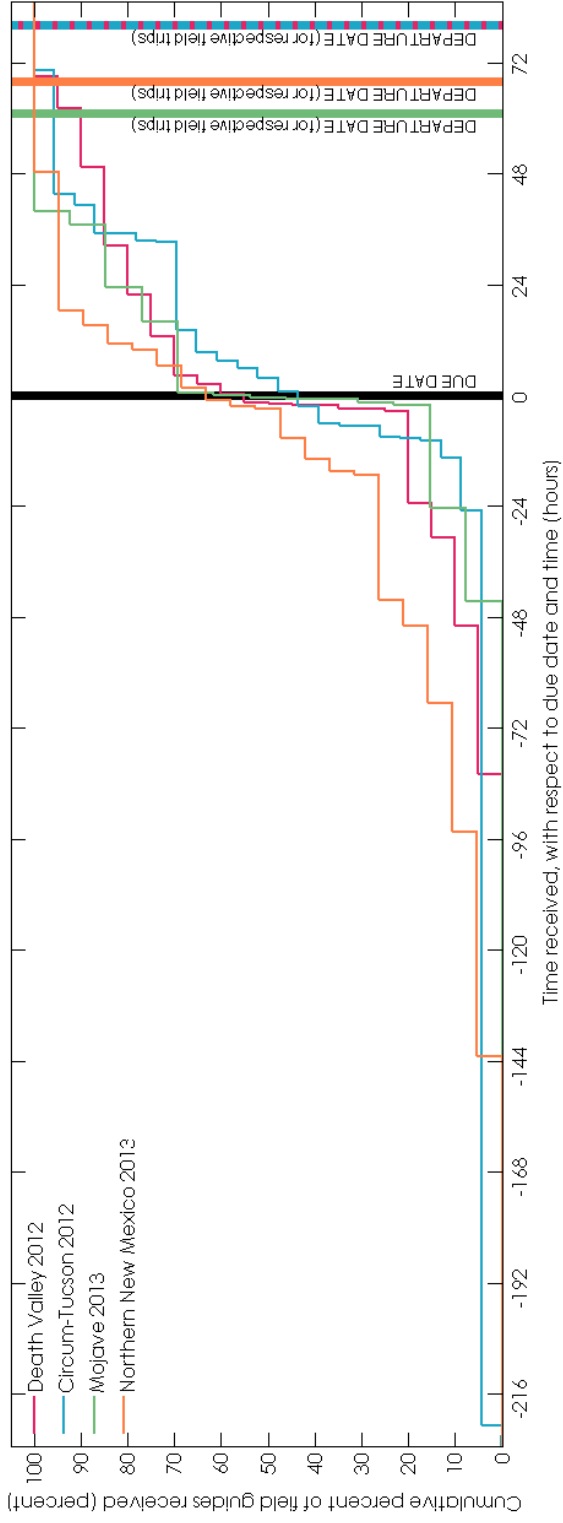
Perform another reverse fold to make the dinosaur's head. Further small folds can shorten the dinosaur's skull, and create downward pointing arms.



Fold down corner "C" (labeled in the last figure above), to form the dinosaur's leg. Repeat on the other side to get the second leg. Then crimp the legs to form the dinosaur's feet. To slim the body, you can fold the lowermost part of the body inside of itself.



You now have an origami dinosaur!











# Scale bar

